Studies on the structure and function of phenazine modifying enzymes PhzM and PhzS involved in the biosynthesis of pyocyanin

DISSERTATION

zur Erlangung des akademischen Grades
eines Doktors der Naturwissenchaften (Dr. rer. nat.)
des Fachbereichs Chemie der Universität Dortmund

Angefertigt am Max-Planck-Institüt für Molekulare Physiologie
In Dortmund

Eingereicht von

Neelakshi Gohain
Aus Mumbai/Indien

Dortmund, 2008

1. Gutachter :   Prof. Dr. R.S.Goody

2. Gutachter :   Prof. Dr. H.Mootz

Studies on the structure and function of phenazine modifying enzymes PhzM and PhzS involved in the biosynthesis of pyocyanin

DISSERTATION

Submitted towards partial fulfillment of requirement
for the degree of

DOKTOR DER NATURWISSENCHAFTEN
(DR. RER. NAT.)

in the Department of Chemistry,
University of Dortmund, Germany

By

Neelakshi Gohain
Max Planck Institute for Molecular Physiology

&

Department of Chemistry, University of Dortmund

2008

Die vorliegende Arbeit wurde in der Zeit von September 2004 bis September 2008 am Max- Planck-Institut für Molekulare physiologie in Dortmund unter der Anleitung von Prof. Dr. Roger S Goody, Dr. Wulf Blankenfeldt und Prof. Dr. H.Mootz durchgeführt.

Hermit versichere ich an Eides statt, dass ich die vorliegende Arbeit selbständig und nur mit den angegeben Hilfsmitteln angefertigt habe.

Dortmund, 2008   Neelakshi Gohain

c

Dedicated to my mother…

CONTENTS

iii

SYMBOLS AND ABBREVIATIONS

Å	Ångstrom (0.1nm)
CAN	Acetonitrile
ADIC	2-amino-2-deoxychorismic acid
AdoHcy	S-Adenosyl-L-Homocysteine
APCI	Atmospheric Pressure Controlled Ionization
APS	Ammonium Persulfate
bp	base pair
BSA	Bovine Serum Albumin
CCD	Charge Coupled Devices
C-terminus	Carboxyterminus
Da	Dalton
DMSO	Dimethyl Sulfoxide
DNA	Deoxyribonucleic acid
DTT	Dithiothreitol
EDTA	Ehtylendiamintetraacetate
ESRF	European Synchrotron Radiation Facility
E. coli	*Escherichia coli*
ESI-MS	Electrospray Ionisation Mass Spectroscopy
Fcalc, Fobs	Structure-factor amplitudes (calc:calculated, obs: observed)
FAD	Falvin Adenine Dinucleotide
FPLC	Fast Performance Liquid Chromatography
GC	Gas Chromatography
1-oh-phz	1-Hydroxy Phenazine
HPLC	High Performance Liquid Chromatography
IPTG	Isopropyl-β-D-1-thiogalactopyranosid
ITC	Isothermal Titration Caloriemetry
kb	kilo-base pair
kDa	kilo-Dalton
kJ	kilo-Joule
LB	Luria-Bertani
λ	Wavelength, Lambda
MAD	Multiple Wavelength Anomalous Dispersion
MALDI	Matrix Assisted Laser Desorption/Ionization
Min	Minute

MIR	Multiple Isomorphous Replacement
MM	Millimolar
MR	Molecular Replacement
Mw	Molecular Weight
NADH	Nicotinamide Adenine Dinucleotide
NADPH	Nicotinamide Adenine Dinucleotide Phosphate
NCS	Non-Crystallographic Symmetry
Nm	Nanometer
NMR	Nuclear Magnetic Resonance
N-terminus	Aminoterminus
O.D	Optical Density
P.aeruginosa	*Pseudomonas aeruginosa*
PCA	Phenazine-1-carboxylic acid
PCR	Polymerase Chain Reaction
PDB	Protein Data Bank
PDC	Phenazine-1,6-dicarboxylic acid
PEG	Polyetheleneglycol
PMSF	Phenylemethylsulphonylfluoride
Pyo	Pyocyanin
RNA	Ribonucleic acid
Rmsd	Root mean square deviations
RT	Room temperature
SAM	S-Adenosyl methionine
SAD	Single-Wavelength Anomalous Dispersion
SDS-PAGE	Sodiumdodecylsulphate-Polyacrylamide Gel Electrophoresis
Se	Selinium
SeMet	Seleno-L-Methionine
TB	Terrific Broth
TEMED	N,N,N,N -Tetramethyl-Ethylenediamine
TFA	Trifluoro acetic acid
TRIS	Tris-(hydroxymethyl)-aminomethane
U	Units
UV	Ultraviolet
V	Volt
µl	Microliter
µM	Micromolar

Amino Acids Abbreviations

Amino Acids	3-letter-code	1-letter Code
Alanine	Ala	A
Arginine	Arg	R
Asparagine	Asn	N
Aspartate	Asp	D
Cysteine	Cys	C
Glutamine	Glu	E
Glutamate	Gln	Q
Glycine	Gly	G
Histidine	His	H
Isoleucine	Ile	I
Leucine	Leu	L
Lysine	Lys	K
Phenylalanine	Phe	F
Methionine	Met	M
Proline	Pro	P
Serine	Ser	S
Threonine	Thr	T
Tryptophane	Trp	W
Tyrosine	Tyr	Y
Valine	Val	V

INTRODUCTION

1.0 Introduction

1.1 Introduction to phenazines

For more than a century, chemists have been concerned with the discovery, isolation, and characterization of chemical substances in the earth's biota. That the inventory is not yet complete becomes apparent from perusal of any journal recording current research on natural products. New substances continue to be discovered in substantial numbers. By, and large, these do not fit into the well-established systems for intermediary metabolism, and so add to that diverse collection of compounds called *secondary metabolites,* a term invented by plant physiologists (1) and brought into general use for microbial products by J. D. Bu'Lock in 1961 (2). Historically, microbiologists and chemists alike have categorized 'secondary metabolites' as a broad class of molecules produced at late stages of microbial growth in laboratory cultures. In particular, the traditional view is that secondary metabolites (i) do not contribute to the growth or survival of the producer (ii) are highly sensitive to the conditions stimulating their production (for example, medium composition) (iii) often have complex structures and (iv) have production rates that are decoupled from the doubling time of the cells (3). Secondary metabolites have diverse chemical structures, and their intricate molecular frameworks often appear to the biochemist to be quite idiosyncratic. They are usually distinctive products of particular groups of organisms sometimes even of a single strain.

Amongst the secondary metabolites that have gained interest in pharmaceutical and clinical research groups for the last 50 years is a class of compounds called 'phenazines'. They are heterocyclic nitrogen-containing compounds synthesized by some strains of fluorescent *Pseudomonas* species and some other bacterial genera. Phenazine-excreting bacteria have become popular model organisms for the study of quorum sensing and biofilm formation, two of the most active areas of research in the field of microbiology, whereas pharmaceutical and clinical groups have been focused on the physiological effects of these compounds in non-producing organisms, microbial physiologists and geneticists have typically

viewed phenazines as metabolites that perform only secondary functions. That phenazines and other excreted compounds (i) react with common primary metabolites (ii) are potentially transformed by enzymes active in central metabolic pathways and (iii) induce gene expression calls into question their categorization as secondary metabolites (4). Here I will discuss the recent discoveries that lead to new hypotheses about the relevance of phenazine metabolism in the context of the lifestyles of their producers.
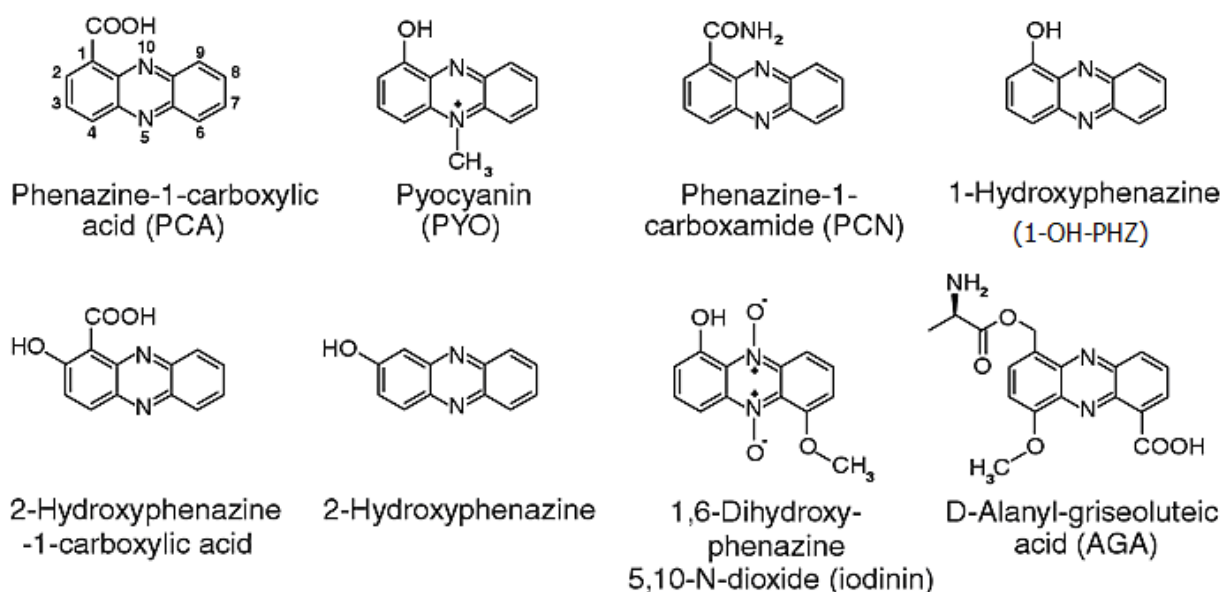
Fig1.1. Some phenazine derivatives

1.2 Occurrence of Phenazine Production:

The discovery of phenazines dates back to as early as 1860 when French researchers and clinicians noticed a blue coloration in the pus and sputum, or respiratory secretion, of infected patients (5). In 1882 Carle Gessard and others examined the pus microscopically and identified a rod-shaped bacterium residing in these wounds, and upon isolating the organism discovered that it was responsible for the bluish tint. For this trait, they named the species *Bacillus pyocyaneus*, and it has since been renamed *Pseudomonas aeruginosa*, for the Latin *aerugo*, which refers to the blue-green rust of copper. The antibiotic properties of phenazines have been known for over 150 years, but it is only within the past few years that significant progress

has been made in understanding how these compounds are synthesized, how they affect other organisms, and how they function in the environment. Phenazines are nitrogen containing heterocyclic compounds produced by diverse bacterial genera, including *Erwinia*, *Burkholderia*, *Streptomyces* and fluorescent *Pseudomonas* species under quorum sensing control. Of more than 6000 phenazine-containing compounds that have been described over the past century, fewer than 100 are of natural origin, but most of these possess broad-spectrum antibiotic activity toward bacteria, fungi, and plant and animal tissues (6). Most studies on the production and biosynthetic pathways of the various phenazine pigments have been conducted with the representatives of the fluorescent pseudomonads. Pseudomonads represent the major group of non-differentiating microorganisms producing antibiotics. The lack of cytological and physiological differentiation makes it possible to study the effect of various factors on secondary metabolism without interference from genetically programmed development cycles. The pseudomonads may therefore offer experimental advantages over the filamentous fungi, the actinomycetes, and the bacilli for studying certain facets of secondary metabolism (T.Leisinger and R.Margraff 1979). The practical use of antibiotics from pseudomonads date back to the period before the 'antibiotic era'. In 1899 some researchers reported that the cell free culture fluid of *P. aeruginosa*, concentrated to one-tenth of its original volume, killed several kinds of bacteria. It has been used extensively in the therapy of diphtheria, influenza, and meningitis during the first two decades of this century (7).

Phenazine-producing species are more abundant among the high G+C Gram-positive lineage, but they also occur within two clades of Gram-negative Proteobacteria. All known phenazine-producing Gram-positive bacteria are Actinobacteria. Many are members of the genus *Streptomyces*, with over a dozen species that synthesize both simple and more complex phenazines (6).Amongst all phenazine producing fluorescent pseudomonads bacteria *Pseudomonas aeruginosa* has been most widely studied because it is a ubiquitous environmental bacterium that is one of the top three causes of opportunistic human infections that is, it exploits some break in the host defences to initiate an infection (8-10). One of the reasons why *P. aeruginosa*

is a successful opportunistic pathogen is that it produces a battery of secreted virulence factors (11). The bacterium almost never infects uncompromised tissues, yet there is hardly any tissue that it cannot infect if the tissue defences are compromised in some manner. It causes urinary tract infections, respiratory system infections, dermatitis, soft tissue infections, bacteraemia, bone and joint infections, gastrointestinal infections and a variety of systemic infections. *Pseudomonas aeruginosa* infection is a serious problem particularly in patients hospitalized with cancer, cystic fibrosis, severe burns and AIDS patients who are immunosuppressed (12;13) Apart from this the antibiotic activity of the secondary metabolites produced by *P.aeruginosa* made its investigation more interesting in the scientific research field. In 1899 Emmirich and Low reported that the cell free culture fluid of *P.aeruginosa*, concentrated to one-tenth of its original volume, killed several kinds of bacteria. Because the preparation exhibited enzymatic activities, it is called pyocyanase. It has been used extensively in the therapy of diphtheria, influenza and meningitis during the first two decades of 20th century (T.Leisinger and R.Margraff 1979). *Pseudomonas aeruginosa* strains produce two types of soluble pigments, the fluorescent pigment pyoverdin and the blue pigment pyocyanin. The latter is produced abundantly in media of low-iron content and functions in iron metabolism in the bacterium (14). Pyocyanin (from "pyocyaneus") refers to "blue pus" and is a characteristic of suppurative infections caused by *Pseudomonas aeruginosa.* My work mainly deals with giving an insight to the biosynthesis of pyocyanin.

1.2.1. Pyocyanin

1.2.1.1 Chemical nature of pyocyanin

Pyocyanin is a blue redox-active secondary metabolite and a member of the large family of the tricyclic compounds 'phenazines' (13). Because of its solubility in chloroform it can be easily isolated. Pyocyanin or 1-hydroxy-5-methylphenazine is considered as a resonance hybrid of the mesomeric forms of N-methyl-1-hydroxyphenazine (Hillemann, 1938) (15) and is capable of undergoing a two-electron reduction to a colourless product, leukopyocyanin. The elucidation of the structure of pyocyanin represents the first reported

instance of the occurrence of the phenazine nucleus as a natural product (16). Pyocyanin can exist in either oxidized or reduced form, the later being an unstable form of pyocyanin that reacts rapidly with molecular oxygen (17). The pigment is wine-red at acid condition due to the basic property of one of the N atoms and blue at alkaline reaction (Friedheim *et al* 1931).
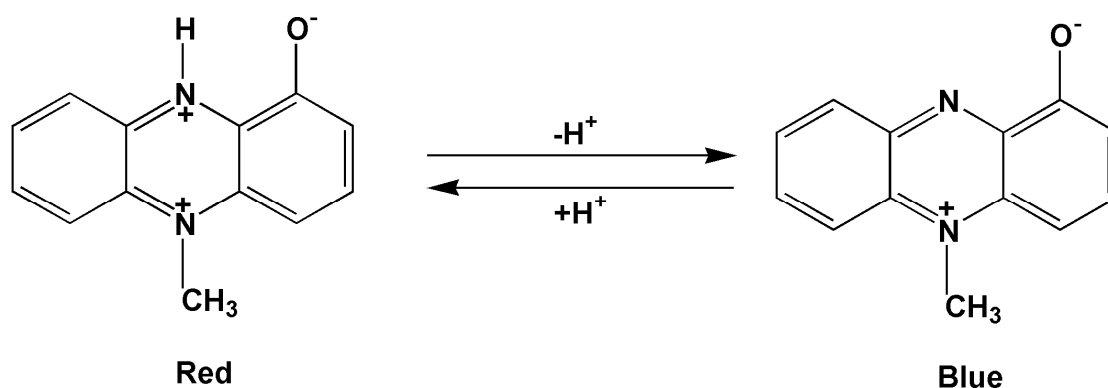
Fig 1.2 (a) Structure of pyocyanin

Fig 1.2. (b) colours of pyocyanin in acid and alkaline solution (c) the intermediary green colour

When the alkaline blue solution is reduced, say by a trace of colloidal palladium in a stream of hydrogen, the colour vanishes and is reestablished on exposure to the air. However, when the acid red form of the pigment is reduced there is an intermediary green stage (fig. 1.2(c)) before the complete

decolouration. In the same manner when the completely reduced colourless form of the pigment is titrated with a colourless oxidant (such as ferricyanide) in an alkaline solution, the colourless form directly turns blue, whereas in an acid solution the colour first turns green and just when the half of the equivalent amount of the oxidant is being exceeded (judged from the potentiometric end-point of titration) begins to turn red (Friedheim *et al* 1931).
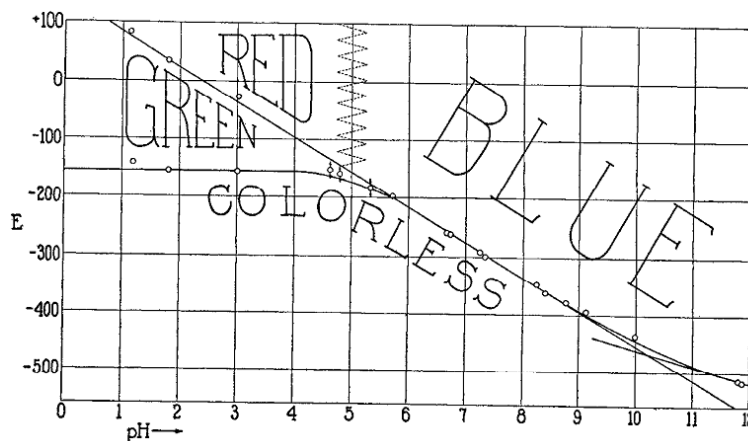
Fig 1.3 The normal potential of pyocyanin at varied pH at 30°c (Friedheim and L. Michaelis Journal of biological chemistry Feb, 1931)

The blue pigment pyocyanin is reversibly oxidizable and reducible. In ranges of pH>6 it behaves entirely as a reversible dye of a quinoid structure. The slope of the titration curve indicates that one molecule of the dye combines with two hydrogen atoms simultaneously. At pH ranges<6 the titration curves show a different shape which can be interpreted by the assumption that the two hydrogen atoms are accepted in two separate steps. The existence of these two steps of reduction is confirmed by the fact that in acid reaction the colour, on reduction, changes in two different steps, whereas at alkaline reaction the color change takes place in one step as mentioned earlier. The normal potentials of the dye at various pH are summarized in Fig. 1.3.

1.2.1.2 III effects of pyocyanin

Pyocyanin is toxic at micro molar concentrations to a wide range of bacterial and mammalian cells. *In vivo* virulence of pyocyanin was studied on alternative model hosts and mice, which revealed that pyocyanin has crucial role in *P. aeruginosa* infection. It causes multiple and omnious effects on human cells like inhibition of cell respiration (18), ciliary function (19), epidermal cell growth and disruption of calcium homeostasis. It may interact with endothelium derived relaxing factor nitric oxide (20), which plays an important role in the control of blood pressure, blood flow and immune function, through the formation of a complex or it may act by inhibition of nitric oxide synthase (21). It also inactivates the α1 protease inhibitor (22) and contributes to the imbalance of protease–antiprotease activity, which is readily detected in the airways of patients with Cystic Fibrosis lung disease. It has been shown recently that *P. aeruginosa* strains with defective pyocyanin biosynthesis are less virulent and more susceptible to the immune response in the lung infection mouse model (23). Pyocyanin can increase oxidant formation in human airway epithelial cells through a number of mechanisms including the oxidation of glutathione and NADH and inhibition of antioxidant enzymes. Once it is reduced, pyocyanin can then react with oxygen, forming superoxide radical and hydrogen peroxide (24). Pyocyanin radical is also formed as an intermediate during its redox cycling and can then further contribute to the formation of reactive oxygen species (ROS) (25). These insults to the host cell's internal redox balance may lead to increased secretion and thereby contribute to the generation of sputum, the physical and nutritional substrate for *P.aeruginosa* in the lungs of individuals with Cystic Fibrosis.

Bacteria of the genus *Pseudomonas*, like most heterotrophic bacteria (26), oxidize organic carbon sources via the activity of the citric acid cycle. Several of the oxidative steps in these pathways are coupled to the reduction of NAD^+ to NADH, and NADH must be reoxidized so that these pathways can proceed and generate anabolic precursors. In pseudomonads, the primary mechanism whereby this is accomplished is through reduction of one of the NADH

dehydrogenases at the start of the respiratory chain, which ultimately transfers the electrons to oxygen or nitrate (27). It has therefore been assumed that pseudomonads, organisms that rely on respiration for growth under most conditions, accumulate NADH when terminal electron acceptors become limiting (28). Some of these compounds, including pyocyanin, the best-studied phenazine due to its role in the pathology of *P. aeruginosa* infections, have been shown to react with NADH in vitro (29;30). This has led to the hypothesis that electron transfer to phenazines may represent an adaptation that allows bacteria to modulate their intracellular redox state (31;32). This physiological role would be consistent with the fact that phenazine biosynthesis is regulated such that phenazines are produced at high cell densities (33-35), a condition that typically correlates with electron acceptor limitation (36). Friedheim theorised that the reducible nature of pyocyanin was important for the respiration of *P.aeruginosa* because addition of pyocyanin could function as an extracellular respiratory pigment. In human alveolar epithelial cells, pyocyanin causes oxidative stress accompanied by direct inhibition of catalase, depletion of cellular cAMP and ATP, and depletion of the intracellular pool of reduced glutathione (GSH) that serves as a major antioxidant (37); (38). Instead of acting as a protectant under these conditions, GSH can further enhance the damage to lung tissues by reducing pyocyanin with the production of pyo free radical and $O^{2-\cdot}$(6).

1.3. Chemical properties of Phenazine

Phenazines are heterocyclic compounds that are produced naturally and substituted at different points around their rings by different bacterial species. Small modifications of the core phenazine structure give rise to a full spectrum of colours (Fig 1.4), ranging from the deep red of 5-methyl-7-amino-1-carboxyphenazinium betaine (aeruginosin A) to the lemon yellow of phenazine-1-carboxylic acid (PCA), to the bright blue of 1-hydroxy-5-methylphenazine (pyocyanin) (39). The combination and variety of functional groups added also determine the redox potential and solubility of these compounds, thus affecting their biological activity (40). Early studies on phenazines were motivated by the fact that phenazines possess broadband

antibiotic activity towards other microorganisms (41). Most of the phenazines produced by *Pseudomonas* species are simply carboxy- and hydroxyl-substituted derivatives but their physical properties and consequently the antibiotic activity differ according to the nature and position of the substitutents on the heterocyclic ring. The lack of obvious metabolic functions of phenazines has led to several hypotheses on their role in nature. As phenazine-producing organisms survive longer than non-phenazine-producing species, it is likely that the phenazine production, due to the apparent antibiotic activity, helps the producing organism to protect its habitat against other microbial competitors. Apart from this leukopyocyanin has the ability to reduce iron and causes the release of iron from transferrin, a protein that normally sequesters iron so that it is available only to the human host (17). Thus, phenazine reduction could act to make the iron more available to the producing organism.

a   b
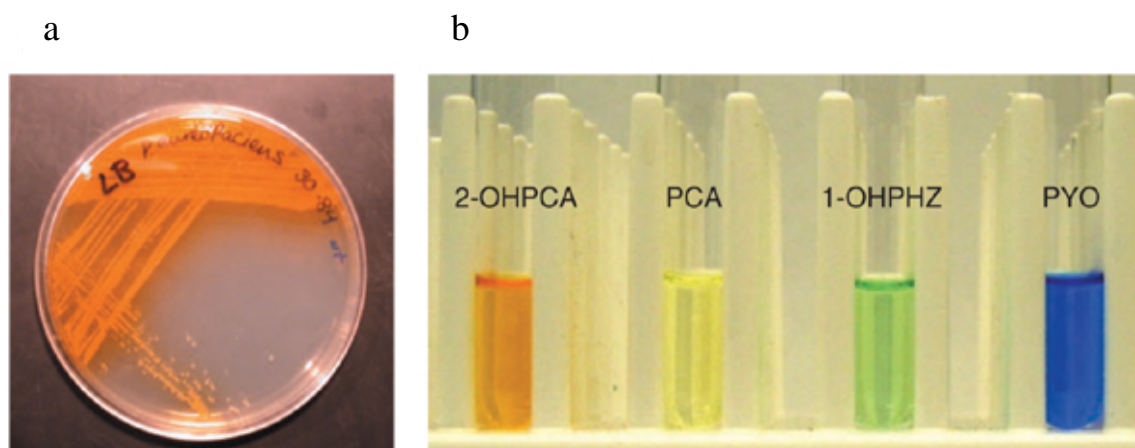
Fig.1.4. (a) Streak plate of the bio-control strain P. aureofaciens 30-84. The phenazine 2-OH-PCA turns the agar bright orange. (b). Aqueous solutions of some of the phenazines produced by various Pseudomonas strains (42).

1.4. Mode of Action

The biological activities of phenazines have interested chemists for a long time and an estimated 6000 phenazine compounds have been synthesised or modified after their discovery from biological sources. These include chemically synthesised phenazines which play an important role in physical and electrochemical research, e.g. construction of microbial fuel cells for

10

generation of renewable energy source (43). Additionally, phenazines were designed to exploit their DNA intercalative properties, e.g. [5,4-*ab*]-phenazine and phenazine-5,10-dioxide to investigate their anti-proliferative, thus anti-tumour and anti-cancer activities (44-46). Among the models that have been advanced to explain the unusually broad activity of phenazines, those that remain the focus of contemporary research involve interactions with polynucleotides, topoisomerase inhibition and the generation of free radicals (6). Although the exact mechanism of intercalation of DNA by phenazines is not well understood, it is thought that phenazines act by hindering DNA biosynthesis, replication or processing (47). These examples clearly indicate that phenazines, rather than performing one dedicated purpose, seem to be capable of performing multiple roles. This has led to intensification in research towards understanding the mode of action of phenazines. The evident non-selective toxicity of phenazines was thought to arise from a mode of action directed against one of the more universal primary metabolic pathway reactions (48). In 1934, Friedheim and co-workers showed through potentiometric study that pyocyanin in mixture with its reduced derivative acted as a reversible redox system.

Almost all the effects of phenazines mentioned in the previous paragraph (except DNA intercalation) can be attributed to this one essential feature of phenazines - their capacity for undergoing redox transformations (24;49-51). Phenazines are thought to diffuse across or insert into membranes and readily undergo redox-cycling in the presence of molecular oxygen, resulting in the uncoupling of oxidative phosphorylation and generating reactive oxygen species like superoxide ($O^{2-\cdot}$) hydroxyl (OH^-) and hydrogen peroxide (H_2O_2) (24;41) (Fig 1.5).

The accumulation of these radicals is toxic not only to bacterial but also fungal and eukaryotic cells (52;53) thus conferring host-nonspecific pathogenicity to organisms producing phenazines. The finding of Friedheim about increased rates of respiration has been reiterated by O'Malley *et al*., (54) and Lau *et al*. (55;56), who showed that the effects of PCA and PYO on both bacterial and eukaryotic host cells result from oxidative activity and the inactivation of proteins involved in oxidative stress responses. Moreover, Hassett and co-workers (53;57) have found that the superoxide dismutases of pyocyanin

producing *P. aeruginosa* possess a higher activity than other known dismutases, which would protect this organism from the harmful effects of phenazines.
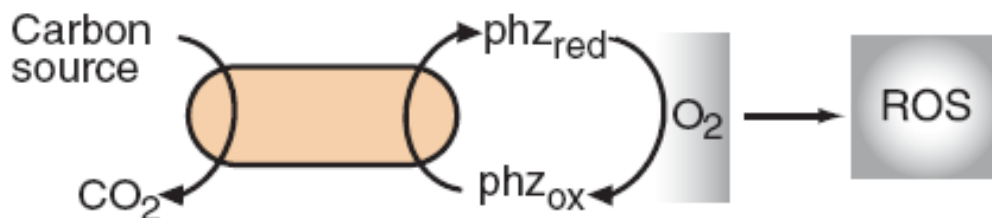
Fig1.5 Phenazine reduction and auto-oxidation (58)

Though the redox activity of phenazines is well known and the mode of action is hypothesised, the exact mechanism of how phenazines generate these species is not well understood. A more detailed understanding of mode of action of various phenazines, their influence on the molecular level and their metabolism is only just emerging (59;60).

1.5. Biosynthesis of Phenazines

All secondary metabolites are known to arise from some modification of the primary metabolic pathways of cells. The shikimate pathway is an essential metabolic route by which microorganisms and plants synthesise the aromatic amino acids phenylalanine, tyrosine and tryptophan, as well as a number of other aromatic compounds, which are critical to sustaining the primary functions of living organisms. It links the metabolism of carbohydrates to the biosynthesis of ring containing compounds (61). The absence of this pathway in animals makes it an attractive target for metabolic intervention in the development of chemotherapeutic agents as well as herbicides. However, the significance of the shikimate pathway extends well beyond the manufacture of these primary cellular metabolites. The pathway is also the source of a vast number of secondary metabolites of plants and microorganisms, natural products which, although not critical to the immediate survival of the producing organism, help it in a variety of ways to maintain its position in its ecological environment (62). The majority of these shikimate-derived natural products

are formed from the end products of the shikimate pathway, *i.e.* the aromatic amino acids (63).

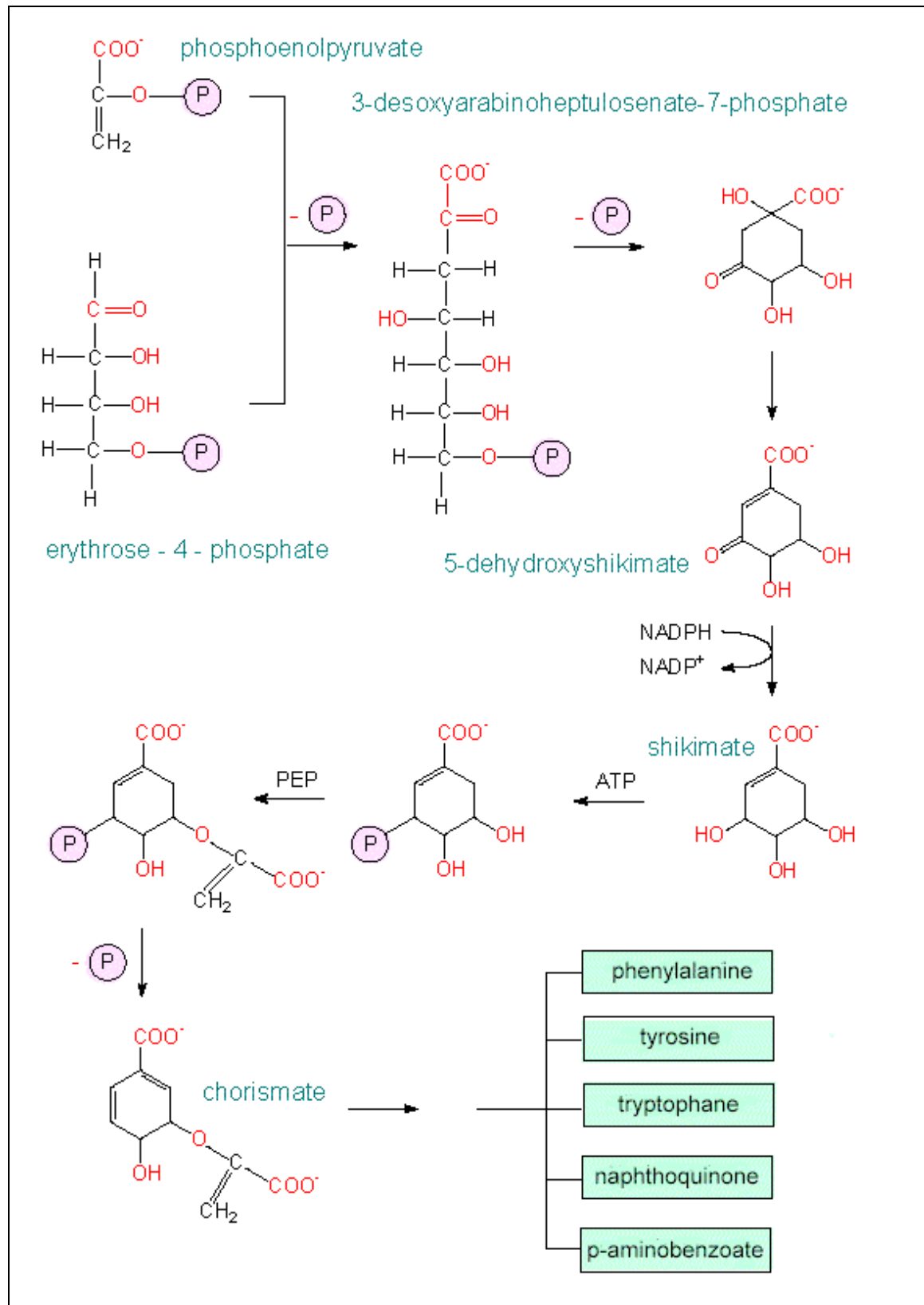*Fig 1. 6.The Shikimate Pathway (www.biologie.uni-hamburg.de/b-online/ge19/26.gif)*

The discovery of the Shikimic acid pathway for the biosynthesis of aromatic amino acids - tryptophan, tyrosine and phenylalanine in the 1960s (Balinsky and Davis, 1961) and the availability of isotopically labelled compounds resulted in the investigation of some metabolic intermediates of the shikimate pathway as a possible precursor. Information on the assembly of the first-formed phenazine from a derivative of shikimate has been obtained from the elegant studies by Hollstein & McCamey (64) and Herbert *et al*. (1974, 1976) of iodinin biosynthesis (65).

Three important studies in the 1960-70 period established beyond doubt that the Shikimic acid pathway was indeed the primary metabolic pathway which branched into the phenazine biosynthesis. The first of these studies was carried out in 1963 by Millican (66) and showed that biosynthetically prepared [U14-C] shikimic acid was the precursor of pyocyanin synthesised by *P. aeruginosa;* with the recovery of around 16% of this radiolabelled shikimate in pyocyanin. A second set of experiments using isotope-competition technique (67;68) confirmed that shikimic acid was the precursor for biosynthesis not only of pyocyanin but also phenazine-1-carboxylic acid and oxychlororaphin.
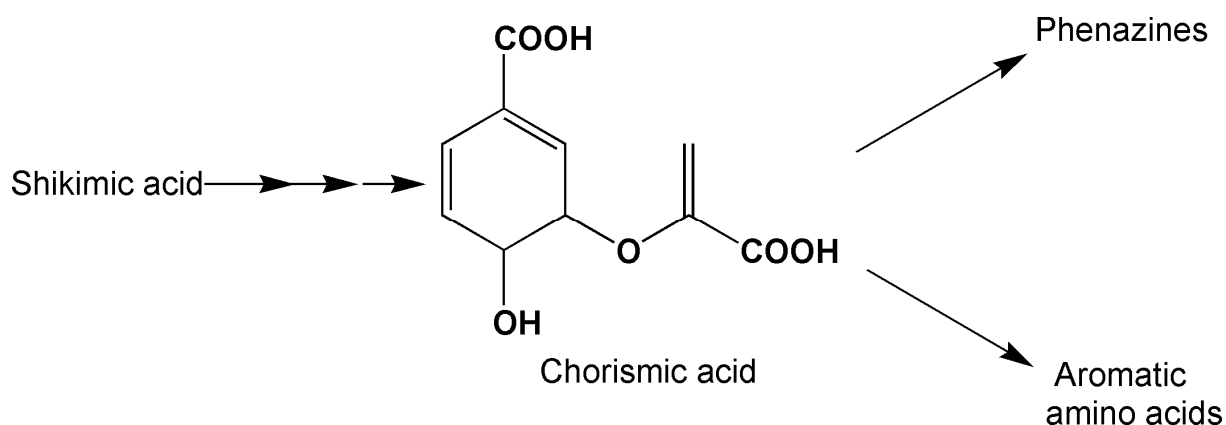
Fig. 1.7 Shikimate to chorismate and then to phenazines and to aromatic amino acids

Lastly, experiments by Longley *et al*. and Calhoun *et al*., (1972) used mutants unable to degrade shikimic acid and blocked at various points on the branched pathway to aromatic amino acids. Their experiments not only validated the conclusions by the previous two sets of experiments, but went

further and identified chorismic acid as the branching point of the shikimic acid pathway to phenazine biosynthesis (Figure1.7).

The next question in elucidating the phenazine biosynthesis pathway was the identification of the compound that led to the formation of the tricyclic scaffold of phenazines.

Chorismate   **Phenazine-1-carboxylic acid**
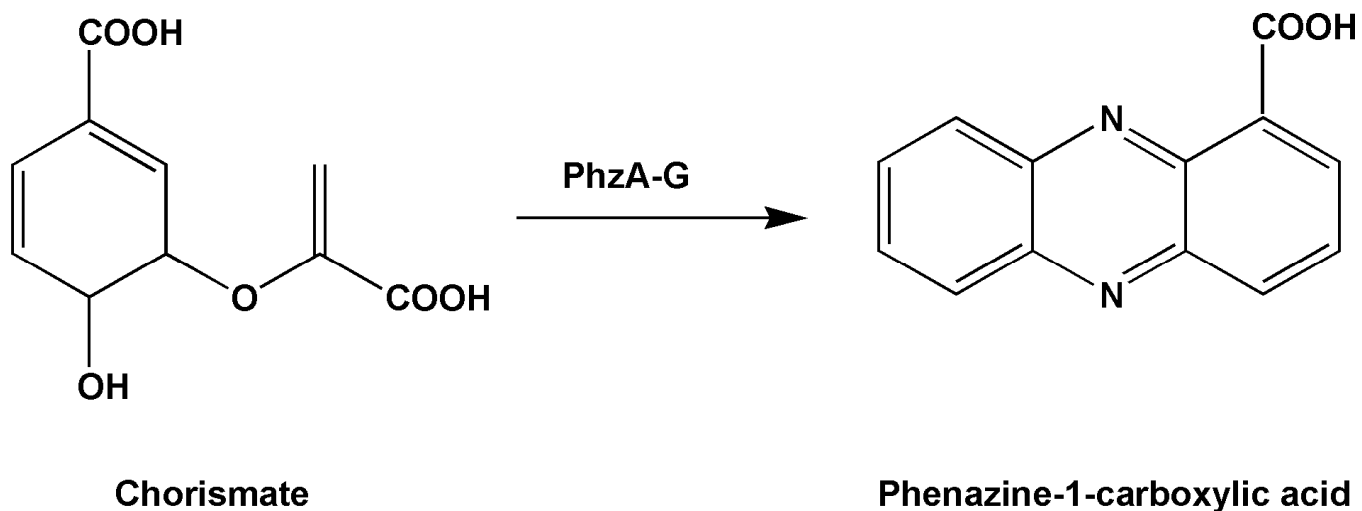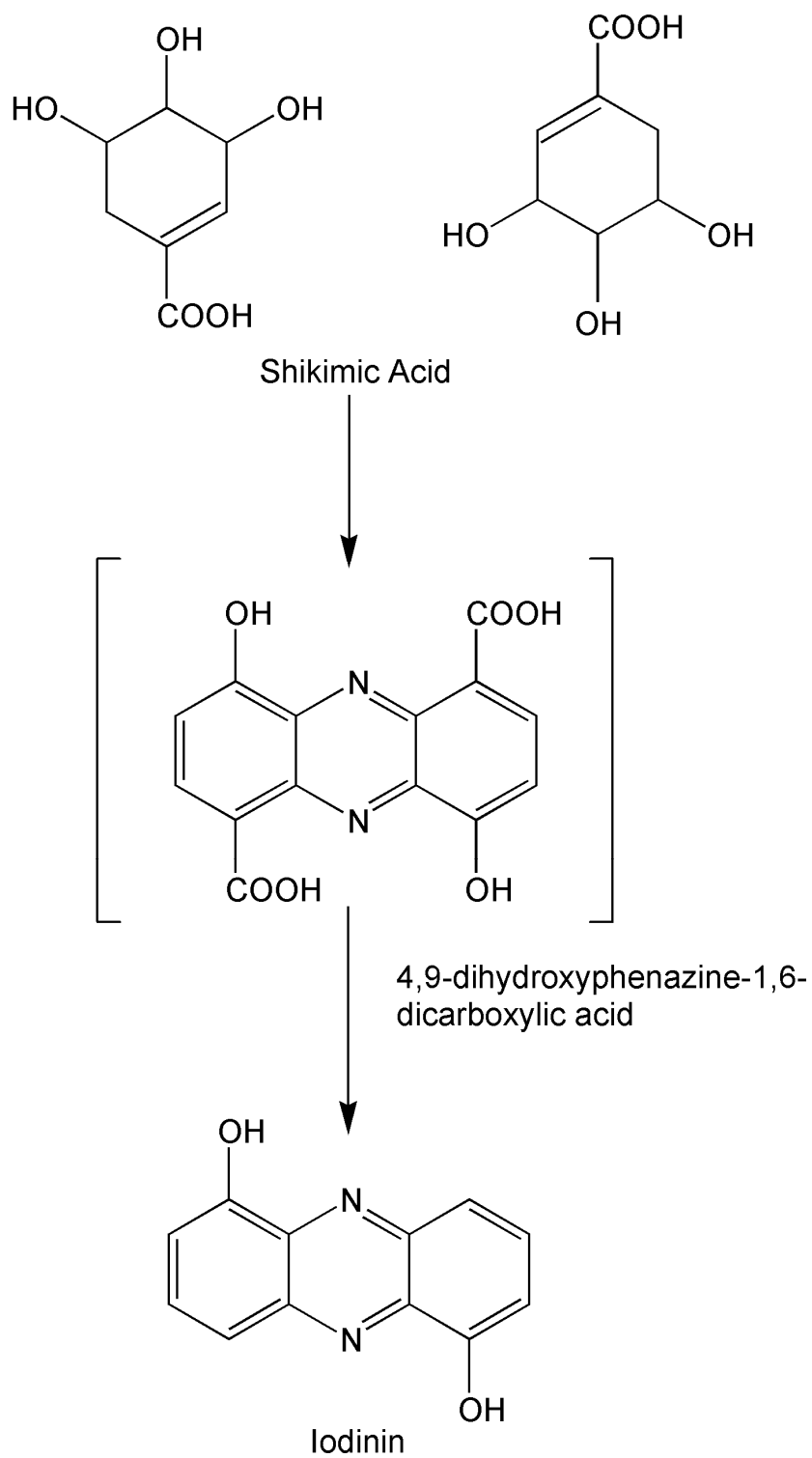
Fig. 1.8 (a)

Fig. 1. 8(a) & (b) The proposed intermediates of the phenazine biosynthesis pathway

1.6. Assembly of the tricyclic phenazine ring scaffold

Initial studies on Iodinin led to the hypothesis that the phenazine moiety was formed by the diagonal, asymmetrical incorporation of two shikimic acid units. 4,9-dihydroxyphenazine-1,6-dicarboxylic acid was hence proposed as the key intermediate in the biosynthesis of all phenazines (69).

The biosynthesis of phenazines has been extensively studied in *Pseudomonas* species, particularly by the groups of Herbert and of Hollstein. The Shikimate origin of the phenazine skeleton in these organisms was amply demonstrated by feeding experiments with labelled precursors. These gave good incorporations of shikimic acid into the phenazine skeleton, they showed that both halves of the phenazine ring are labelled by shikimic acid and they demonstrated the coupling mode shown in Fig. below by which two molecules of shikimic acid are linked to each other to give the phenazine ring system.

2 molecules of shikimic acid   Phenazine ring system
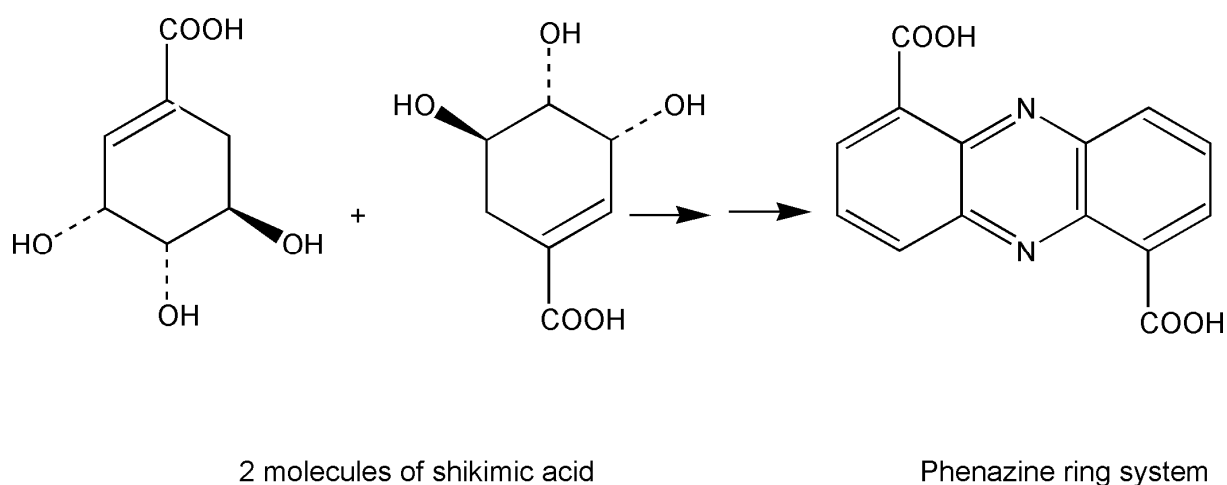
Fig 1.9 Shikimic acid to the phenazine ring system

Meanwhile, search continued for more evidence for chorismic acid being the compound that dimerises to form the phenazine ring system, with anthranilic acid also being considered. The discovery of two sets of anthranilate synthase genes in pyocyanin producing strains of *P. aeruginosa* by Essar *et al.*, (1990) gave some credence to this hypothesis, although all previous attempts to demonstrate incorporation of isotopically labelled anthranilate into phenazine were unsuccessful (70;71). Thus, although the shikimic acid pathway was

accepted as the primary metabolic pathway, which branched off into phenazine biosynthesis, the mechanism of assembly of the tricyclic scaffold of phenazines and identity of the intermediate formed in this process remained unclear.

1.7. Genetic basis of phenazine biosynthesis in *pseudomonads*

Further progress in understanding the phenazine biosynthesis pathway came in 1995, when Pierson and co-workers identified the biosynthetic genes responsible for the production of phenazine in *P. aureofaciens* (72). Soon, a phenazine biosynthesis locus was also identified, cloned and sequenced in *P. fluorescens* (73) and *P. aeruginosa* (74). This locus comprised of a conserved seven-gene operon *phzABCDEFG,* which was found to be sufficient for the production of PCA from chorismic acid. (Fig. 1.9). Both *P. aureofaciens* and *P. fluorescens* contain one, whereas *P. aeruginosa* possesses two copies of the phenazine biosynthesis operon. PCA is the end product of this 'core' phenazine biosynthesis pathway.
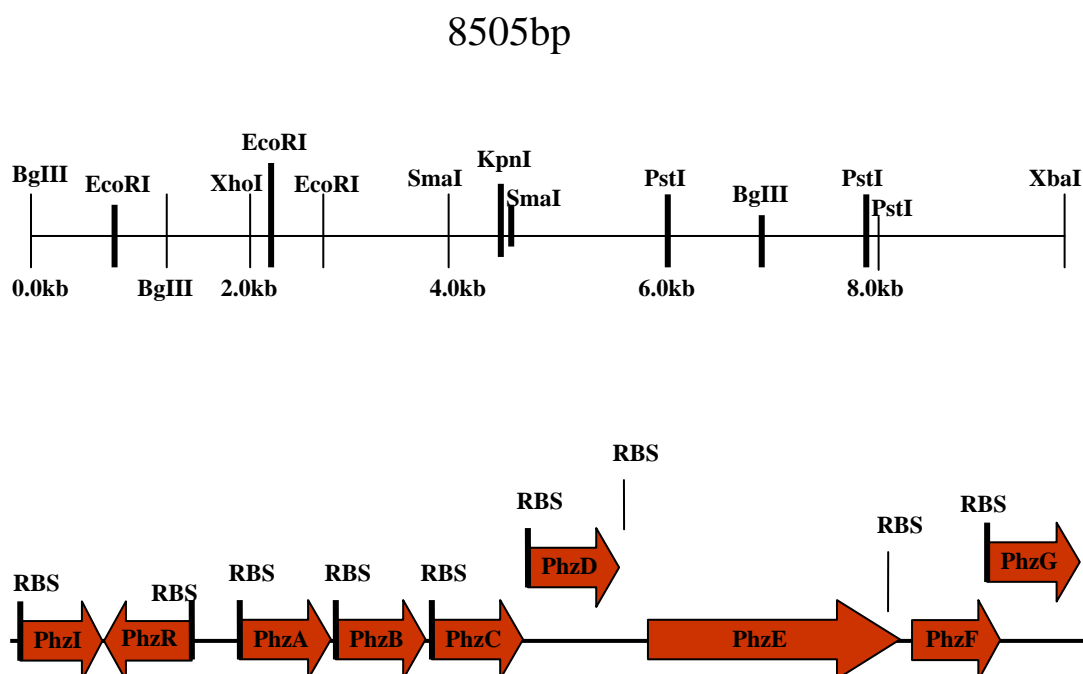
8505bp

Fig. 1.10 Phenazine biosynthesis operon from Pseudomonas fluorescens 2-79

The discovery of this 'core' phenazine biosynthesis operon in *Pseudomonas* led to further investigation into the presence of this operon in other phenazine producing species.

1.7.1. Phenazine biosynthesis in *Pseudomonas*

McDonald *et al*., (2001) expressed all or a subsets of the seven genes of the phenazine biosynthesis operon of *P. fluorescens* in *Escherichia coli*. Feeding experiments were then carried out using exclusively, chorismic acid, anthranilic acid or 2-amino-2-deoxychorismic acid (ADIC), to re-examine the branching point of phenazine biosynthesis from the shikimic acid pathway and the process of phenazine ring assembly.

Their results proved conclusively that chorismic acid was the branching point and that it was converted to 2-amino-2-deoxychorismic acid (ADIC) by the enzyme PhzE. Also, neither anthranilic acid (no conversion to PCA) nor chorismic acid (conversion to ADIC by PhzE, but no PCA formation) were utilised for the assembly of the phenazine scaffold. ADIC however, was completely converted to PCA. Moreover, incubation of ADIC with the enzyme PhzD yielded trans-2,3-dihydro-3-hydroxyanthranilic acid (DHHA) and incubation of DHHA with PhzA-G showed complete conversion to PCA. Both these compounds were thus confirmed as intermediates of phenazine biosynthesis. PDC, the previously hypothesised intermediate, was not detected in these experiments. To further explore the possibility of PDC formation, [11-C13]-labelled PDC was incubated with PhzA-G extract. Less than 1% of this labelled PDC was found to be converted into PCA. Moreover, the incubation of radiolabelled PDC in the presence of radiolabelled ADIC with the same set of enzymes (PhzA-G) yielded no conversion of labelled PDC to PCA. Thus, PDC was ruled out as an intermediate of the phenazine biosynthesis pathway of *P. fluorescens*. Instead, the dimerisation of two molecules of oxidised DHHA was suggested as a possible mode of phenazine scaffold assembly.

These observations were collated and presented in the form of a scheme for the biosynthesis of PCA from chorismic acid by McDonald and co-workers (Fig 1.11), which included the newly identified intermediates and the role of enzymes involved.

1.8. Enzymes of the phenazine biosynthesis operon

While studying the various enzymes involved in the phenazine biosynthesis operon of *P. fluorescens*, McDonald *et al*. compared the sequences of these seven enzymes with proteins of known function. Their results are tabulated in table below.

Protein	Size (amino acids)	Similar Enzymes
PhzA	163	PhzB
PhzB	162	PhzA
PhzC	400	Plant 3 –deoxy-D-arabino-heptulosonate-7-phosophate (DHAP) synthase.
PhzD	207	Bacterial Isochorismate
PhzE	637	Bcterial anthranilate synthase
PhzF	278	Unknown
PhzG	222	Bacterial pyrodoximine 5'-phosphate oxidase

Fig. 1.11 Enzymes similar to those of the phenazine biosynthesis pathway.

There is more than 70% similarity between the genes *phzA* and *B*, which were found to be important for quantitative synthesis, but not essential for the biosynthesis of PCA (74). Both these enzymes however, are conserved in the phenazine biosynthesis operons of all *Pseudomonas* species. The enzymes

PhzA-B were thought to act past the formation of DHHA, but no further information, either structural or biochemical was available, since these enzymes showed no similarity to any enzymes of known function in the NCBI database. Of the rest of the enzymes PhzC, D, E, F and G, which are essential for PCA production, PhzC, D, E and G were found to have counterparts in the bacterial world. PhzC is a 3-deoxy-arabino heptulosonate-7-phosphate (DAHP) synthase and acts more upstream (prior to formation of chorismic acid), ensuring adequate availability of chorismate for phenazine biosynthesis. PhzE, which acts after PhzC, shows similarity to bacterial anthranilate synthase and catalyses the conversion of chorismate to ADIC. This enzyme is followed by PhzD, an Isochorismatase, which catalyses the conversion of ADIC to DHHA. This conclusion was recently confirmed by the crystal structural analysis of PhzD by Parson *et al.*, (2003).
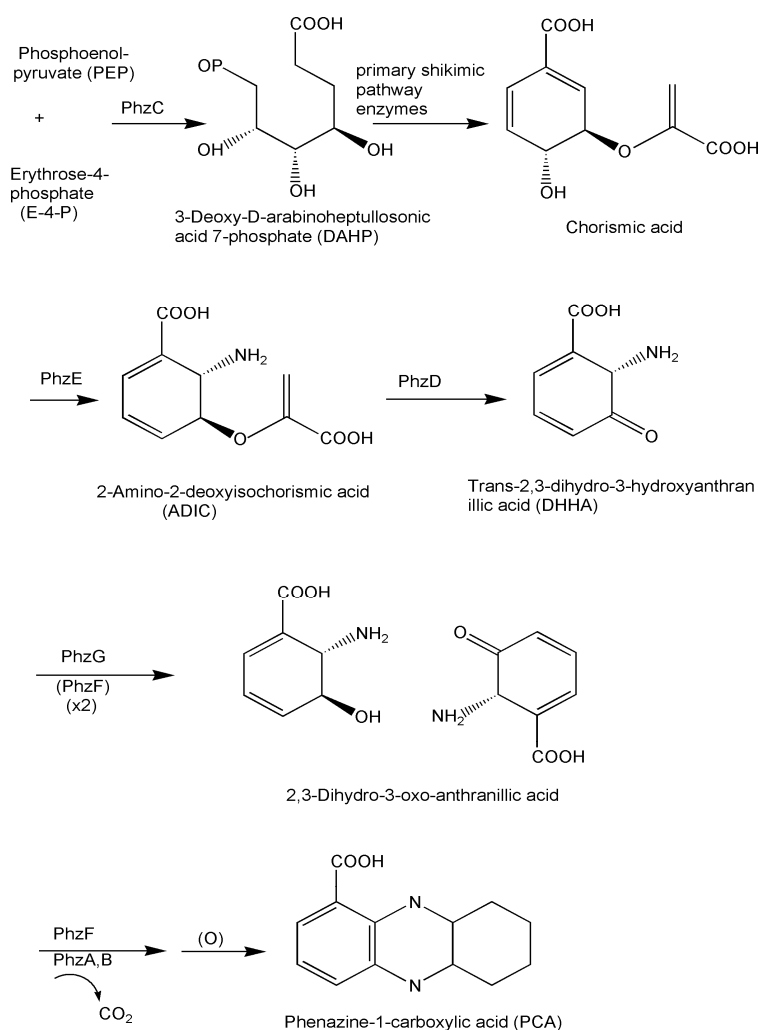
Fig. 1.12 Proposed biosynthetic pathway for PCA in Pseudomonas fluorescens

Thus, the phenazine biosynthetic gene cluster from *P. fluorescens* strain 2-79 (Fig. 1.10) contains 7 genes; of which five (*phz C-G*) are essential and two others (*phzA* and *B*) substantially enhance the level of synthesis of phenazine-1-carboxylic acid (PCA), the phenazine produced by this organism (75). Mc Donald and his coworkers found in their experiments that ADIC is the phenazine precursor.

Recently, Blankenfeldt *et al.*, (2004) shed more light on the mode of action of the homodimeric enzyme PhzF through structural and biochemical analysis. They showed that PhzF acts as an isomerase, converting DHHA to its highly reactive ketone form - 1,2,4-trihydro-3-oxo-anthranilic acid. Blankenfeldt and co-workers also hypothesised that PhzF is an enzyme with dual functions and also catalyses the condensation of two molecules of this ketone to form the phenazine ring scaffold.

Fig. 1.13 Scheme of phenazine biosynthesis modified by Blankenfeldt et al., 2004

The modified scheme proposed by Blankenfeldt *et al* is depicted in the Fig. 1.12. The last of the seven enzymes, PhzG, is similar to bacterial

pyridoxamine-5-oxidase. It was thought to act in steps past the formation of 2,3-dihydro-3-oxo anthranilic acid, but its exact role in PCA biosynthesis could not be deduced. The functions of the enzymes PhzC, D, E and F were thus known or could be accurately surmised (76). However, no such conclusion could be drawn for PhzA, B and G.

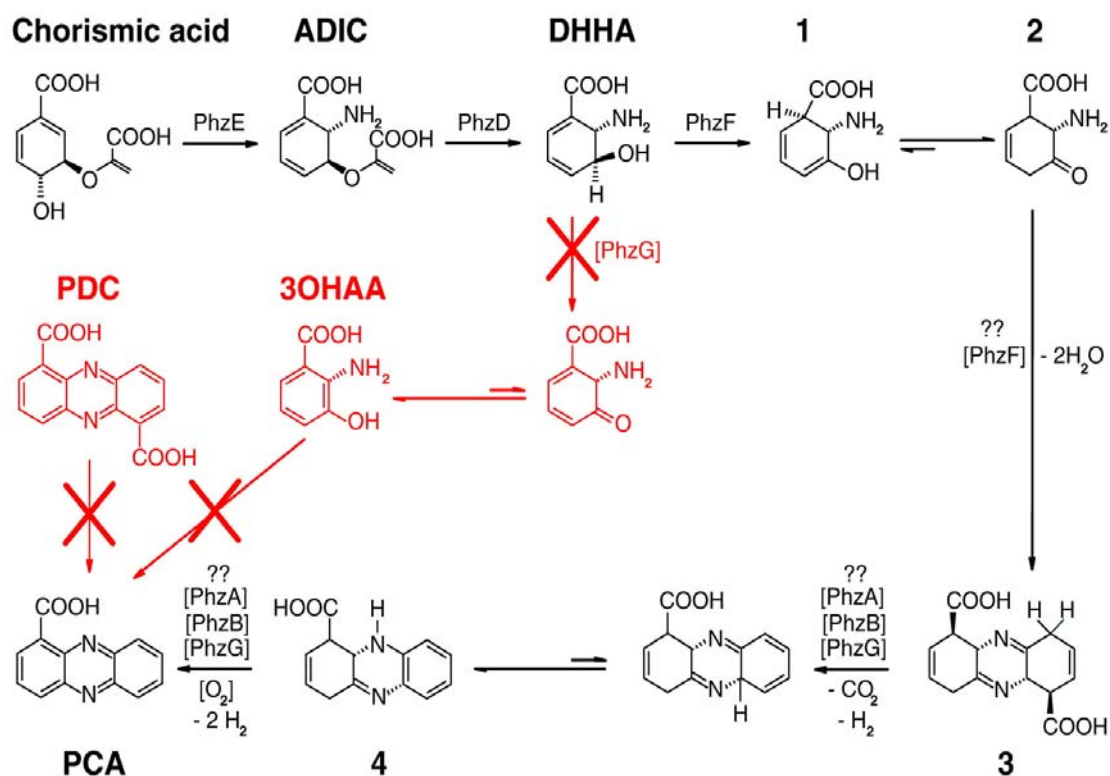As mentioned previously, the end product of core phenazine biosynthesis operon, *phzABCDEFG*, is PCA, which is the only phenazine compound synthesised by *P. fluorescens.* PCA, however is modified to other phenazine derivatives in case of *Pseudomonas* strains like *P. aeruginosa, P. chlororaphis* etc. The genetic basis of generation of phenazine diversity and the organization of phenazine biosynthesis operon in other organisms is described herewith.

1.8.1. Phenazine modifying enzymes

In *Pseudomonas* species., the phenazine biosynthetic pathway branches off from the shikimic acid pathway, which is also the source for metabolites such as the aromatic amino acids, siderophores and quinines (Fig 1.14) (77). Genes encoding the phenazine biosynthetic enzymes are arranged in one core operon, *phzABCDEFG*, in most phenazine producing pseudomonads. Such an operon exists in the genome of *P.aeruginosa* in duplicate, and the expression of the two copies of the operon is differently regulated. In many strains additional genes involved in phenazine decoration, such as *phzM, phzS, phzO* and *phzH*, are present in single copy and can be located proximally to the core operon or elsewhere in the genome; currently, little is known about how these genes are regulated (74;76). This project involves the study of structure and functional relationship of phenazine modifying enzymes encoded by genes *phzM* and *phzS,* which are involved in the biosynthesis of pyocyanin, a virulence factor for humans.
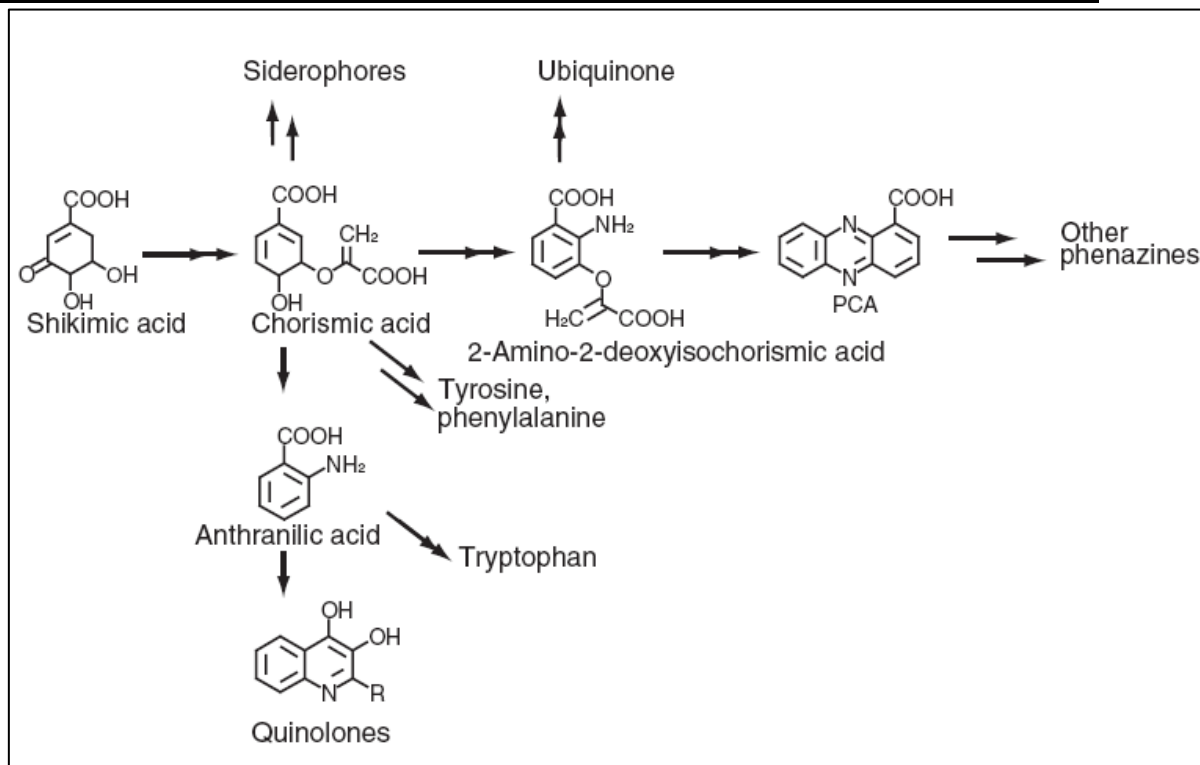
Fig 1.14 Phenazine biosynthesis and its relation to shikimic acid pathway
(Price-Whelan 2006)

PhzM is a predicted 36.4-kDa protein similar to enzymes involved in the methylation of polyketide antibiotics by *Streptomyces* spp. Streptomycetes produce a variety of bioactive polyketides, many of which contain methyl groups introduced via the action of *N*- and *O*-methyltransferases. PhzM most closely resembles *O*-methyltransferases from *Streptomyces* spp. and shares with them a putative catalytic domain (residues 137 to 177) that might be universal among S-Adenosyl methionine or SAM-dependent methyltransferases. The presence of a potential SAM binding site in the N-terminal part of PhzM (residues 67 to 176) further supports the idea that PhzM functions as a methyltransferase (74;78).

The second putative phenazine-modifying gene, *phzS*, is located immediately downstream of *phzA1B1C1D1E1F1G1* and encodes a predicted 43.6-kDa protein similar to putative salicylate hydroxylases from *S. coelicolor* (GenBank accession numbers T36193 and CAB95795), *Bordetella pertussis* (AAC46266), *Acinetobacter* sp. strain ADP1 (AAC27110), and *P. aeruginosa* (AAG06716) and NahW from *P. stutzeri* AN10 (AAD02157). NahW is of particular interest as it is the best-characterized enzyme related to PhzS (74;78;79). According to Bosch *et al.*, *nahW* encodes a flavoprotein

monooxygenase with broad substrate specificity that catalyzes conversion of salicylic acid and its derivatives to catechol. In a detailed sequence analysis of NahW, they identified several conserved motifs present in bacterial salicylate hydroxylases. A sequence comparison of PhzS with NahW and other salicylate hydroxylases revealed that PhzS contains the consensus NADH binding domain (159-DVLVGADGIHSAVR-172), putative N-terminal flavin adenine dinucleotide binding site (11-GAGIGG-16), and substrate active site (303-GRITLLGDAAHLMYPMGANGA-323).

1.8.2. AdoHcy nucleosidase
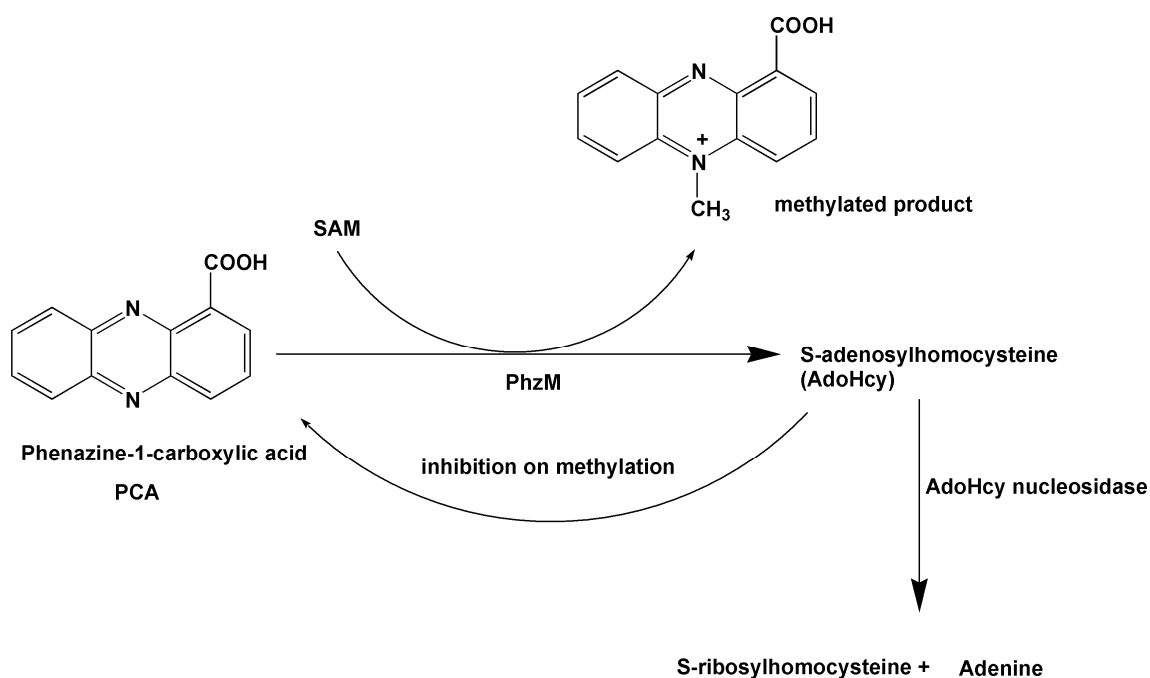
Fig 1.15 Role of AdoHcy nucleosidase

All methyltransferase reactions involve the transfer of the methyl group to a specific substrate with the release of one molecule of S-adenosyl-L-homocysteine (AdoHcy or SAH) (80). In this case PCA is the substrate and SAM transfers one methyl group to PCA and itself gets converted to SAH, the common product of all SAM dependent methyltransferase reactions (81). Under normal physiological conditions, AdoHcy is hydrolyzed to homocysteine (Hcy) and adenosine in a reversible reaction catalyzed by SAH hydrolase.

However, because the equilibrium constant of SAH hydrolase favours SAH synthesis rather than hydrolysis, SAH hydrolysis depends on the efficient removal of homocysteine (Hcy) via remethylation to methionine or degradation to cysteine. However, it has been found that SAH acts as a competitive inhibitor or a potent inhibitor of almost all the SAM dependent methyltransferases (82;83). Thus, SAH removal is essential for the continued transmethylation activity. This is done by an enzyme termed as adenosyl homocysteine (AdoHcy) nucleosidase. This enzyme breaks down AdoHcy to adenine and S-ribosylhomocysteine, thereby preventing the inhibition of the methyltransferase activity (84-86).

1.8.3. Biosynthesis of pyocyanin

Two steps have been suggested to be involved in the synthesis of pyocyanin from phenazine-1-carboxylic acid (PCA), which is the common precursor for many different species-specific phenazines. Theoretically, there can be two reaction strategies by which PCA can be converted to pyocyanin. In the first reaction mechanism, PCA is first acted upon by the enzyme PhzM, an S-adenosyl methionine (SAM) dependent methyltransferase, and gets converted to 5-methylphenazine-1-carboxylic acid betaine by transfer of a methyl group to an N atom of the phenazine-ring moiety. This is followed by the action of the enzyme PhzS, a FAD-dependent monooxygenase, which involves the hydroxylative decarboxylation of 5-methylphenazine-1-carboxylic acid betaine to pyocyanin (74). On the other hand in the other reaction strategy leading to the biosynthesis of pyocyanin, PCA first gets converted to hydroxyphenazine in presence of the enzyme PhzS followed by its methylation to pyocyanin in presence of the SAM dependent methyltransferase, PhzM (Fig. 1.11). Although the role of pyocyanin in *P. aeruginosa* infections is well established, little is known about the enzymes involved in its biosynthesis. As these proteins are potential targets whose inhibition could alleviate the situation of affected patients, we have initiated studies to elucidate their structure–function relationships.
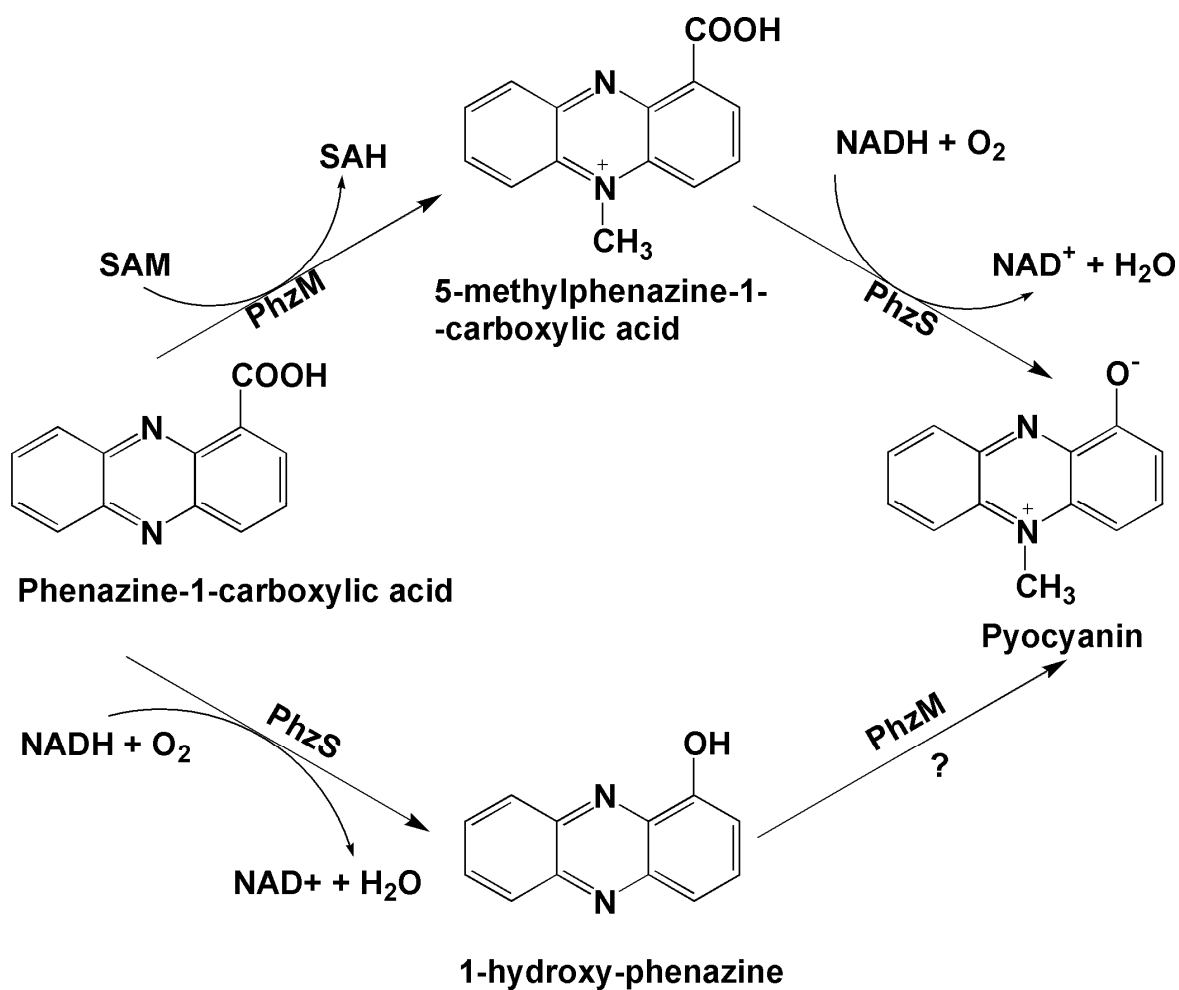
Fig. 1.16 Proposed biosynthetic pathway for pyocyanin

The synthesis of pyocyanin is affected by carbon and nitrogen sources in growth media, but most nutrients support pyocyanin production as long as the phosphate ion concentration is low and there is adequate sulfate ion present. Synthesis of this pigment also appears to be under the control of iron concentration since addition of iron to a medium containing low phosphate stimulates the synthesis of pyocyanin and related phenazine pigments by other species of bacteria (14).

1.9. Regulation of phenazine biosynthesis

The discovery that bacteria are able to communicate with each other changed the general perception of many single, simple organisms inhabiting this world. The mode of communication amongst bacteria are signalling molecules, which are released into the environment. As well as releasing the signalling molecules, bacteria are also able to measure the number (concentration) of the molecules within a population.

The term used for this is quorum sensing which is defined as a phenomenon whereby the accumulation of signalling molecules enables a single cell to sense the number of bacteria (cell density). Quorum sensing was discovered and described over 25 years ago in two luminous marine bacterial species, *Vibrio fischeri* and *Vibrio harveyi*. Quorum sensing is the regulation of gene expression in response to fluctuations in cell-population density. Quorum sensing bacteria produce and release chemical signal molecules called autoinducers that increase in concentration as a function of cell density. The detection of a minimal threshold stimulatory concentration of an autoinducer leads to an alteration in gene expression. Different bacterial species use different molecules to communicate. Gram-positive and Gram-negative bacteria use quorum sensing communication circuits to regulate a diverse array of physiological activities. In general, Gram-negative bacteria use acylated homoserine lactones as autoinducers, and Gram-positive bacteria use processed oligo-peptides to communicate.

In *P. fluorescens*, *P. aureofaciens* and *P. chlororaphis*, two genes, phzI and phzR, located directly upstream to the phenazine biosynthesis operon function as regulators of N-acyl-homoserine lactone mediated gene expression of the 'phz' operon. Thus, these two genes link quorum sensing to phenazine biosynthesis and act as regulating sub-circuit in these Pseudomonas strains. However, this is not the only mode of regulation. As mentioned earlier one of the primary factors governing the phenazine production is population density and in *P.aeruginosa* this dependency is effected by three Quorum sensing systems of which two quorum-sensing (QS) systems that belong to the LuxR/I family have been well characterized.
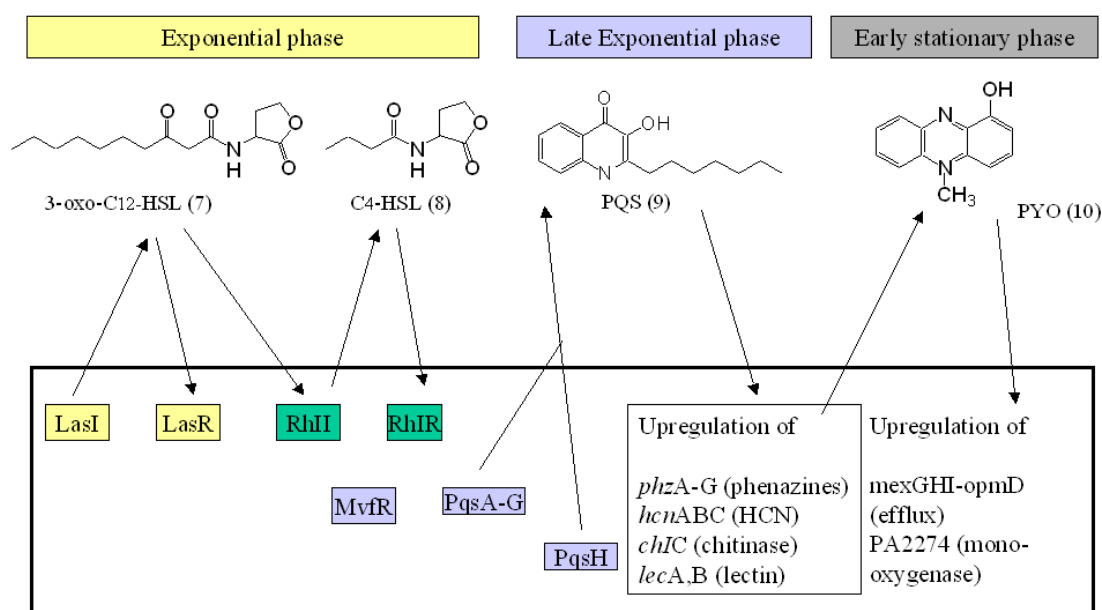
Fig 1.17. Quorum sensing network in Pseudomonas aeruginosa (A.P. Whelan et al 2006)

In *P. aeruginosa*, the genes regulating phenazine biosynthesis are not located upstream of the core biosynthetic pathway, but elsewhere in the genome. In this organism, the expression of phenazine biosynthesis is thought to be regulated in a more complex manner. There are two QS systems in *P. aeruginosa*, which have been extensively studied. The las system consists of the transcriptional activator protein LasR, the acyl-HSL (homo serine lactone) synthase LasI and the acyl homoserine lactone (acyl- HSL) 3O-C12-HSL.The rhl system consists of the regulator RhlR, the synthase RhlI and C4-HSL (9;87).The las and rhl quorum-sensing circuitries operate in a hierarchical cascade responsible for regulating the expression of many virulence determinants, secondary metabolites, the type-II secretion machinery, stationary phase genes and genes involved in biofilm formation (88;89) (Withers *et al* 2001). Recently, a third signal has been found to participate in the *P.aeruginosa* QS network, the quinolone 2-heptyl-3-hydroxyl-4-quinolone that has been named the Pseudomonas quinolone signal (PQS) adds further complexity to the regulatory pathway in *P. aeruginosa* (87;90;91). Till now,

PQS has been thought to be the terminal signal in the *P.aeruginosa* QS cascade but recently Dietrich *et al* in his paper reported that phenazine pyocyanin is a terminal signaling molecule in the *P.aeruginosa* QS network, and suggested that phenazines may, in this capacity, control their own cycling (92). Pyocyanin is both necessary and sufficient to upregulate the expression of a limited set of genes known as the pyocyanin stimulon. As mentioned earlier pyocyanin is a good antimicrobial agent and the fact that it can act as intercellular signals underscores the possibility that secondary metabolites may infact be of primary importance in tuning the cell response to particular physiological states (93). This is a good example where secondary metabolites prove to have functions that transcend their antibiotic activities and enable the coordinated response of microbial communities to changes in their environment. Studying the function and structure relationship of enzymes PhzM and PhzS can help to understand more about the biosynthesis of pyocyanin.

Objectives of this work

As discussed in the earlier section, phenazines are versatile and multi-functional compounds; but relatively little information is available about the biosynthesis of these molecules in nature. A blue, redox active modified phenazine compound called pyocyanin is a virulence factor of the opportunistic human pathogen *P.aeruginosa* even in micro molar concentrations it is toxic to a wide range of bacterial and mammalian cells. Although the role of pyocyanin in *P.aeruginosa* infections is well established, little is known about its biosynthesis and the enzymes involved. Understanding the structure of these two enzymes is needed to design inhibitors, which could be powerful antibacterial agents and thus, can help us tackle the problem of fatal infections caused by phenazine-producing micro-organisms in immuno-compromised individuals.

Although it is known that two enzymes are involved in pyocyanin biosynthesis but the exact mechanism or the pathway leading to its formation is yet to be discovered. The main aim of this project is to better understand reaction pathway involving the two enzymes leading to the formation of the virulence factor pyocyanin. The specific aims of this work encompasses firstly, the over expression, crystallisation and elucidation of the three dimensional structures of the enzymes PhzM and PhzS from *P.aeruginosa* to discover the role played by these enzymes. In addition, this project intends to investigate the exact mechanism of pyocyanin biosynthesis to establish the identity of the substrates and products of the various enzymes as well as the intermediates formed during the production of pyocyanin by using some biochemical and mass spectroscopic methods.

MATERIALS AND METHODS

3.1 Materials

3.1.1 Chemicals

Chemicals from the following companies were used:

Amersham-Pharmacia (Freiburg), Baker (Deventer Holland), Fluka (Neu-Ulm), GERBU (Gaiberg), Merck (Darmstadt), Pharma-Waldhof (Düsseldorf), Qiagen (Hilden), Roche (Mannheim), Roth (Karlsruhe), Serva (Heidelberg), and Sigma-Aldrich (Deisenhofen).

3.1.2 Materials

Sterile Filter FP 030/3 0.2 µm (Schleicher and Schuell , Dassel)

Ultrafiltration device VIVASPIN 10, 30 (Vivascience; Lincoln USA)

0.2 µM and 0.45 µM sterile filters (Schleicher and Schuell)

HiTrap Chelating affinity column HP 5 ml (Amersham Biosciences)

Superdex 75 and 200 (Amershem Pharmacia, Freiburg)

Limbro 24 flat bottom well tissue culture plates (ICN Biomedicals Inc, Ohio)

Garnier TM 96 well flat bottom sitting drop crystallization plates.

3.1.3 Kits

QIAprep Spin Miniprep Kit   Qiagen

QIAquick Gel Extraction Kit   Qiagen

Perfect 1kb-DNA standard   Invitrogen (Karlsruhe)

Wide Range, SDS7 protein marker   Sigma (Deisenhofen)

1kb ladder for Agarose Gels   Gibco

Crystal Screen, 2TM, Index Screen TM   Hampton Research,

Nextal Classic, PEG ion   Nextal

An ÄKTA Prime FPLC machine (Pharmacia) was used throughout for chromatography.

3.1.4 Microorganisms

E. coli BL21 (DE3) B, F-, hsdSB (rB-, mB-), gal, dcm, ompT, λ (DE3) (Novagen)

E. coli BL21 (DE3) F– ompT hsdSB(rB– mB–) gal dcm (DE3) pRARE2 (CmR)

E. coli Rosetta (Novagen) pRARE containing the tRNA genes argU, argW, ileX, glyT, leuW, proL, metT, thrT, tyrU, and thru

3.1.5 Plasmid Vectors

pET15b(Novagen). pET15b is a plasmid containing the 6x Histidine sequence for use in Nickel chromatography for protein purification. It carries an N-terminal His-Tag sequence followed by a thrombin site and three cloning sites.

3.1.6 Media and Antibiotics*:*

Luria-Bertani (LB) medium : 10 g/l Bacto-Tryptone, 10 g/l NaCl, 5 mM NaOH, 5 g/l yeast extract.

Terrific Broth (TB) medium: 12 g/l Bacto-Tryptone, 24 g/l Bacto-yeast-extract, 4 g/l glycerol, 17 mM KH_2PO_4, 72 mM K_2HPO_4.

GYT medium: 10g/L glucose, 1g/L Yeast extract, 2g/L Tryptose, 1mg $FeSO_4$, 20g/L Agar.

TSS medium: 10% PEG8000, 5% DMSO, 50mM $MgCl_2$ in LB medium and pH adjusted to 6.5.

SeMet Medium**:** The medium was prepared according to (94). It is a minimal medium excluding methionine but containing high concentrations (250 mg/l) of the amino acids V, L, I, K, T, F and 50 mg/ml of the other amino acids to aid suppression of bacterial methionine biosynthesis.

Antibiotics from GERBU (Gaiberg) were used at the concentration 100 mg/l for ampicillin and 34 mg/l for chloramphenicol.

3.1.7 Buffers

Method	Buffers Used
Nickel Affinity Chromatography	Buffer A: 50mM Na_2HPO_4, 300mM NaCl pH8.0 Buffer B: Buffer A + 1M Imidazole
Gel Filtration Chromatography	20mM Tris/HCl, 150mM NaCl pH 8.0
SDS sample buffer	50mM Tris, pH = 8.9 100mM DTT 2% (w/v) SDS 0.25% (w/v) Bromophenol blue 10% Glycerin
SDS running buffer	25mM Tris, pH = 8.3 192mM Glycine 0.1% (w/v) SDS
ITC measurements	20mM Tris/HCl, 150mM NaCl pH 8.0
HPLC measurements	Buffer A: Water + 0.1% TFA Buffer B: TFA + 0.1% CH_3CN

Buffers were prepared in sterile water and degassed before being used.

3.2 COMPETENT CELLS AND TRANSFORMATION

Sterile media and solutions were chilled prior to use unless otherwise indicated.

Competent cells for protein expression (Rosetta pLysS) or plasmid amplification (XL1-Blue) were prepared as follows:

Electrocompetent cells were prepared by inoculating a single colony *Escherichia coli* cells in 100 ml Luria Broth (LB) medium and grown overnight at 37ºC under continuous shaking. The next day, 5 ml preculture were diluted with 500 ml LB medium and grown further to optical density OD_{600} = 0.6. The cells were harvested by centrifugation at 3000xg for 15 minutes. The pellet was washed with 500 ml sterile H_2O at 4ºC twice. The pellet was then resuspended in 10 ml 10% glycerol (4ºC) and recentrifuged. The resulting cell pellet was finally resuspended in approximately 2.5 ml GYT media (4ºC) and aliquoted into 75 µl portions flash frozen in liquid nitrogen and stored at -80ºC till further use.

Heat shock competent cells were prepared by growing the cells in 30 ml of LB medium at 37ºC with continuous shaking. Next day the overnight culture was then inoculated with 100 ml of LB starting with an OD_{600} of 0.2-0.3. The cells were grown at 37ºC to an OD_{600} of 0.7-0.8. The growth was stopped by putting the culture on ice. The cells were then centrifuged in 50 ml falcon tubes at 2000 rpm for 15 mins at 4ºC. The resulting cell pellet was finally resuspended in approximately 2.5 ml TSS media (4ºC) and aliquoted into 100 µl portions flash frozen in liquid nitrogen and stored at -80ºC till further use.

3.2.1 Transformation by heat shock

100 µl of the competent cell were incubated with approximately 1 ng of DNA on ice for 30 mins. After this the cells were subjected to heat shock treatment by placing them at 42ºC for 90 mins. This opens up the cell walls for the introduction of the plasmid DNA. This is followed by transferring the cells on ice for 5mins. The cells are then transferred to 1ml of LB medium and allowed to incubate at 37ºC while shaking. The cells are centrifuged carefully discarding 900 µl supernatant; the bacteria were resuspended and plated on an agar selection medium containing the appropriate antibiotic.

3.2.2 Transformation by electroporation

50 µl of the competent cells were incubated with approximately 100 ng of DNA in a dry and previously chilled electrocompetent cuvette and then transformed using a transformation apparatus controlled at a voltage of 2.5 kV. The cells were then transferred to 1 ml of LB medium and were grown at 37ºC for 1 hr. The cells were then centrifuged carefully discarding 900 µl supernatant; the bacteria were resuspended and plated on an agar selection medium containing the appropriate antibiotic.

3.3 PROTEIN OVEREXPRESSION AND PURIFICATION

3.3.1 Protein Expression

The proteins were expressed in *E.coli* strain Rosetta pLysS (DE3) (Novagen). An overnight culture from a single colony was grown and diluted the next morning with fresh medium suspended with 100 mg/l ampicillin and 34 mg/l chloramphenicol. The cells were grown at 37ºC with vigorous shaking until an OD_{600} = 0.6. Protein expression was induced using 1mM isopropyl-ß-D-thiogalactoside (IPTG) for 3 hours at 37ºC. The cells were harvested by centrifugation for 15 minutes at 6000×g. When not immediately used for protein purification, the pellets were flash frozen and stored at -80ºC.

3.3.2 Protein Purification

The cell pellet was resuspended in Buffer A containing 1 mM protease inhibitor PMSF (Phenylmethylsulfonyl fluoride, protease inhibitor). The cells were lysed in a microfluidizer (model 110S, Microfluidics Cooperation, USA). The lysate was then ultracentrifuged at 150000×g (Beckman ultracentrifuge model Optima L-70K, rotor Ti45) for 45 minutes and the resulting supernatant was filtered through a 0.2 µm filter. The supernatant was loaded onto a nickel-chelation column (Hi-Trap Chelating, Qiagen), equilibrated in Buffer A on an Äkta Prime FPLC system (Pharmacia). The column was washed with 6-8 column volumes of Buffer A containing 2% Buffer B after which the bound protein was eluted in an imidazole gradient of 2 to 100% Buffer B. The

fractions containing the desired protein were identified by SDS-PAGE and pooled.

3.3.3 SDS-PAGE

Separation of proteins of different molecular weight was performed according to Laemmli (*Nature 227, 1970*) using denaturing 15% SDS-polyacrylamide gel electrophoresis (SDS-PAGE) (95;96). The running gel was composed of 15% acrylamide, 0.4% bisacrylamide, 0.1% (w/v) SDS and 375 mM Tris, pH 8.8. The polymerisation of the gel material was initiated by adding 14 µM/µl N,N,N,N-Tetramethyl-Ethylenediamine (TEMED) and 0.5 mg/ml ammonium persulphate (APS). The gel was casted by pouring it into the casting chamber and covering it with isopropanol/water 1:1. After polymerisation, the isopropanol/water mixture was replaced by the stacking gel composed of 5% acrylamide, 0.13% bisacrylamide, 0.1% (w/v) SDS, 125 mM Tris, pH 6.8, 14 µM/µl TEMED and 0.5% mg/ml APS. Prior to application on the gel, the protein samples were denatured by incubation for 2 mins at 95ºC in SDS sample buffer. The protein molecular weight marker (LMW-Standard, Amersham Biosciences) was composed of protein phosphorlylase b (97 kDa), albumin (67 kDa), ovalbumin (43 kDa), carboanhydrase (30 kDa), trypsin inhibitor (20.1 kDa) and lysozyme (14.4 kDa). The electrophoresis took place at 60 mA in SDS running buffer. The gels were stained with a Commasie Blue solution and then destained with destaining solution containing 5% Ethanol and 10% Acetic Acid to display the protein bands.

3.3.4 Size exclusion chromatography

The fractions collected from the affinity chromatography column were collected and dialysed overnight at 4ºC against dialysis buffer to remove imidazole. The dialysed protein sample was then concentrated and subjected to the final step of purification involving gel filtration. This purification was carried out in a Superdex G75/200 HR 26/60 column (Amersham Pharmacia Biotech), which was pre-equilibrated with the gel filtration buffer. The concentrated protein was injected and FPLC was then carried out at a flow-

rate of 2 ml/min and 4 ml fractions were collected. The protein fractions were analyzed with SDS PAGE.

3.3.5 Determination of protein concentration

Protein concentration was determined according to Bradford (1976) using the Biorad protein assay solution. This solution was calibrated prior to use by Bovine Serum Albumin (BSA).

3.3.6 Final concentration and storage of protein

Finally, the purified protein was concentrated using an Amicon chamber with the respective cut off membrane. The concentrated protein was then aliquoted to 30-50 μl fractions, flash frozen and stored at -80ºC.

3.3.7 Seleno-L-methionine labelled protein

The preparation of selenomethionine- labelled proteins has become a fundamental part of many crystallographic studies. For the purpose of structural solution using SAD (Single-wavelength Anomalous Diffraction)/MAD (Multi-wavelength Anomalous Diffraction), inhibition of methionine biosynthesis in synthetic media (Doublie, 1978) was undertaken to incorporate seleno-L-methionine in the protein (97). Proteins labelled with selenomethionine are useful for determining structures of proteins by X-ray crystallography. *E.coli* Rosetta pLysS cells bearing the pET-15b plasmid incorporating 6xHis-tagged protein were grown overnight in LB media supplemented with ampicillin and chloramphenicol. The cells were then pelleted and resuspended in SeMet media containing 50 μg/ml ampicillin and 17 μg/ml chloramphenicol. This culture was grown at 37ºC to OD_{600} of 0.8 and the amino acids lysine, phenylalanine and threonine (100 mg/L) and isoleucine, leucine and valine (50 mg/L) were added. The culture was then supplemented with 60 mg/L seleno-L-methionine and allowed to cool to 20ºC before induction with 1mM IPTG and incubated at 20ºC overnight, with continuous shaking. The protein purification protocol remained identical to that

for the native protein. Incorporation of selenium was confirmed by MALDI-TOF mass spectrometry.

3.3.8 High Pressure Liquid Chromatography (HPLC)

The HPLC separations were run under the following conditions: A gilent 1100HPLC equipped with degasser, auto-sampler, two binary pumps, diode array detector connected on-line to a Finnigan LCQ Advantage mass spectrometer; C18 Atlantis column; flow rate 1 ml/min; solvent A: 0.1 % formic acid in water, solvent B 0.1 % formic acid in acetonitrile; gradient: 0-1 min 0 % B, 1-15 min 0-50 % B 15-25 min 50-100 % B, re-equilibration of the column in 5 min; positive ion mode detection.

3.4 Methods for protein analysis

3.4.1 Isothermal Titration Calorimetry (ITC)

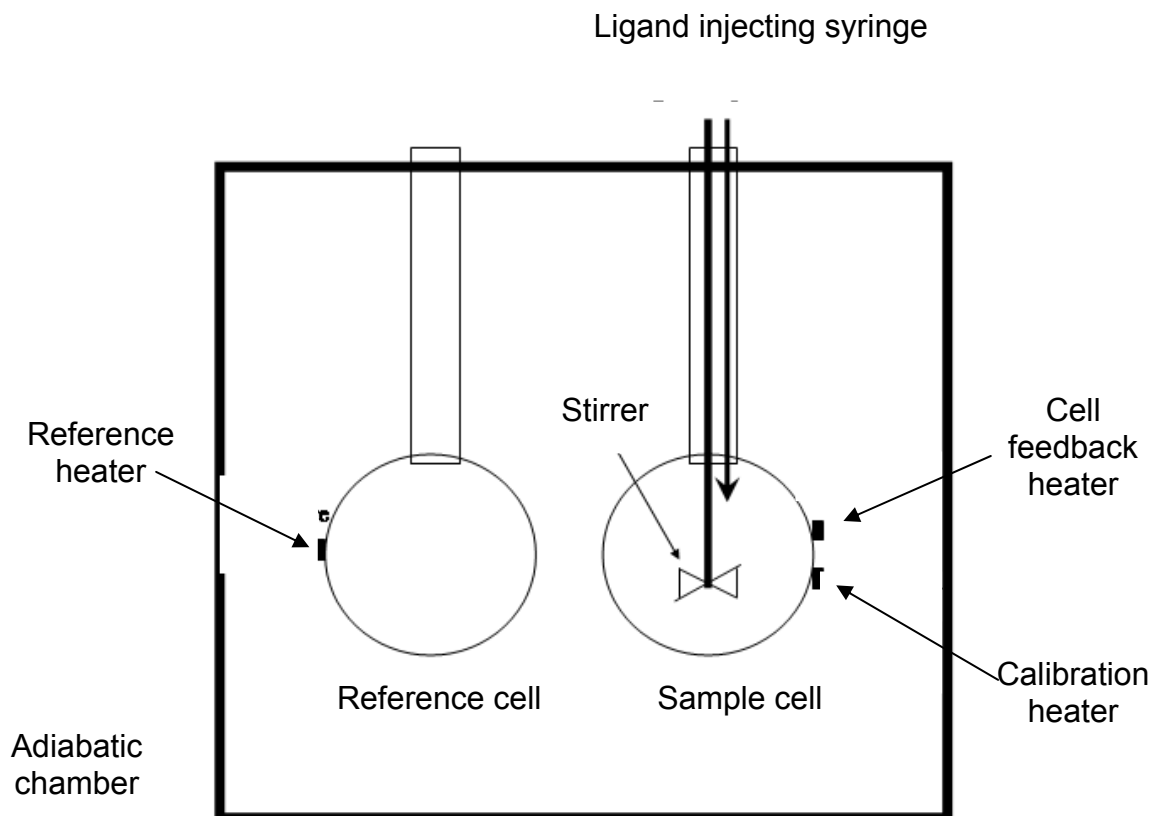Isothermal Titration Calorimetry (ITC) is a biophysical technique used to

Fig 2.1 Schematic of an ITC instrument

determine the thermodynamic parameters of interactions between ligands such as proteins and peptides, or proteins and other ligands (e.g. lipid heads groups). In other words Isothermal Titration Calorimetry is a thermodynamic technique for monitoring any chemical reaction initiated by the addition of a binding component, and has become the method of choice for characterizing biomolecular interactions. Measurement of this heat allows accurate determination of binding constants (K_B), reaction stoichiometry (n), enthalpy (ΔH) and entropy (ΔS), thereby providing a complete thermodynamic profile of the molecular interaction in a single experiment.

The entropy change (ΔS) of binding is calculated from ΔH and K_B

$$\Delta G = -RT\ln K_B = \Delta H - T\,\Delta S$$

Where, G is Gibbs free energy, R is gas constant, T is absolute temperature.

An ITC instrument consists of two identical cells composed of a highly efficient thermal conducting material such as Hastelloy alloy or gold, surrounded by an adiabatic jacket (Figure 2.1) The jacket is usually cooled by a circulating water bath. Sensitive thermopile/thermocouple circuits detect temperature differences between the two cells and between the cells and the jacket. Heaters located on both cells and the jackets are activated when necessary to maintain identical temperatures between all components.

In an ITC experiment, the macromolecule solution is placed in the sample cell. The reference cell contains buffer or water minus the macromolecule. Prior to the injection of the titrant, a constant power (1 mW) is applied to the reference cell. This signal directs the feedback circuit to activate the heater located on the sample cell. This represents the baseline signal. The direct observable measured in an ITC experiment is the time-dependent input of power required to maintain equal temperatures in the sample and reference cell. During the injection of the titrant into the sample cell, the two materials (macromolecule and ligand) interact and heat is taken up or evolved depending on whether the macromolecular association reaction is endothermic or exothermic. For an exothermic reaction, the temperature in the sample cell will increase, and the

feedback power will be deactivated to maintain equal temperatures between the two cells. For endothermic reactions the reverse will occur, meaning the feedback circuit will increase power to the sample cell to maintain the temperature. As the macromolecule in the cell becomes saturated with ligand, the heat signal diminishes until only background heat of dilution is observed.
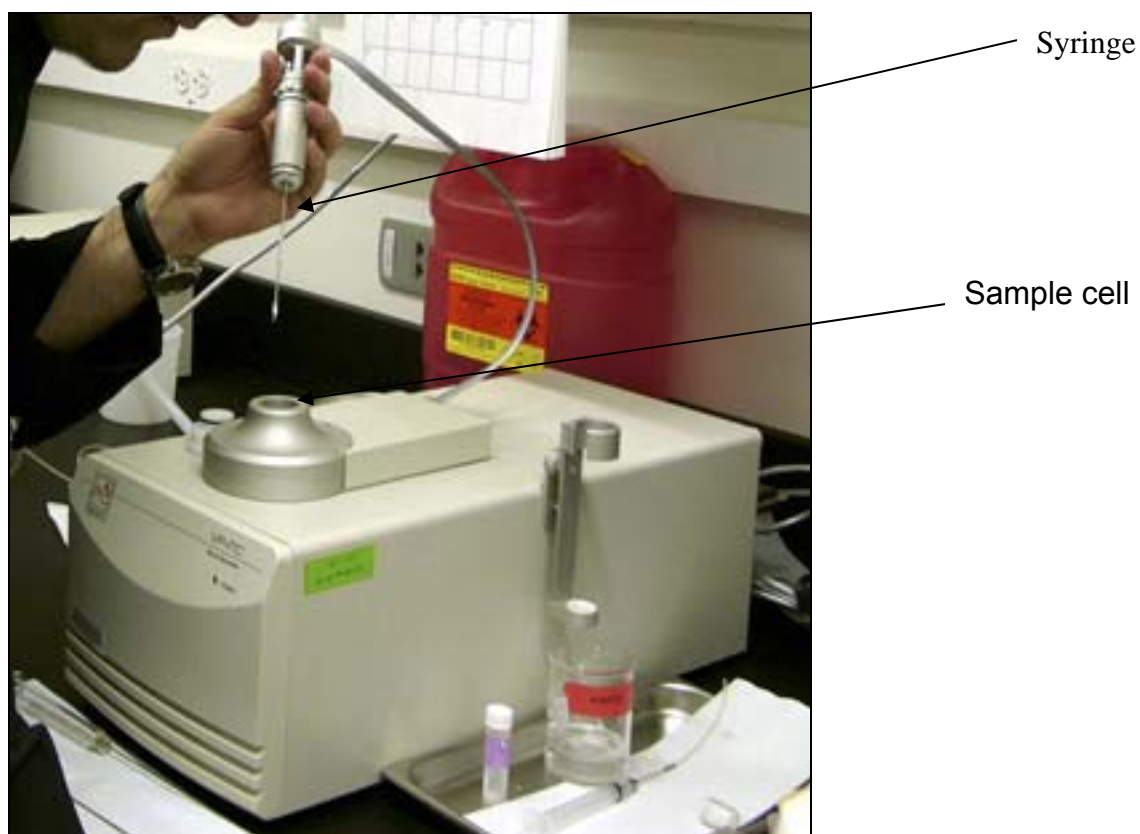
Fig 2.2 MicroCal Isothermal Titration Calorimeter

3.4.2 Mass Spectrometry

Mass spectrometry is an analytical technique used for measuring the Molecular Weight (Mw) of samples. Mass spectrometers use the difference in mass-to-charge ratio (m/z) of ionized atoms or molecules to separate them from each other. Mass spectrometry is therefore useful for quantitation of atoms or molecules and also for determining chemical and structural information about molecules. Molecules have distinctive fragmentation patterns that provide structural information to identify structural components. Mass spectrometers can be divided into three fundamental parts, namely the ionisation source, the analyser, and the detector.

3.4.2.1 HPLC-APCI-MS

An important enhancement to the mass resolving and determining capacity of mass spectrometry is the combination of mass spectrometry with analysis techniques that resolve mixtures of compounds in a sample based on other characteristics before introduction into the mass spectrometer. One effective method or way to determine small amount of substance is to combine or couple these two different analytical methods. Mass Spectrometry (MS) combined with the separation power of chromatography has revolutionised the way we do chemical analysis today. Here we have coupled High Performance Liquid Chromatography (HPLC) with Mass Spectrometry. High performance liquid chromatography mass spectrometry is an extremely versatile instrumental technique whose roots lie in the application of more traditional liquid chromatography to theories and instrumentation that were originally developed for gas chromatography (GC). As the name suggests the instrumentation comprises a high performance liquid chromatograph (HPLC) attached, via a suitable interface, to a mass spectrometer (MS) (Figure 2.3). The primary advantage HPLC/MS has over GC/MS is that it is capable of analysing a much wider range of components. Compounds that are thermally labile exhibit high polarity or have a high molecular mass can all be analysed using HPLC/MS, even proteins are routinely analysed using HPLC/MS. Solutions derived from samples of interest are injected onto an HPLC column that comprises a narrow stainless steel tube (usually 150 mm length and 2 mm internal diameter, or smaller) packed with fine, chemically modified silica particles. Compounds are separated on the basis of their relative interaction with the chemical coating of these particles (stationary phase) and the solvent eluting through the column (mobile phase). Components eluting from the chromatographic column are then introduced to the mass spectrometer via a specialised interface. The two most common interfaces used for HPLC/MS are the electrospray ionisation and the atmospheric pressure chemical ionisation (APCI) interfaces. In this case we have used the later for the analysis.

Fig 2.3 A HPLC-APCI mass spectrometer

3.4.2.1.1 HPLC

High-performance liquid chromatography or High-pressure liquid chromatography is an analytical chromatographic technique used to separate components of a mixture by using a variety of chemical interactions between the substance being analyzed (analyte) and the chromatography column. The basic operating principle of HPLC is to force the analyte through a column of the stationary phase (usually a tube packed with small spherical particles with a certain surface chemistry) by pumping a liquid (mobile phase) at high pressure through the column. The sample to be analyzed is introduced in small volume to the stream of mobile phase and is retarded by specific chemical or physical interactions with the stationary phase as it traverses the length of the column. The amount of retardation depends on the nature of the analyte, stationary phase and mobile phase composition. The time at which a specific analyte elutes (comes out of the end of the column) is called the retention time and is considered a reasonably unique identifying characteristic of a given analyte.

3.4.2.1.2 APCI or Atmospheric Pressure Chemical Ionisation

Atmospheric Pressure Chemical Ionisation or APCI produces ions using a reagent gas generated from solvent vapour. The solvents are solvent A containing 0.1% formic acid in water and solvent B containing 0.1% formic acid in acetonitrile and the flow rate used was 1 ml/min. Liquid spray is produced by passing co-axial nebuliser gas (nitrogen) over the tip of a fused silica capillary, housed within the probe. The solvent spray is vaporised by a heater coil at 400°C. Once formed, the vapour is ionised by a strong electric field emanating from a corona pin held at 3 kV (Figure 2.4).
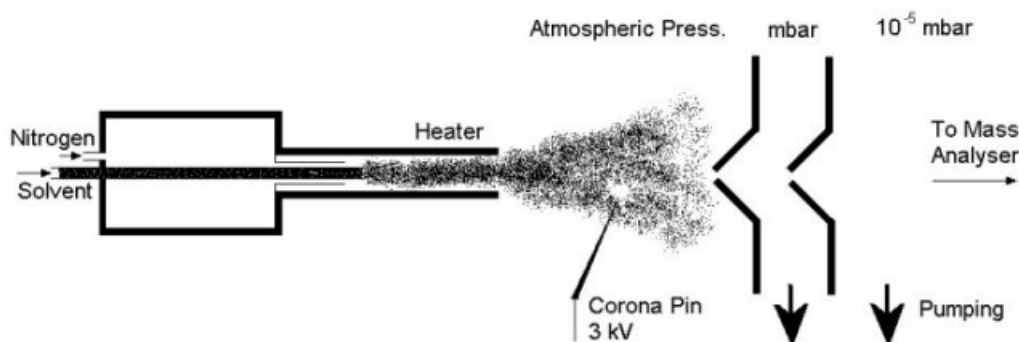
Fig 2.4 Atmospheric Pressure Chemical Ionisation

Atmospheric pressure chemical ionisation (APCI) is an analogous ionisation method to chemical ionisation (CI) and has its primary applications in the areas of ionisation of low mass compounds (APCI is not suitable for the analysis of thermally labile compounds). In ESI, ionisation is brought about through the potential difference between the spray needle and the source-sampling cone along with rapid but gentle desolvation. In APCI, the analyte solution is introduced into a pneumatic nebulizer and desolvated in a heated quartz tube before interacting with the corona discharge creating ions. The corona discharge replaces the electron filament in CI - the atmospheric pressure would quickly "burn out" any filaments - and produces primary $N2^{\circ+}$ and $N4^{\circ+}$ by electron ionisation. These primary ions collide with the vaporized solvent molecules to form secondary reactant gas ions. These reactant gas ions then undergo repeated collisions with the analyte resulting in the formation of analyte ions. The high frequency of collisions results in a high

ionisation efficiency and thermalisation of the analyte ions. This results in spectra of predominantly molecular species and adduct ions with very little fragmentation. Once the ions are formed, they enter the pumping and focussing stage in much the same as ESI (Figure 2.5).
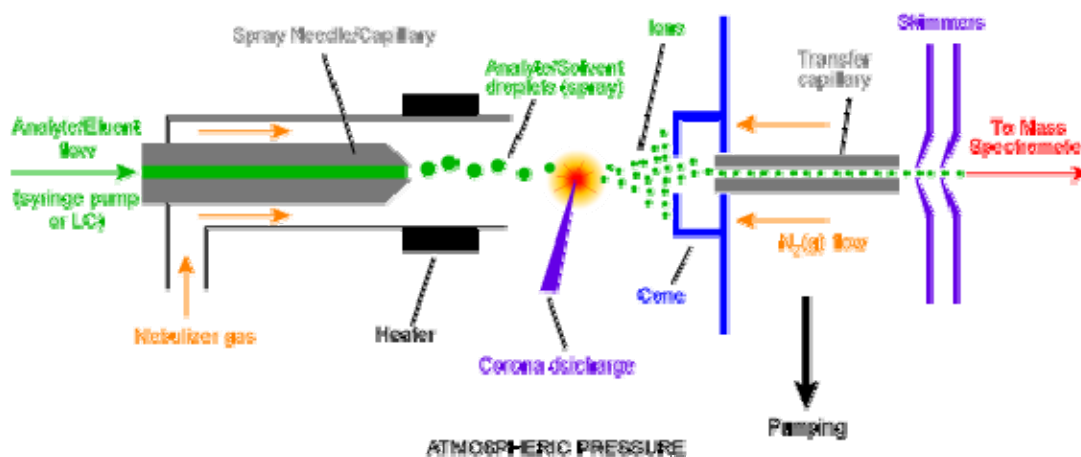

Fig 2.5 A schematic of the components of an APCI source
(http://www.bris.ac.uk/nerclsmsf/techniques/hplcms.html)

3.4.2.1.3 Reaction Mixture for HPLC-APCI-MS

To monitor the reaction catalysed by enzymes PhzM and PhzS and to detect the intermediates that were formed, various combinations of the reaction mixtures (as mentioned in the table below) were prepared. Samples were prepared in 50 mM Tris Buffer (pH 7.5) containing 10µM of the marker molecule caffeine. The inclusion of caffeine allowed a comparison of the various spectra obtained during the course of this work. Buffers used for the whole reaction were Buffer A containing H_2O and 0.1% HCOOH and Buffer B containing ACN and 0.1% HCOOH. In a glass vial (Agilent Technologies) 100 µM of the substrate in Tris buffered (50 mM; pH 7.5) solution was prepared and 1.0 µl of this solution injected directly into the spectrometer and analysed to get a time zero (t=0; blank reading). After this, the enzymes along with the respective cofactors were added to initiate the reaction. A spectrum was recorded every 10 mins for a period of approximately 150-200 mins. Manufacturer's software 'Xcalibur' (Voyager Mass Spectroscopy Systems)

was used for data analysis and Excel (Microsoft) for representation of the data.

Substrate (100 µM)	Cosubstrate (1mM)	Enzyme (10 µM)	Reducing agent
PCA	SAM	PhzM	TCEP
1-oh-phz	NADH	PhzS	DTT
	NADPH	AdoHcy	$Na_2S_2O_4$ (1mM, 5mM)

3.4.3 UV-VIS SPECTROSCOPY

UV-Visible spectroscopy is the measurement of the wavelength and intensity of absorption of near-ultraviolet and visible light by a sample. The absorption of visible light is what makes things coloured. For example, the oxidized form of pyocyanin appears blue because the light at the red end of the spectrum is absorbed. This leaves the blue light to be reflected to the observer's eye. This principle is used to determine the effect in the quantity of pyocyanin formed in the presence or absence of AdoHcy nucleosidase.

The basic parts of a spectrophotometer are a light source (often an incandescent bulb for the visible wavelengths, or a deuterium arc lamp in the ultraviolet), a holder for the sample, a diffraction grating or monochromator to separate the different wavelengths of light, and a detector (Figure 2.6). The detector is typically a photodiode or a CCD. Photodiodes are used with monochromators, which filter the light so that only light of a single wavelength reaches the detector. Diffraction gratings are used with CCDs, which collects light of different wavelengths on different pixels.
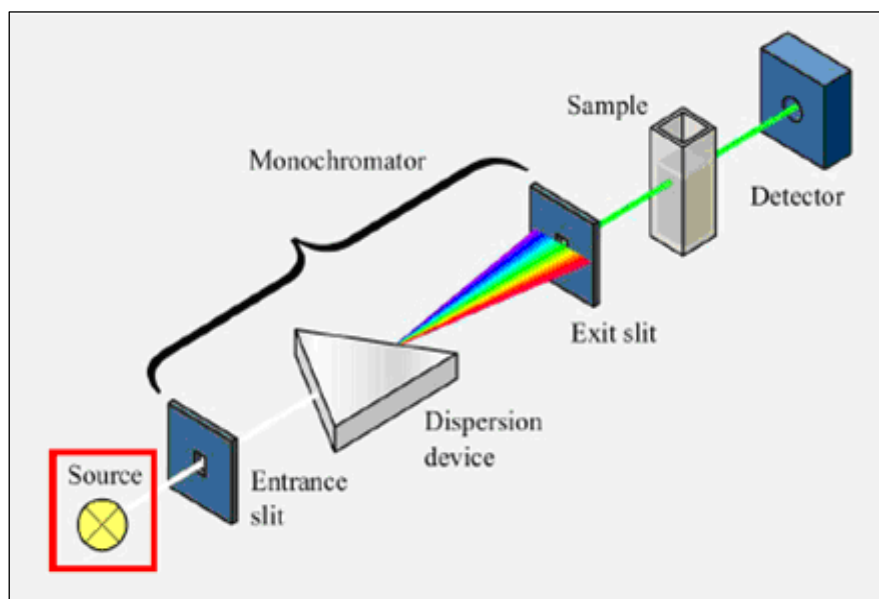
Fig 2.6 A schematic diagram of a single beam UV-Visible Spectrometer

Samples are used in solution and are placed in a small silica cell. Two lamps are used. A hydrogen or deuterium lamp for the ultraviolet region and a tungsten/halogen lamp for the visible region. In this case first 1 ml of the reference solution was prepared containing 1 mM of PCA, SAM, NADH in Tris/HCl-Buffer in a cuvette. Spectra were measured within the wavelength range of 210 to 800 nm. After this 10 μM of the enzymes PhzM and PhzS were introduced and mixed well in the cuvette. Spectra were measured after an interval of 5 mins for 25 mins within the wavelength range of 210-800 nm. Similarly another sample mixture was prepared containing all the components mentioned earlier and 10 μM of AdoHcy nucleosidase and spectra were measured. This showed how the presence of AdoHcy nucleosidase in the reaction can effect the quantity of pyocyanin formed.

3.5 Crystallographic methods

Proteins, like many molecules, can be prompted to form crystals when placed in the appropriate conditions. Determining the structure of a protein by X-ray crystallography entails growing high-quality crystals of the purified protein, measuring the directions and intensities of X-ray beams diffracted from the

crystals, and using a computer to stimulate the effects of an objective lens and thus produce an image of the crystal's contents. Finally that image must be interpreted, which entails displaying it by computer graphics and building a molecular model that is consistent with the image. Thus, the goal of crystallization is usually to produce a well-ordered crystal that is lacking in contaminants and large enough to provide a diffraction pattern when hit with x-ray. This diffraction pattern can then be analyzed to discern the protein's three-dimensional structure.

Crystals of an inorganic substance can often be grown by making a hot saturated solution of the substance and then slowly cooling it. Polar compounds can sometimes be crystallized by similar procedures or by slow precipitation from aqueous solutions by addition of organic solvents. However in case of proteins these conditions won't apply as the proteins are denatured by heating or exposure to organic solvents. In order to crystallize a protein, the purified protein undergoes slow precipitation from an aqueous solution. As a result, individual protein molecules align themselves in a repeating series of "unit cells" by adopting a consistent orientation. The crystalline "lattice" that forms is held together by noncovalent interactions (98;99). Protein crystallization is inherently difficult because of the fragile nature of protein crystals. In addition to overcoming the inherent fragility of protein crystals, the successful production of x-ray worthy crystals is dependent upon a number of environmental factors because so much variation exists among proteins, with each individual requiring unique conditions for successful crystallization. Some factors that require consideration are:

- Purity of the protein: In order for sufficient homogeneity, the protein should usually be at least 97% pure.
- Concentration of the protein and the precipitant
- pH conditions are also very important, as different pH's can result in different packing orientations. Buffers, such as Tris-HCl, are often necessary for the maintenance of a particular pH *(Branden and Doze, 1999).*

Apart from the conditions mentioned above there are some subtle conditions like cleanliness, vibration and sound, convection, source and age of protein, and the presence of ligands that also influence the formation of macromolecular crystals A protein will stay in solution only up to a certain concentration. Once this limiting concentration is reached, the solution will no longer remain homogeneous, but a new state or phase will appear. This phenomenon forms the basis of all protein crystallization experiments. By changing the solution conditions, the crystallographer tries to exceed the solubility limit of the protein so as to produce crystals. However, merely changing the concentration doesn't not guarantee the formation of protein crystals in majority of the cases. Many things can happen instead of getting crystals (a) nothing happens i.e., the protein solution remains homogenous, (b) a new phase appears but its not a crystal instead an aggregate or a liquid, (c) the crystals appear but unsuitable for structural determination because of poor diffraction pattern obtained.

An important tool in this work is the phase diagram (Fig 2.7). A complete phase diagram shows the state of a material as a function of all of the relevant variables of the system. For a protein solution, these variables are the concentration of the protein, the temperature and the characteristics of the solvent (e.g., pH, ionic strength and the concentration and identity of the buffer and any additives) *(Neer Asheri ,Methods , Mar 2004).*

In principle, supersaturation is the key for the crystallization of the proteins. In practice, crystals hardly ever form unless the concentration exceeds the solubility by a factor of at least three. The large supersaturation is required to overcome the activation energy barrier, which exists when forming the crystal. This barrier represents the free energy required to create the small microscopic cluster of proteins—known as a nucleus—from which the crystal will eventually grow.
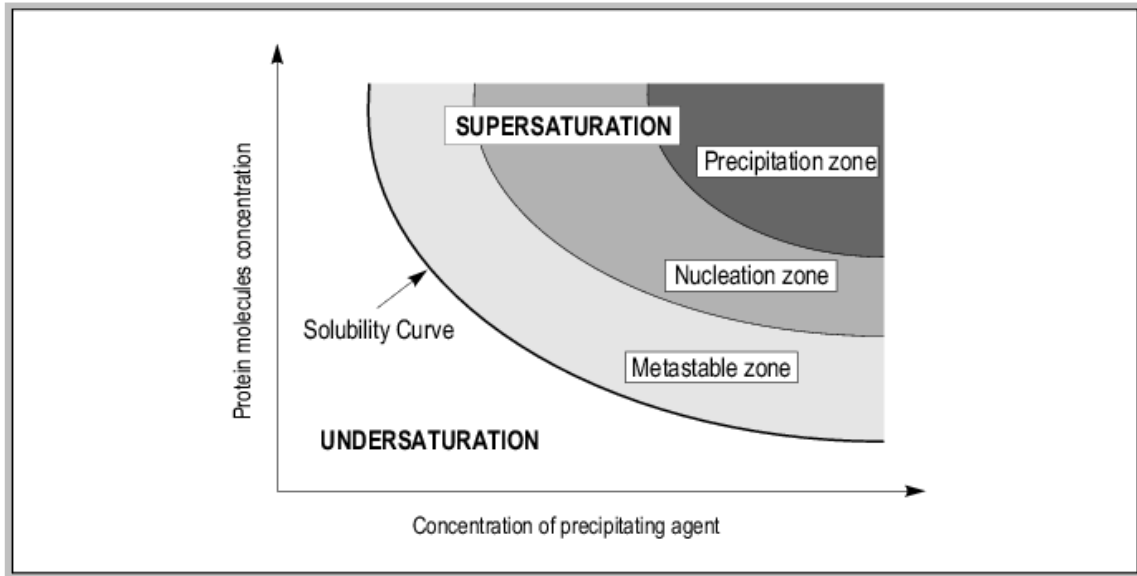
Fig 2.7 Phase Diagram showing zones for crystal nucleation, growth, precipitation.

Since there is an energy barrier, nucleation (the process of forming a nucleus) takes time. If the supersaturation is too small, the nucleation rate will be so slow that no crystals form in any reasonable amount of time. The corresponding area of the phase diagram is known as the "metastable zone". In the "labile" or "crystallization" zone, the supersaturation is large enough that spontaneous nucleation is observable. If the supersaturation is too large, then disordered structures, such as aggregates or precipitates, may form. The "precipitation zone" is unfavorable for crystal formation, because the aggregate and precipitates form faster than the crystals. The precipitation zone is where the excess of protein molecules immediately separates from the solution to form amorphous aggregates. To grow well-ordered crystals of large size, the optimal conditions would have to begin with the formation of a preferably single nucleus in the nucleation zone just beyond the metastable zone. As the crystals grow, the solution would return to the metastable region and no more nuclei could occur. The remaining nuclei would grow, at a decreasing rate that would help to avoid defect formation until equilibrium is reached. The three zones are illustrated schematically in the Fig 2.7. Since these zones are related to kinetic phenomena, the boundaries between the zones are not well defined.

3.5.1 Crystallisation by Vapour-Diffusion

In the most common methods of growing protein crystals, purified protein is dissolved in an aqueous buffer containing a precipitant such as ammonium sulfate or polyethylene glycol at a concentration just below that is necessary to precipitate the protein.

By far the vapour diffusion method is the most common and popular technique for crystallising proteins. It was first used for the crystallisation of tRNA. In this technique a drop containing protein, stabilizing buffers, precipitants and crystallization aids is allowed to equilibrate in a closed system with a much larger reservoir. The reservoir usually contains the same chemicals minus the protein but at an over all higher concentration so that water preferentially evaporates from the drop. If conditions are right this will produce a gradual increase in protein and precipitant concentrations so that a few crystals may form. Usually there are two different techniques in which the vapour diffusion method is carried out; ''*the sitting drop* "and "*the hanging drop*'' method (Fig 2.8 (a) and (b)).
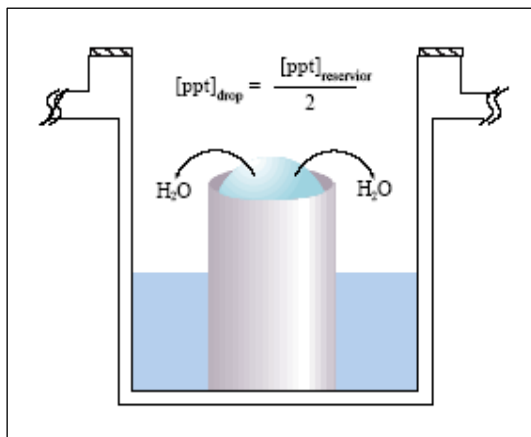
Fig 2.8 (a). The sitting drop method   Fig 2.8 (b). The hanging drop method
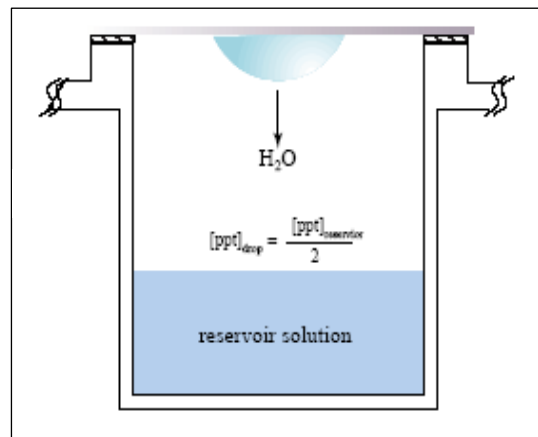
For the crystallising purpose in our case the concentrated aliquots of native proteins (PhzM and PhzS) were thawed and subjected to screening using Crystal Screen and Crystal Screen 2 of Hampton Research (100-102). The protein concentration was screened at 10 and 15 mg/ml for PhzS and 5, 10 and 15 mg/ml for PhzM by dilution of the protein stock with gel filtration buffer. The hanging drop vapour diffusion method with drops consisting of 1.2 µl

protein and 1.2 µl precipitant solution was used throughout. All crystallization trials were carried out at 20 °C. The conditions were checked for the appearance of crystals periodically. Conditions that produced micro crystals were optimized with respect to precipitant concentration and pH to reduce the amount of nucleation and increase the size and appearance of crystals obtained.

3.5.2 Selecting a cryoprotectant

After optimised crystals are obtained they need to be exposed to X-rays for collecting diffraction data and to prevent them from being destroyed by radiation they are flash cooled in liquid nitrogen (yields the highest cool-down rate). Flash-cooled crystals are much less prone to radiation damage than their room-temperature counterparts, allowing data to be accumulated over extended periods of time. In theory lowering the temperature should increase the molecular order in the crystal and improve diffraction. In practice, however, early attempts to freeze crystals resulted in damage due to formation of ice crystals. In recent years techniques were developed for flash freezing crystals in presence of agents like sugar or glycerol, which prevent ice formation. These ice-preventing agents are called cryoprotectants. In all cases of ice formation on cooling to cryogenic temperatures the process starts in a layer of liquid on the surface of the crystal. It is therefore necessary to remove or modify this layer with a cryoprotectant. Typically the cryoprotectant is added to a portion of mother liquor, usually in the range 10-25% by volume. Because the action is at the surface of the crystal, it is normally not necessary to soak the crystal for any length of time. A few seconds (<10 s) of rinsing will often suffice.

In order to check for a suitable cryo first the solution to be used as the cryoprotectant is flash frozen in liquid nitrogen. Then the cryo solution is checked for ice formation either visually or with X-ray diffraction. Upon cooling, a transparent drop and x-ray diffraction pattern free of powder diffraction rings or "ice rings," indicates success. The appearance of a cloudy drop or "ice rings" indicates an inappropriate cryoprotectant concentration or

cryoprotectant. Some precipitants for example polyethylene glycol (PEG), act as cryoprotectant and often just increasing their concentration in the mother liquor is sufficient to use the mother liquor as the cryo and in some cases additional compounds need to be added to the mother liquor eg. glycerol or sugar.

In addition to better diffraction, other benefits of using a cryoprotectant include reduction of radiation damage to the crystal and hence possibility of collecting more data form a single crystal; reduction of X-ray scattering from water (resulting in cleaner backgrounds in diffraction patterns) because the amount of water surrounding the crystal Is far less than that in a droplet of mother liquor; and the possibility of safe storage, transport and reuse of crystals.

3.5.3 Data collection and processing

All cryoprotected crystals were initially tested at home source - a copper rotating anode with Osmic mirrors (λ = 1.5419 Å, 50 kV, 100 mA, 0.1 mm collimator) at 100 K. Final datasets were then obtained at the synchrotron sources mainly, the ESRF at Grenoble, France and the SLS at Basel, Switzerland.

It is important to collect as complete data as possible, i.e., to record nearly all reflections up to the resolution limit (which is often due to the crystal quality). In order to understand which reflections are collected, one can look at the Ewald Sphere, which is constructed in reciprocal space. When a lattice point crosses the Ewald sphere, a reflection occurs in the direction determined by the centre of the sphere and the point of intersection.
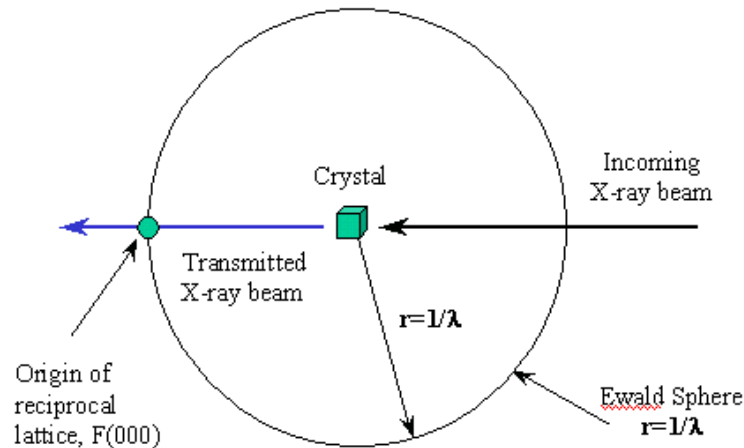
Fig 2.9. The Ewald Sphere

In order to collect a diffraction data, a monochromatic (single wavelength) source of X-ray is needed or desirable because the diameter of the sphere of reflection is 1/ λ, and a source producing two distinct wavelengths of radiation gives two spheres of reflection and two interspersed sets of reflections making indexing difficult or impossible because of overlapping reflections.

3.5.3.1 Data Collection

X-ray data processing is a key stage for protein crystallography. The final quality of X-ray data is related with the data processing procedure, which includes integration of the crystallographic data and scaling. Absolute requirement for the successful analysis of a protein structure is a well-ordered protein crystal, grown from protein of highest purity. During the central experiment of data collection a protein crystal is positioned into an X-ray beam. Through the combination of scattering and interference a diffraction pattern is generated, which is recorded in an X-ray sensitive device. The diffraction is described by the following term

$$\text{Bragg's Law} \qquad n\,\lambda \;=\; 2\,d\,\sin\theta$$

Where, d = distance between two parallel reflecting planes of the crystal,

λ = the wavelength and

n = an integral number

In order to collect X-ray diffraction data the crystals were rotated around an axis perpendicular to the beam in steps of $\Delta\varphi$ = 0.5 – 1.0 degrees over a range of typically 90° – 180°. Per rotation step one diffraction image was recorded and all reflections from all diffraction images ("frames") together constitute a complete data set. This raw data obtained is subsequently processed by a series of different steps mainly Indexing, Integrating and Scaling (103).
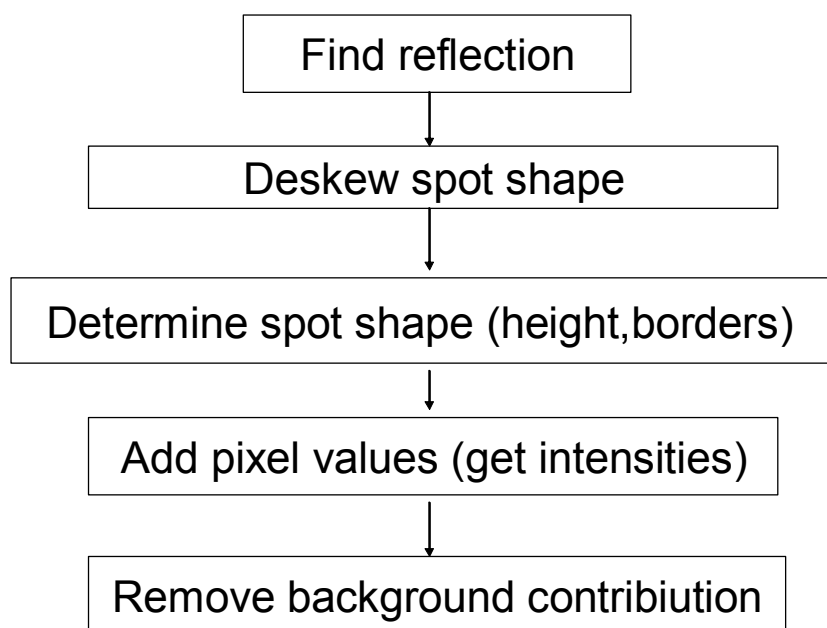
3.5.3.2 Data Processing
Indexing

The positions of the diffraction maxima on the X-ray detector are directly related to shape and size of the crystal unit cell. The unit cell of the crystal and the diffraction pattern are related by a reciprocal relationship. Each reflection can be assigned three coordinates or indices in the imaginary three-dimensional space of diffraction pattern. This space where the reflections live, is called the reciprocal space due to a reciprocal relation between diffraction pattern and crystal lattice. Usually set of integral indices h, k, and l, the so called Miller indices are used to designate the position of an individual reflection in the reciprocal space of the diffraction pattern.

Integration

Data collection results in a list of images, each representing a wedge of the rotation of the crystal in the beam. The images are distorted sections of reciprocal space. Data integration has to reconstitute the original, undistorted lattice in 3 dimensions.

```
┌─────────────────────────┐
│      Find reflection      │
└─────────────────────────┘
            │
            ▼
┌─────────────────────────┐
│     Deskew spot shape     │
└─────────────────────────┘
            │
            ▼
┌───────────────────────────────────┐
│ Determine spot shape (height,borders) │
└───────────────────────────────────┘
            │
            ▼
┌─────────────────────────────────┐
│   Add pixel values (get intensities)  │
└─────────────────────────────────┘
            │
            ▼
┌─────────────────────────────────┐
│  Remove background contribiution   │
└─────────────────────────────────┘
```

Fig 2.10 The data integration flow chart

Scaling

"Scaling" refers to putting single diffraction images/frames to the same scale such that "partially" recorded reflections (extending over several frames) can be summed up and symmetry-equivalent reflections can be "merged". The (experimental) differences in intensities necessitates the scaling of the data: All reflections must be put on a common scale. To do so, one takes symmetry related reflections into account: Reflections that are related by one of the symmetry operators of the crystal's space group must have equal intensities.

Data processing was carried out using the program XDS (104), which incorporates all of the above-mentioned steps. Other parameters affecting data processing like mosaicity, Matthew's coefficient etc., were also calculated.

The regular repetition of the unit cells is normally interrupted by lattice defects. The diffraction pattern of a crystal is infact the sum of diffraction patterns originating from mosaic blocks with slightly different orientations. Mosaicity

values were checked to ensure that the lattice defects are moderate (between 0.2°- 0.5°).

Typically, 30-80% of the unit cell volume is occupied by solvent. Based on the volume of asymmetric unit (determined by x-ray measurements) and molecular weight of the protein one can estimate the number of protein molecules present in a unit cell by calculating Matthew's coefficient (V_M) via the equation:

$$V_M = \frac{V}{Mw \times Z}$$

Where,

V = Volume of the asymmetric unit ($Å^3$) .

Mw = Molecular weight of the protein (k Da).

Z = Number of molecules in the asymmetric unit.

The average Matthew coefficient for a protein crystal is 2.5 $Å^3$/Da, which corresponds to a unit cell solvent content of 50% (Matthews, 1968).

3.5.4 Determination of Phases

The interaction of X-rays with electrons in a crystal gives rise to a diffraction pattern. Because of the physics of diffraction, this diffraction pattern is the Fourier transform of the electron density distribution. Fourier transforms can, in principle, be reversed so it is possible to reconstruct the distribution of electrons (hence of atoms) in the crystal. Unfortunately, to do this we need not only the amplitudes of the diffracted waves, which are obtained from the intensities of the diffraction spots, but also their relative phase shifts, which cannot be measured directly. This problem is known as the phase problem of crystallography. The only relationship is *via* the molecular structure or electron density. Therefore if there is some prior knowledge of the structure or electron density, this can lead to values of phases. One of the major efforts of macromolecular crystallography lies in determining good phases. The following are the most frequently used techniques:

- Direct methods (small molecules and high resolution only)
- Molecular Replacement (MR)
- Isomorphous Replacement
- Anomalous Scattering (MAD, SAD)

For a normal diffraction experiment, Friedel's law is valid, which states that the intensities of the reflection (h, k, l) and (−h,−k,−l) are equal and that the phases of the underlying structure factor have opposite signs, _(h, k, l) −_(−h,−k,−l). One method of obtaining phases is by using heavy atom derivative by taking into advantage the heavy atom's capacity to absorb X-rays of specified wavelength. As a result of this absorption Friedel's law does not hold, and the reflections (h, k, l) and the inverse (–h –k –l) are not equal in intensity. This inequality of symmetry-related reflections is called anomalous scattering or anomalous dispersion. The single wavelength anomalous diffraction method (SAD) has been used for this work.

In practice, selenium is one of the most widely used heavy atoms for SAD/MAD phasing in protein crystallography and was used for labeling proteins for this work. This approach was undertaken after unsuccessful molecular replacement trials using closely related structures. The structure of PhzM was solved from 360° Se-K-edge SAD data collected on ESRF-beamline ID14/4. 16 out of 20 Selenium atoms were located by SHELXD (105). The structure of PhzS was solved from Se-K-edge SAD data collected at station ID29 of the ESRF. Of 360 1°-oscillation frames only the first 180 were usable due to radiation-induced crystal decay. The positions of 8 selenium atoms were determined by SHELXD and subsequently used for phasing in SHARP.

Molecular replacement can be used when one has a good model for a reasonably large fraction of the structure in the crystal. If a homology model available, molecular replacement can be successfully employed to get phase information, which was first described by Rossmann & Blow. In this method, the phases for the model are obtained from the coordinates and the structure factor amplitudes (F_{Calc}) of the known structure. In general the space group

and the orientation differ between the known and the unknown structure, therefore the known search model needs to be reoriented in the new unit cell properly. This is achieved by comparing the Patterson functions, obtained from the structure factor amplitude (F_{Obs}) of the measured diffraction intensities and from the search model (F_{Calc}). This fact was used to solve the structure of PhzM complexed with SAM

3.5.5 Model Building and Refinement

The initial structural model contains errors that can be minimised through iterative model refinement. This is a process of adjustment of the atomic coordinates of the model in order to minimise the difference between experimentally observed structure factor amplitudes (F_{Obs}) and those calculated from the model (F_{Calc}). The progress of refinement was monitored using the conventional crystallographic index 'R factor' and 'R-free'. The R factor is defined by the equation:

$$R_{cryst}(F) = \frac{\sum_{hkl} |F_{obs}(hkl)| - |F_{calc}(hkl)|}{\sum_{hkl} |F_{obs}(hkl)|}$$

An acceptable value for the R-factor depends on the resolution of the structure. For structures determined at high resolution (<2.0 Å) the value of the final R-factor is expected to be below 0.2 or 20%. Given the low observations-to-parameters ratio for protein structures the R-factor can be artificially lowered at the expense of the stereochemistry of the model. To avoid this type of error, Brunger (1992) introduced a new methodology in the refinement process (cross validation) where approximately 5% of the data (a test group of reflections 'T') is isolated from the remainder (the working group) and not used for the purposes of refinement). Instead the refinement is performed by using only the reflections belonging to the working group. At each cycle of refinement the structure factors are calculated for both groups.

Whilst the working group is used for the calculation of the R-factor as defined above, the test group is used to calculate a new parameter, R-free, in an exactly analogous manner.

$$\text{R-free} = \sum_{hkl \subset T} \left| \left| F_{obs}\, hkl \right| - \left| F_{calc}\, hkl \right| \right| \Bigg/ \sum_{hkl \subset T} \left| F_{obs}\, hkl \right|$$

The fundamental difference between these two discordance indices is that the refinement procedure `knows' about the working group (as it is used for the very refinement process) but it has never `seen' the test group. The great advantage of the R-free is that it is a sensitive indicator of over-refinement, that is, a refinement protocol, which attempts to extract more information than the data, is capable of providing.

In case of PhzM the refinement program REFMAC5 (106) was used for refinement and the model further adjusted by hand using the graphics program O or COOT (107). For PhzS the refinement programme REFMAC5 and CNS programme suit (108) was used and the model as in case of PhzM was further adjusted using O or COOT.

RESULTS AND DISCUSSIONS

4.1 Cloning, over-expression and purification

4.1.1 PhzM

The oligonucleotide primers PhzM-up (5'-TTTTTCATATGAATAATTCGAATCTTGCTG-3') and PhzM-low (5'-TTTTTGGATCCGTTGAAAGTTCCGATTCA-3') were used to generate a 1015 base pairs DNA fragment encoding PhzM from *P.aeruginosa* PAO1 by Polymerase Chain reaction (PCR). This fragment was amplified with a PTC-200 thermocycler. The PCR product was digested with NdeI and BamHI, gel-purified, cloned behind a T7 promoter in the N-terminal His-tag fusion vector pET15b and single-pass sequenced to confirm the integrity of the resultant fusion. The plasmid was then transformed into *E.coli* Rosetta pLysS competent strain and initial expression tests were carried out to determine the optimal conditions for growth and expression. The protein was over-expressed (Fig.3.1 (a)) and purified according to the techniques mentioned earlier. A typical purification with nickel affinity chromatography and gel filtration (Fig.3.1 (b)) produced about 95% of pure protein, which was concentrated to 20 mg/ml.
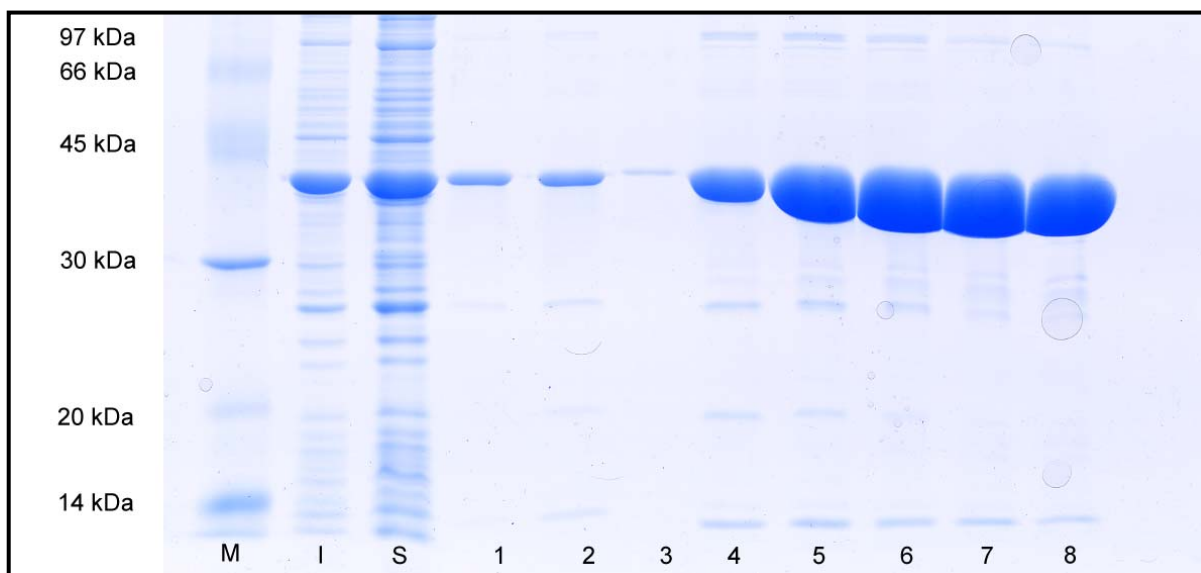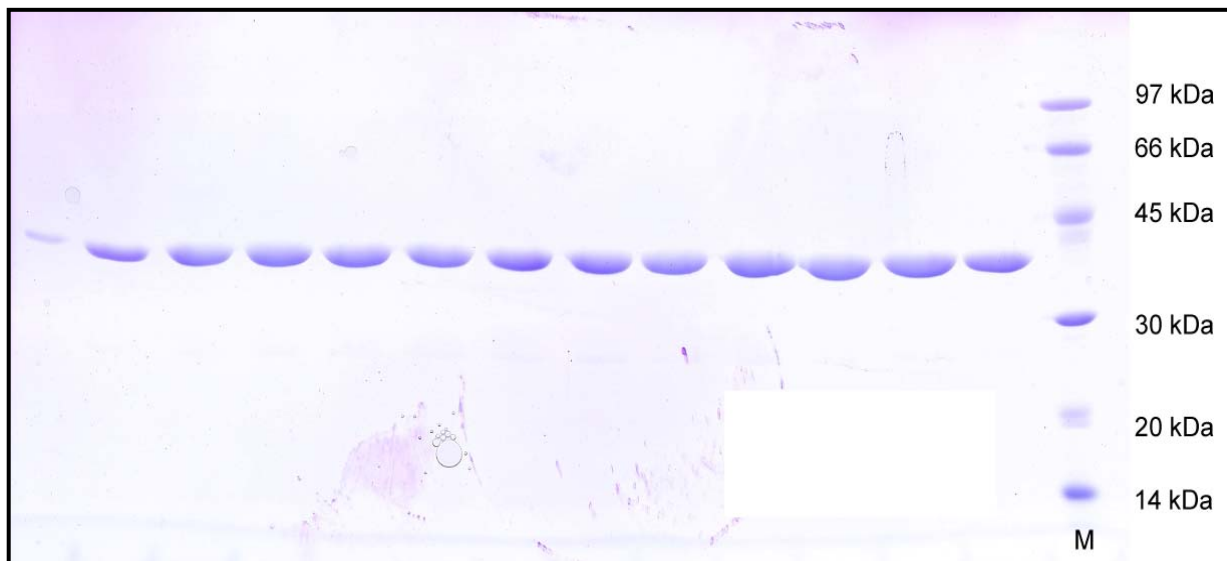

Fig 3.1 (a) Expression and nickel chromatography (M = marker; S= supernatant; I = induced; 1-8 fractions obtained after affinity chromatography)

Fig.3.1 (b) Fractions obtained after gel purification

The purification protocol for the Seleno-L-methionine labelled protein remained same as in the case of native protein. The purified protein was then used for the crystallisation trials.

4.1.2 PhzS

The oligonucleotide primers PhzS-up (5'- TATATACATATGAGCGAACCCATCGAT-3') and PhzS-low (5'- TTTTTTGGATCCTAGCGTGGCCGTTC-3') were used to generate a 1218-bp DNA fragment encoding PhzS from *P.aeruginosa* PAO1 by PCR. Like in case of PhzM the fragment was amplified, the PCR product was digested with NdeI and BamHI, gel-purified, cloned behind a T7 promoter in the N-terminal His-tag fusion vector pET15b and single-pass sequenced to confirm the integrity of the resultant fusion. The plasmid was then transformed into *E.coli* Rosetta pLysS competent strain and initial expression tests were carried out to determine the optimal conditions for growth and expression. The protein was over-expressed (Fig.3.2 (a)) and purified according to the techniques mentioned earlier. A typical purification with nickel affinity chromatography (Fig.3.2 (b)) and gel filtration (Fig.3.2 (c)) produced about 95% of pure protein, which was concentrated to 15 mg/ml
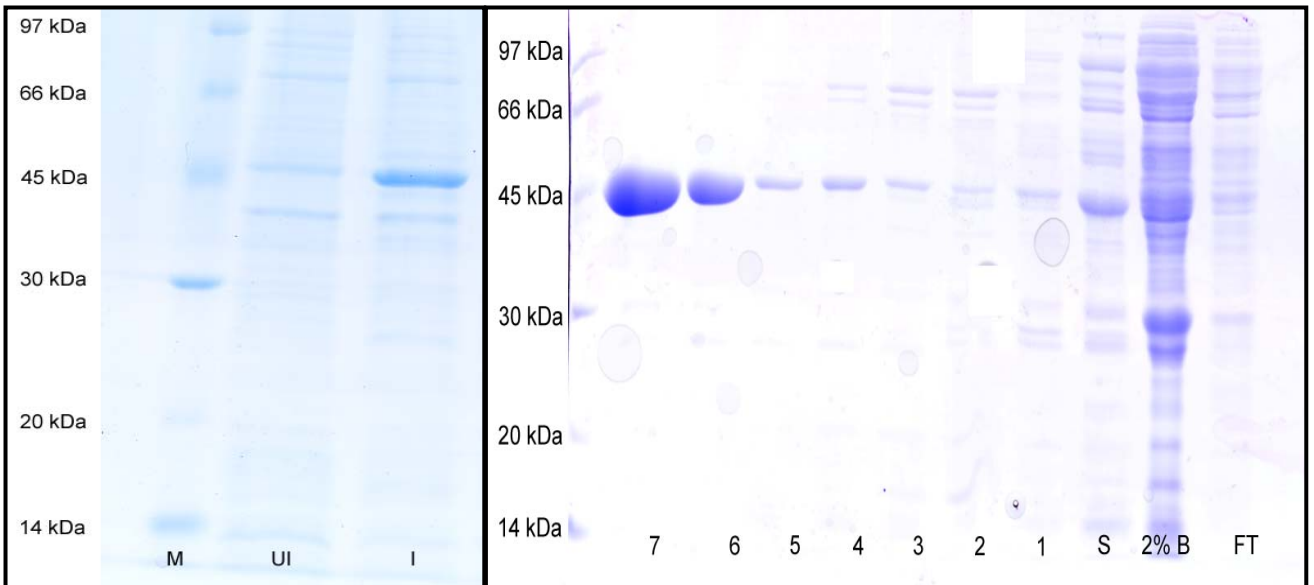
Fig3.2 (a) Expression of PhzS in Rosetta pLysS strain (b) Fractions from Ni affinity column (FT = Flow through; I = induced; UI = uninduced; S = soluble extract ; 1-7 are the fractions of the protein)
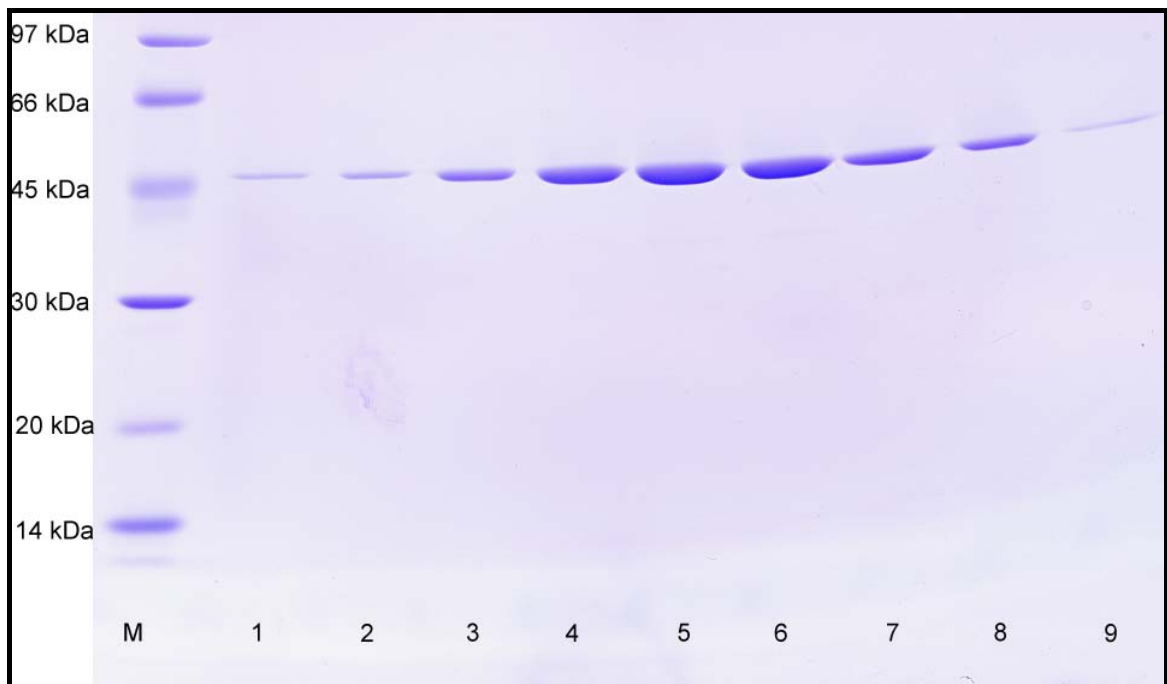
Fig3.2 (c) Fractions from gel purification

4.1.3 S-adenosylhomocysteine nucleosidase

S-adenosyl-homocysteine nucleosidase is a 26-kDalton protein that hydrolyses S-adenosyl-homocysteine. As mentioned earlier SAH acts or creates a negative feedback regulation on the synthesis of the methylated

product so hydrolysing SAH thereby helps in the positive regulation of the methylation reaction. It was expressed in BL21pLysS strain, purified by the methods explained earlier (affinity chromatography and gel filtration) and concentrated to 10 mg/ml.
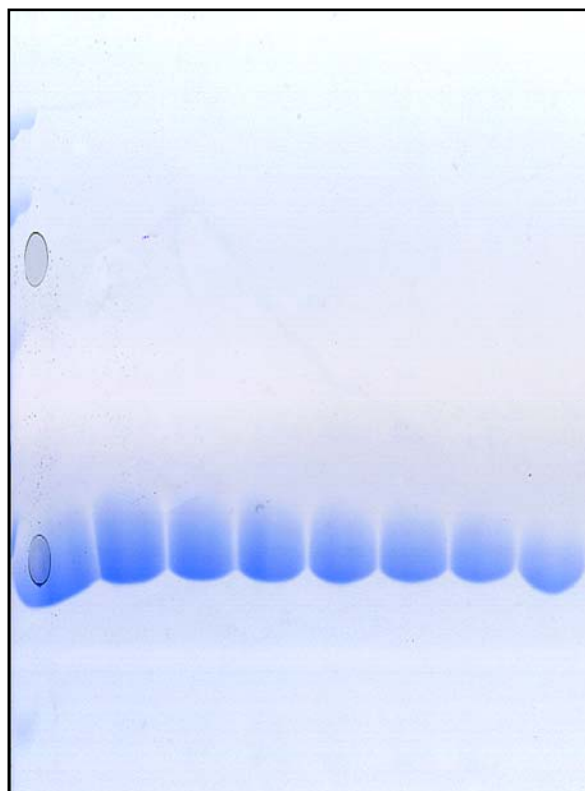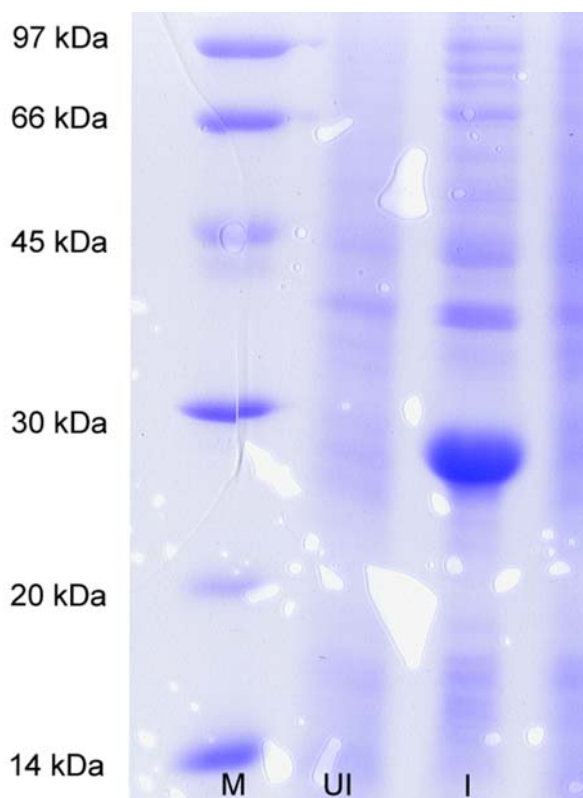

97 kDa

66 kDa

45 kDa

30 kDa

20 kDa

14 kDa

M   UI   I

Fig 3.3 (a) Expression of AdoHcy in BL21pLysS   *Fig 3.3(b) Final purified fractions*

The purified fractions were then used for the biochemical assays in the experiments explained below.

4.2 Crystallisation

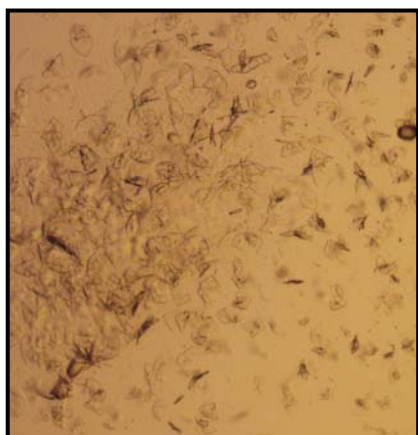### 4.2.1 PhzM

Crystallization was initiated at 293 K using the hanging-drop vapour diffusion method with Crystal Screen and Crystal Screen 2 from Hampton Research (100;101). 5, 10, and 15 mg/ml concentrations of protein in 20 mM Tris–HCl pH 8.0, 150 mM NaCl gel filtration buffer, were used for initial screening, with 1.2 µl of protein solution mixed with a similar amount of precipitant. Conditions

that produced microcrystalline precipitates were optimized with respect to protein concentration, precipitant concentration and pH to reduce the amount of nucleation, increase the size and improve the appearance of the crystals obtained. Diffraction-quality crystals were obtained from a hanging drop containing 1.2 µl protein solution at 8 mg/ml mixed with the same volume of reservoir solution consisting of 18–23% (w/v) PEG 3350, 0.1 M sodium cacodylate pH 5.8–6.8, 0.2 M magnesium acetate. The drops were routinely equilibrated against 500 µl reservoir solution. The crystals have an oblique three-dimensional shape and take about two days to grow to dimensions of approximately 70 X 30 X 20 mm (Fig.3.2 (b)). Crystals of Seleno-L-methionine- labelled PhzM were obtained under similar conditions (Fig.3.2 (c)).

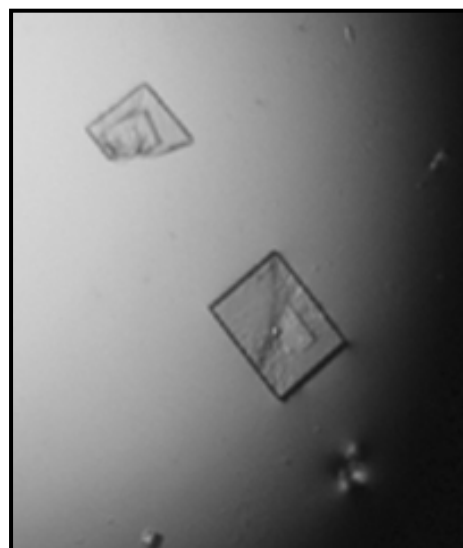*Fig 3.4 (a)*   *3.4 (b)*
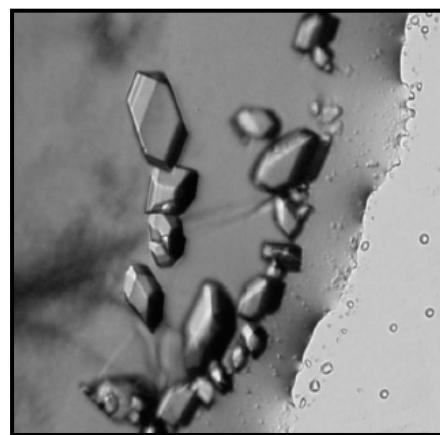

Fig 3.4 (a) and (b) the native crystals of PhzM at different concentrations of PEG 3350 and pH

Fig. 3.4(c) Seleno-L-methionine labelled crystals of PhzM

4.2.2 PhzS

Initial crystallization conditions were determined at room temperature with Crystal Screen and Crystal Screen 2 from Hampton Research (109;110). The protein concentration was screened at 10 and 15 mg/ml by dilution of the protein stock with gel filtration buffer. The hanging drop vapour diffusion method with drops consisting of 1.2 µl protein and 1.2 µl precipitant solution equilibrated against 500 µl reservoir volume at room temperature was used throughout. Conditions that produced microcrystalline precipitates were optimized with respect to protein concentration, precipitant concentration and pH to reduce the amount of nucleation and increase the size and appearance of crystals obtained. Diffraction-quality crystals were obtained at 12 mg/ml PhzS concentration and a reservoir with 0.7 - 1.0 M lithium sulfate, 0.1 M sodium citrate pH 5.0 - 5.5, 0.5 M ammonium sulfate. The crystals are yellow due to the presence of FAD and grow to a size of 0.3 × 0.3 × 0.2 mm (Fig.3.5 (a)) in approximately 3 days. Seleno-L-methionine labelled crystals of PhzS (Fig. 3.5 (b)) grow as thin fragile plates and were obtained at two different conditions consisting of 14 - 17% (w/v) PEG 10000 / 0.1 M ammonium acetate / 0.1M Bis-Tris pH 5.5 and 23 - 26% (w/v) PEG 3350 / 0.1 M Bis-Tris pH 5.8 – 6.0 / 0.2 M ammonium sulfate.
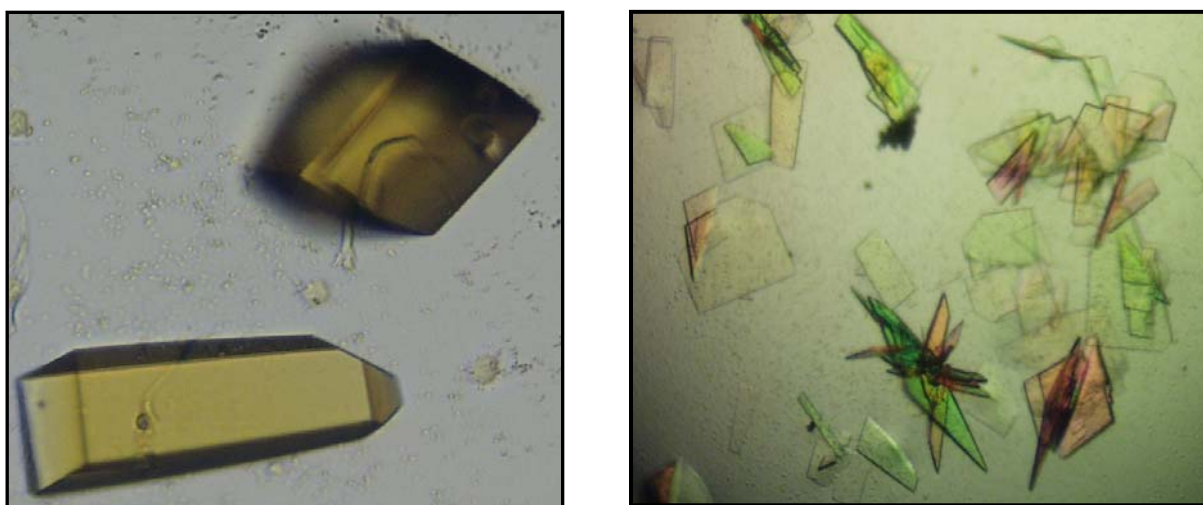
Fig. 3.5 Native (a) and seleno-L-methionine labelled (b) crystals of PhzS

4.3 Data collection, Structure Determination & Quality of Model

Crystals obtained were exposed to synchrotron radiation and datasets were collected for structure solution. Molecular Replacement methods of structure solution being unsuccessful in both the cases, the structures were solved by SAD (Single-wavelength Anomalous Diffraction) using Seleno-L-methionine labelled protein. The initial steps of data processing and phase determination for all structures were similar and are described in detail in the previous section. The particulars of structure determination for each of the proteins are detailed below.

4.3.1 PhzM and PhzM complexed with SAM

In order to achieve cryoprotection, PhzM crystals were washed briefly in mother liquor supplemented with 10% (w/v) sucrose and 10% (w/v) xylitol and flash-cooled in liquid nitrogen prior to data collection The crystals belong to space group P1, with unit-cell parameters a = 46.1, b = 61.8, c = 69.6 Å, α= 96.3, ß = 106.6, γ = 106.9°. Diffraction spots appear to be split in one orientation; however, data reduction statistics as shown below are nevertheless satisfactory.

A data set was collected from a native protein crystal at 100 K as 180° non-overlapping 1° oscillation λ=0.9758Å images at ID14EH1 of the European Synchrotron Radiation Facility (ESRF, Grenoble, France) using a MAR 165 CCD detector with 10 s exposure time.

DATA COLLECTION	NATIVE	Se-SAD	PhzM complexed with SAM
Wavelength (Å)	0.934 / ID14EH1	0.9758 / ID14EH4	0.979/ ID29
Resolution (Highest Shell, Å)	20-1.75 (1.9-1.8)	20-2.3 (2.4-2.3)	20-1.85 (1.95-1.85)
Space group	P1	P1	$P2_1$
Cell constants	a=46.1, b=61.8, c=69.5; α= 96.3, β =106.5, γ =106.9	a=46.4, b=61.8, c=69.8; α= 96.1, β =106.8, γ =107.1	a=63.3, b=73.7, c=72.8; α= 90, β =91.6, γ =90
V_M	2.4	2.1	4.3
Total measurements	161889	117778	228850
Unique Reflections	61771	59061	56959
Average Redundancy	2.6	2.01	4.5
I/σ	11.27 (3.9)	9.57 (5.5)	13.69 (3.07)
Completeness (%)	95.7	96.1	99.4 (100)
Anom. Completeness (%)[a]	-	96.0	-
R_{sym}[b]	8.0 (33.1)	6.0 (14.5)	7.0 (44.4)

[a]*Completeness calculations treat Friedel pairs as separate observations*
[b]*$R_{sym} = \Sigma \mid I(h)_j - <I(h)> \mid / \Sigma \ I(h)_j$ where $I(h)_j$ is the scaled observed intensity of the i-th symmetry-related observation of reflection h and $<I(h)_i>$ is the mean value*

Radiation damage precluded higher redundancy data collection. A single strong peak in the κ = 180° section of the self-rotation function reveals the

orientation of one PhzM dimer in the asymmetric unit (Fig.3.6), corresponding to a solvent content of 47%.
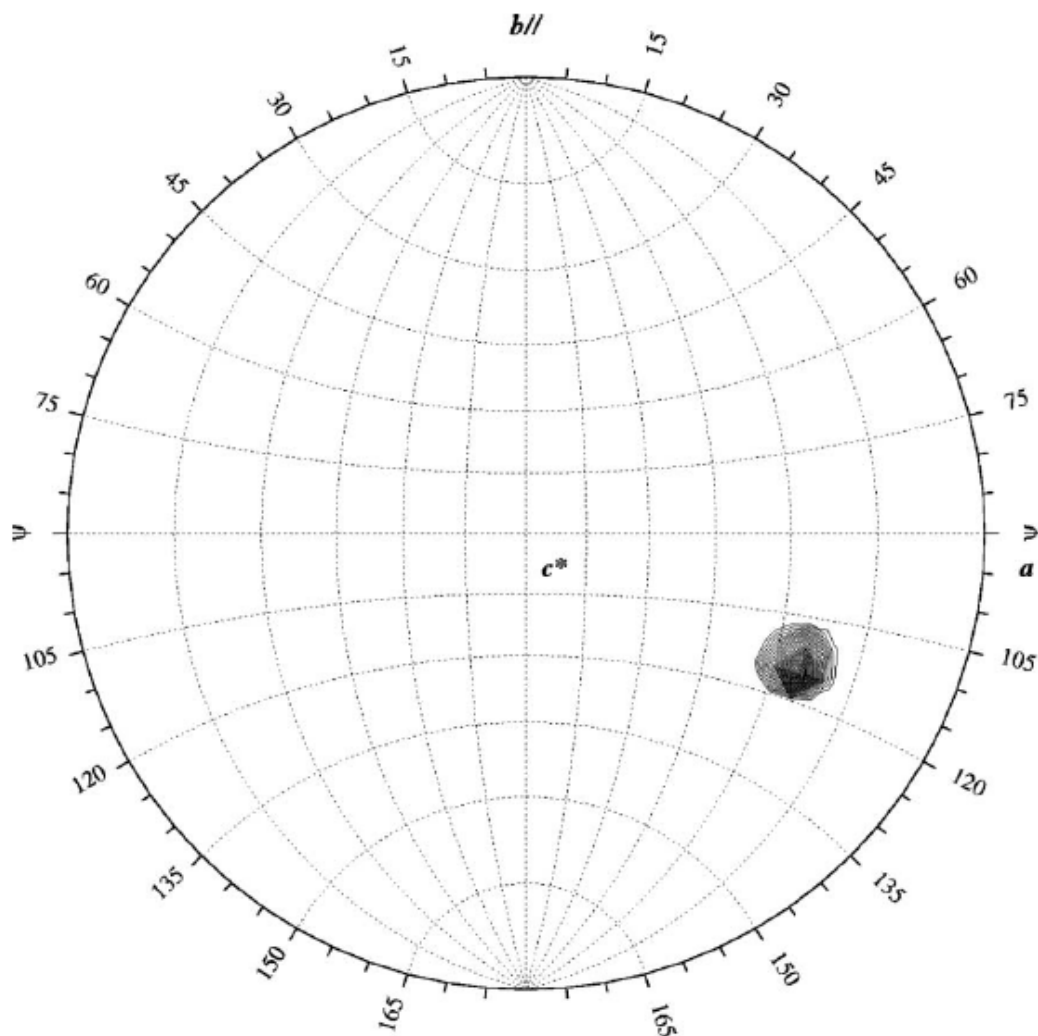
Fig.3.6 κ = 180° section of the self-rotation function of the native PhzM data set, calculated with REPLACE (Tong & Rossmann, 1997). Search angle, polar XYK; orthogonalization, AXABZ.

As molecular replacement was not successful, the structure of PhzM was solved from 360° Se-K-edge SAD data collected on ESRF-beamline ID14/4. 16 out of 20 expected selenium atoms were located by SHELXD (105). Subsequent refinement, phasing and density modification was carried out in SHARP (111) including data of a native crystal to 1.8 Å resolution. This allowed determining the handedness of the system but the resulting electron density was of poor connectivity, making de novo tracing impossible. It was,

however, sufficient for positioning of a related structure (Caffeic acid 3-o-methyltransferase, PDB-access code 1KYZ) within the solvent boundary and to use this structure as a guide for editing bones in O (112). It became obvious that the two PhzM monomers contained in the AU possess a different domain arrangement and that two different operators should be used in NCS averaging. Subsequent density modification in DM (105;113-115) yielded excellent electron density, which was then used in RESOLVE to automatically build a partial model. Using the Se atoms as anchor points and bulky aromatic (Trp, Tyr, Phe) residues as "light houses", side chains were incorporated into this poly-alanine model and 330 of the total 334 residues (per monomer) were fitted. The first 4 residues could not be fitted, as there was no electron density in that region. This model was then further refined using the program REFMAC5 (106). The structure was completed by hand in O and refined with REFMAC5 (106).

The current model of dimeric PhzM consists of 330 residues starting with residue number 4, which codes for Ala till Ala 334 (per monomer). The final structure of PhzM at 1.75 Å resolution has R-factor of 13.9% and R_{free} of 18.4%. The Ramachandran plot (Figure 3.7) obtained by the validation programme 'PROCHECK' shows 92.9 % of the total amino acids in the most favoured region 7.0 % and 0.2 % in the additionally allowed and generously allowed regions respectively. The model of PhzM complexed with SAM has a final resolution of 3.2 Å and contains one SAM molecule per dimer in addition to the molecules present in the native structure. Of the total residues for both the native and complex structure, 92.2% lie in the most favoured region of the Ramachandran plot (PROCHECK) (116). Most of the residues with poorer electron density are located in the additionally allowed regions, with two residues in the disallowed region. The final data collection statistics for the structure of PhzM and its complex with SAM are tabulated in page no 73
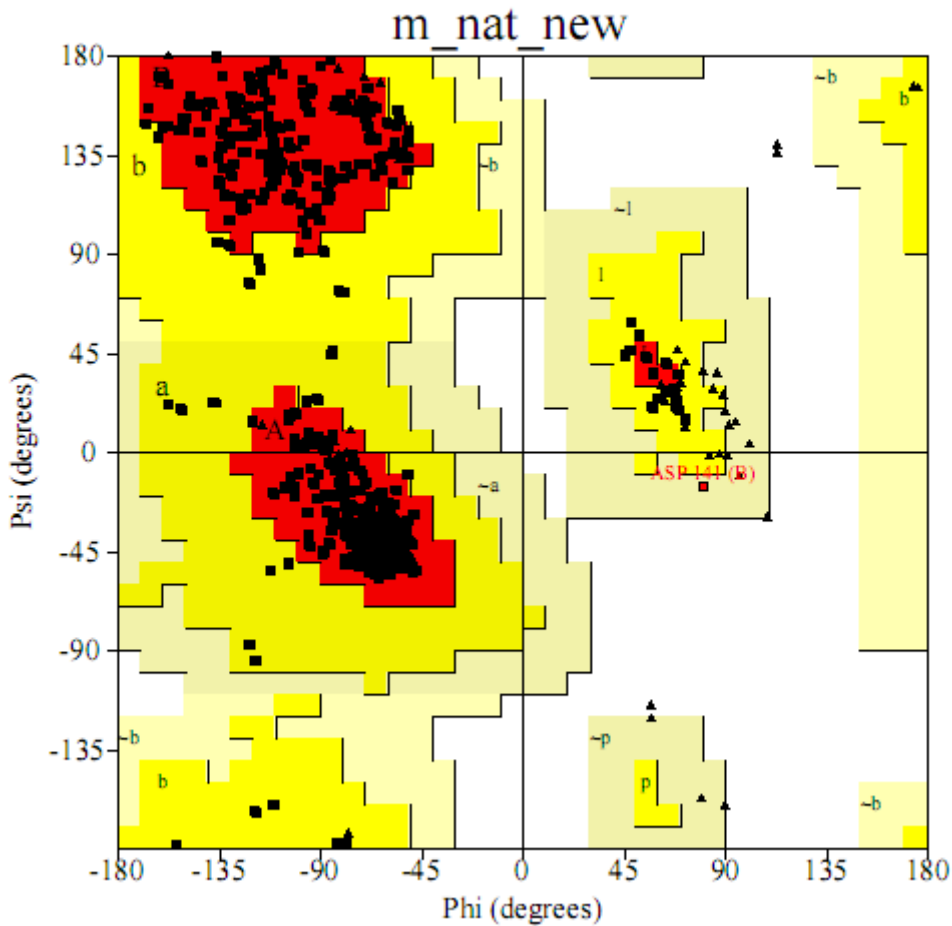
Fig 3.7 Ramachandran plot of the final model of PhzM.

4.3.2 PhzS

To achieve cryoprotection prior to data collection, PhzS crystals were washed briefly in mother liquor supplemented with 10 % (w/v) sucrose and 10 % (w/v) xylitol and then flash cooled in liquid nitrogen. Crystals of the native protein belong to the C2 group with the cell parameters a = 144.2, b = 96.2 and c = 71.7 Å; α = γ = 90, β = 110.5°, indicative of two PhzS monomers contained in the asymmetric unit. A data set of a native protein crystal to 2.4 Å resolution was collected at 100 K in 110 non-overlapping 1° oscillation images at ID14EH1 of the European Synchrotron Radiation Facility (ESRF, Grenoble, France), using a MAR165 CCD detector with 10s exposure time.

| DATA COLLECTION	Se SAD	NATIVE
Wavelength (Å)[a]	0.9791 / E-ID29	0.931 / E-ID14/3
Resolution (Highest Shell, Å)	20.0 – 2.7 (2.8 –2.7)	20.0 – 2.4 (2.5 –2.4)
Space group	C2	C2
Cell constants	a=70.6, b=76.2, c=80.2; $\alpha = \gamma = 90$, $\beta = 110.5$	a=144.2, b=96.2, c=71.7; $\alpha = \gamma = 90$, $\beta = 102.7$
V_M	2.3	2.8
Total measurements	40759	141768
Unique Reflection	10933	37329
Average Redundancy	3.8 (3.7)	3.8 (3.8)
I/σ	11.3 (5.3)	18.6 (3.2)
Completeness (%)	98.9 (100)	99.7 (99.3)
Anom. Completeness (%)[b]	96.8 (97.1)	-
R_{sym}[c]	7.5 (24.9)	5.7 (46.8)
Wilson B-factor ($Å^2$)	43	47
R-merge%	8.5 (26.9)	9.3 (50.1)

Data collection statistics for PhzS
[b]Completeness calculations treat Friedel pairs as separate observations
[c]$R_{sym} = \Sigma \mid I(h)_j - <I(h)> \mid / \Sigma I(h)_j$ where $I(h)_j$ is the scaled observed intensity of the i-th symmetry-related observation of reflection h and $<I(h)_i>$ is the mean value

SAD data from a Seleno-L-methionine labeled crystal were collected at 100K from 360 non-overlapping 1º oscillations at λ = 0.975756 Å (Se-absorption edge) at ID29 of the same synchrotron, using a Quantum (Q4R)-ADSC detector with 1.5 s exposure time and three passes per image. These crystals belong to space group C2 as well, however they possess different unit cell parameters of a = 70.6, b = 76.2 and c = 80.2 Å; α = γ = 90, β = 110.5°, allowing for the presence of one PhzS monomer in the asymmetric unit only.
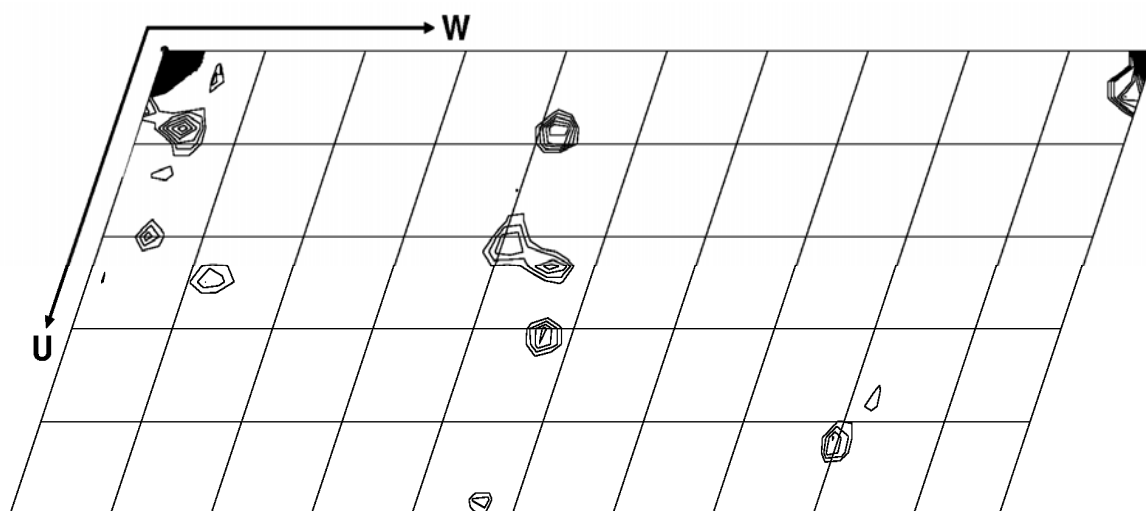
Fig 3.8 Harker section at v = 0 contoured at 3 σ, calculated from the anomalous differences of the Se-SAD data.

The crystals diffract to a resolution of 2.7 Å and are radiation sensitive. Peaks in the Harker section at v = 0 (Fig. 3.8) indicate the presence of anomalous scatterers.

The structure of PhzS was determined from Se-K-edge SAD data collected at station ID29 of the ESRF. Of 360 1°-oscillation frames only the first 180 were used due to radiation-induced crystal decay. The positions of 8 selenium atoms were determined by SHELXD and subsequently used for phasing in SHARP. The resulting electron density was poor and it was not possible to use the phase set for the better native data in the other crystal form. Instead, a related structure (p-hydroxybenzoate hydroxylase, PDB-access code 1PHH) was positioned within the solvent boundary and used as a guide to edit bones in O. The resulting trace was used to trim a poly-alanine version of 1PHH, resulting in a rough model, which was refined against the selenium-derivative data in REFMAC5. A crystallographic dimer was constructed and used as a molecular replacement model for the native data in PHASER. A unique solution was obtained and the superimposition operators with respect to the selenium-derivative were used in DMMULTI (106;115;117-120) for cross crystal averaging, starting from the experimental phase set. The resulting electron density was of good quality and was used for model building.
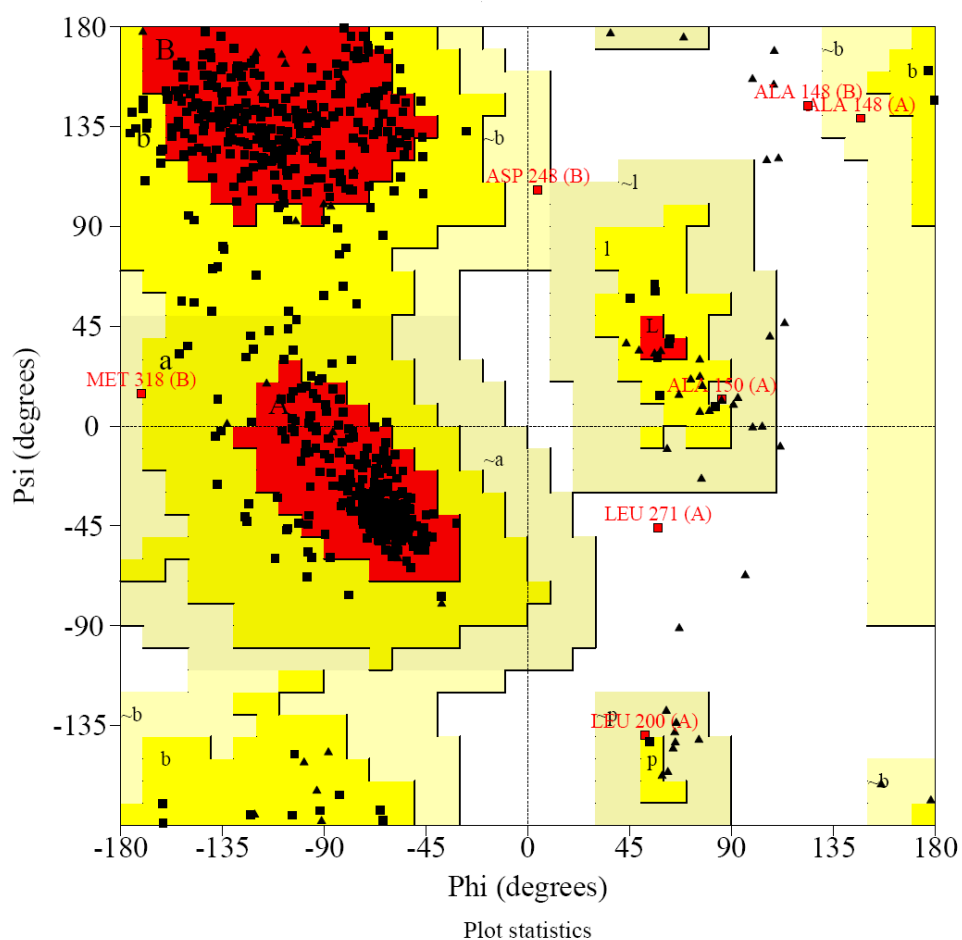
Ramachandran Plot

Fig 3.9 Ramachandran plot of the final model of PhzS.

The current model of dimeric PhzS consists of 384 residues starting with residue number 4 which codes for Pro till E384 (per monomer). The final structure of PhzS at 2.4 Å resolution has R-factor of 20.3% and R_{free} of 22.9%. The Ramachandran plot (Figure 3.9) obtained by the validation programme 'PROCHECK' shows 85.6 % of the total amino acids in the most favoured region 13.4 % and 0.6 % in the additionally allowed and generously allowed regions respectively.

77

4.4 Structural Analysis

4.4.1 Structural Analysis of PhzM from *Pseudomonas aeruginosa*

4.4.1.1 Monomer of PhzM

PhzM is a dimeric protein with a monomer molecular weight of 36.2 kDa. It is a SAM dependent methyltransferase comprising of two identical single subunits of 334 amino acids each. Each polypeptide of PhzM is built up of fifteen helices and seven ß-strands and comprises of three domains, the N-terminal domain, a middle domain and the C- terminal domain (Figure 3.10).
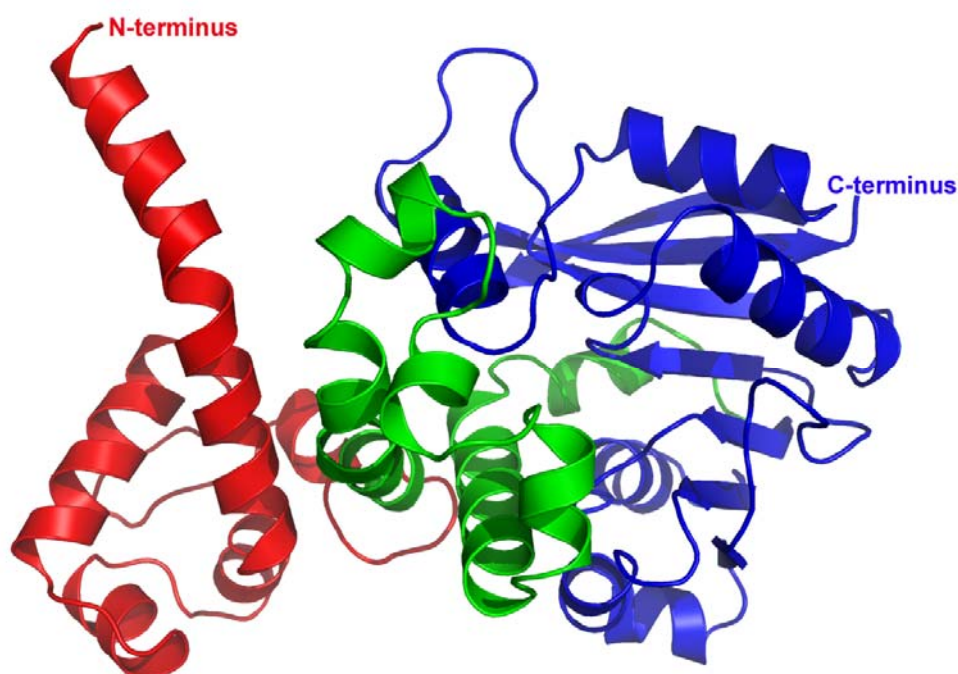
Fig 3.10 Three domains of PhzM

The N-terminal domain mainly consists of alpha helices and spans residues from 1-95. It is the dimerisation domain and contains five helices. It forms relatively few contacts with the other domains of the subunit, but is involved in an extensive dimerisation interface (Figure 3.11 (a)).

Fig 3.11 (a) and (b) First two domains

The middle, the second domain is made up of residues 96-168 and is all helical (Figure 3.11 (b)).

Fig 3.11 (c) The third domain

The C- terminal domain, comprising amino acid residues 169-334 has the typical α/ß fold commonly found in nucleotide binding proteins (Figure 3.11(c)). The C-terminal domain has a structure typical of most small molecule methyltransferases, many of which have been characterized structurally.
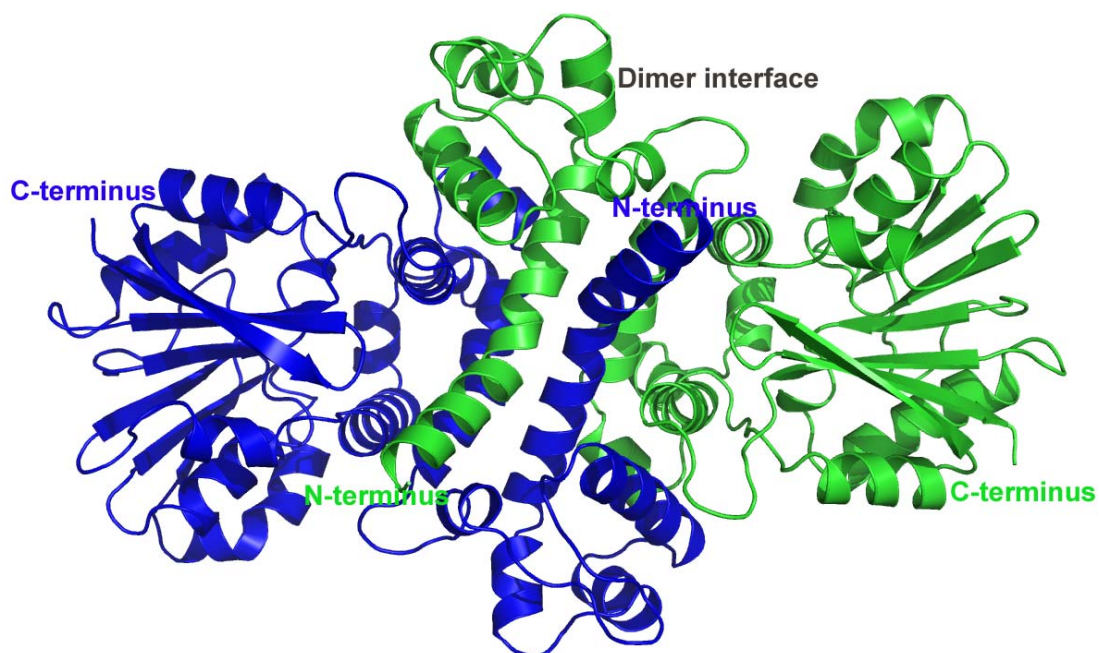
Domain III contains the SAM binding site, has a Rossmann-like fold, and consists of a ß-sheet with a strand topology 3214576 where all except ß7 are parallel to each other. This domain consists of the conserved nucleotide binding fingerprint (DLGGGxG) and SAM binds at the carboxy end of the ß-sheet (Figure 3.12).

```
                   :              :            .   :   *  * *  :  :        ::                         .   : *::*
1tw2  -----GSPNSTAEPTVAARPQQIDALRTLIRLGSLHTPMVVRTAATLRLVDHILAGARTVKALA----------ARTDTRPEALLRLIR   74
1tw3  -----GSPNSTAEPTVAARPQQIDALRTLIRLGSLHTPMVVRTAATLRLVDHILAGARTVKALA----------ARTDTRPEALLRLIR   74
1qzz  -----MSSSSPGEP-LEPTDQDLDVL--LRNLGNLVTPMALRVAATLRLVDHLIAGADTLAGLA----------DRTDTHPQALSRLVR   71
1kyz  MG----STGETQITPTHISDEE-ANLRAMQLASASVLPMILRSALELDLLEIIARAGP-GAQISPIEIASQLP--TTNPDAPVMLDRMLR   82
1fpq  MGNSVITKEDNQISATSEQTEDSACLSAMVITTNLVYPAVINAAIDLNLREIIAKATPPGARMSPSEIASKLPASTQHSDLPNRLDRMLR   90
phzm  ---------------MNNSNLAAARNLIQVVTGEKKSRCVVVATRLGLADLIESGIDSDETLA----------AAVGSDAERIHRLMR   63

      *.     ::    .               *:  :                 :            .:      :        .*     :.
1tw2  HLVAIGLLE--EDAPGERVPTEV-------GELLADDHPAAQRAMHDLTQAVARADISFTRLPDAIRTGRPTVESIVGKPFVEDLAGRPD  155
1tw3  HLVAIGLLE--EDAPGERVPTEV-------GELLADDHPAAQRAMHDLTQAVARADISFTRLPDAIRTGRPTVESIYGKPFVEDLAGRPD  155
1qzz  HLTVVGVLEGGERQGFPLRPTRL-------GMLLADGHPAQCRAWLDLNGAVSHADLAFTGLLDVVRTGRPAMAGRYGRPFWEDLSADVA  154
1kyz  LLACYIILTCSVRTQQDGKVQRLYGLATVAKYLVKNEDGVSISALNLMNQDKVLMESWYHLKDAVLDGGIP-NKAYGMTAREVHGTDPR  171
1fpq  LLASYSVLTSTTRTIEDGGAERVYGLSMVGKYLVPDESRGRLASFTTFLCTPALLQVWMNRKEAVVDEDIDLRKNVHGVTRVEMGKDKK  180
phzm  LLVARFIRQGDTRDGYANTPT--------SHLLRDVE-GSFHDMVLFYGEERFA--AWTPACEALLSGTPGVELARGEDFYSVLKRCPD  141

       *    :       .        ::.  :     :      .:     .: *****:*     *      *      .:     *            :     .  **:: :
1tw2  LRASFDSLLACDQDVARDAPAAARD-WTNVRHVLDVGGGKGGVAAAIARRAPHVSATVLEMAGTVDTARSVLKDEGLSDFVDVVEGDFTE  244
1tw3  LRASFDSLLACDQDVARDAPAAARD-WTNVRHVLDVGGGKGGVAAAIARRAPHVSATVLEMAGTVDTARSVLKDEGLSDFVDVVEGDFTE  244
1qzz  LADSFDALMSCDEDLAYEAPADARD-WSAVRHVLDVGGGNGGMLAAIALRAPHLRGTLVELAGPAEHARRRVADAGLADRVTVAEGDFRK  243
1kyz  TNRVENKGMSDHSTITMKKILETYTGYEGLRSLVDVGGGTGAVINTIVSKYPTIRGINFDLPHVIEDAPSY-------PGVEHVGGDMFV  254
1fpq  MNQIRNKSMVDVCATEMKRMLEIYTGYEGISTLVDVGGGSGHNLELIISKYPLIRGINFDLPQVIENAPPL-------SGIEHVGGDMFA  263
phzm  AGRRFLLAMKAS-NLAFHEIPRLLD-FRG-RSFVDVGGGSGELTKAILQAEPSARGVMLDREGSLGVARDNLSSLLAGERVSLVGGDMIQ  228

      :*   .*   ::.  :   :    :    .:  :*   *  .*:    .*::::  :             :     :             .*   **    *.  :  :
1tw2  PLPRRADAIILSFVLLNWPDHDAVRILTRCAEALEPGGRILIRERDDLHENSINEQR-TELDLRMLVRL---GGALRTREKVDGLAASAG  330
1tw3  PLPRRADAIILSFVLLNWPDHDAVRILTRCAEALEPGGRILIRERDDLHENSINEQR-TELDLRMLVRL---GGALRTREKVDGLAASAG  330
1qzz  PLPVTADVVLLSFVLLNWSDEDALTILRGCVRALEPGGRLLVIDRADVEGDGADRFPSTLLDLRMLTRM---GGRVRTRDEVVDLAGSAG  330
1kyz  SIP-KADAVRMKWICHDWSDEHCLKPLRNCYEALPDNGKVIVAECILPVAPDSSLATKGVVHIDVIMLAHNPGGKERTQREFEDLAKGAG  343
1fpq  SVP-QGDAMILKAVCHNWSDEKCIEFLSNCHKALSPNGKVIIVEFILPEEPNTSEESKLVSTLDNLMRI-TVGGRERTEKQLEKLSKLSG  351
phzm  EVPSNGDIYLLSRIIGDIDEAASLRLLGNCREAMAGDGFRVVVIERTISASEPSP--MSVLRDVHLRMAC---AGRHRTTEEVVDLLGRGG  313

                  :              :
1tw2  LVVEEVRQLPSPTIPVDLSLLVL-------APAATGA-------  360
1tw3  LVVEEVRQLPSPTIPVDLSLLVL-------APAATGA-------  360
1qzz  LALASERTSGSTTLPRDFSILERTAVSEEAAPAAQASEALPAQE  374
1kyz  QGFRKVHCNARNTY-IMEFLKKV--------------------  365
1fpq  SRRQVACRARNSLGVMEPYR--------------------  372
phzm  RAVERIVDLPMETRMIVAARA-------------------  334
```

Fig 3.12 Sequence alignment of PhzM with other homologues proteins. The SAM binding motif shown in red arrows

4.4.1.2 Dimer of PhzM and dimer interface

The N-terminal domain plays an important role in the dimerisation of PhzM. The figure below (Figure 3.13) shows the dimer of PhzM with monomers highlighted in two different colours.

Fig 3.13 Dimer of PhzM

The dimer interface is formed mainly by Domain I, the N-terminal domain comprising of five helices and one helix from the C- terminal domain. Of the residues participating in the dimer interactions, 55% are polar, 45% non-polar residues.

Polar Residues	Asn5, 11, 81; Arg10, 23, 30, 57, 60, 63, 76, 89, 96; Q14, 72; Thr17, 29, 46, 75, 82, 84, 111, 121; Glu19, 38, 45, 56, 69, 92, 104, 105, 115, 125, 130; Lys21; Ser22, 39, 43, 53, 85, 94, 119, 284; Cys24; 114; Tyr26, 79, 102; Asp35, 42, 44, 54, 74, 77, 90, 97, 131, 288; His59, 86, 107, 290;
Non- Polar Residues	Leu6, 12, 31, 33, 36, 47, 61, 64, 65, 87, 88, 100, 117, 118, 126, 286, 291; Ala7, 8, 9, 28, 34, 48, 49, 50, 55, 67, 80, 108, 109, 113, 116, 127; Ile13, 37, 41, 58, 70; Val15, 16, 25, 27, 51, 66, 91, 99, 285, 289; Gly18, 32, 40, 52, 63, 68, 93, 103, 120, 123, 129; Trp20, 110, 287; Met62, 98, 283, 293; Phe68, 71, 95, 101, 106, 124, 132, 292; Pro83, 112, 122, 282

4.4.1.3 PhzM and homologues structures

The polypeptide chain of PhzM from *Pseudomonas aeruginosa* consists of 334 amino acids and shows significant sequence identity with several SAM-binding enzymes deposited in the structure database PDB (citation PDB: H.M. Berman, J. Westbrook, Z. Feng, G. Gilliland, T.N. Bhat, H. Weissig, I.N. Shindyalov, P.E. Bourne: The Protein Data Bank Nucleic Acids Research, 28 pp. 235-242 (2000).), including isoflavone O-methyltransferase (24 % sequence identity, PDB-access code 1fp2; Zubieta *et al*., Nat.Struct.Biol. v8 pp.271-279, 2001), carminomycin-4-O-methyltransferase (sequence identity 26 %, PDB access code 1tw2; Jansson *et al.,* C v279 pp. 41149-56, 2004), aclacinomycin-10-hydroxylase (sequence identity 24 %, PDB access code 1qzz; Jansson *et al*., J.Mol.Biol. v334 pp.269-280 , 2003) and caffeic acid 3-O-methyltransferase (24 % sequence identity, PDB-access code 1kyz;(121) (Figure 3.14).
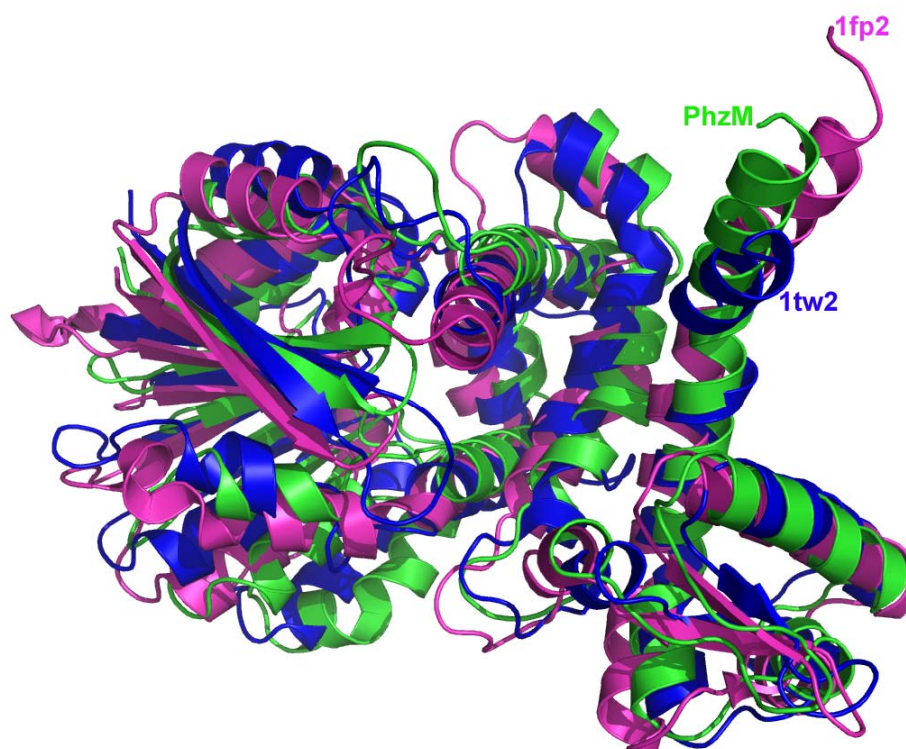
Fig 3.14 Superimposition of PhzM and other related structures

These relatives belong to the class of small molecule SAM-dependent methyltransferases (122) and like these enzymes, PhzM contains the DXGGGXG fingerprint motif, characteristic for the nucleotide-binding site of S-adenosyl-L-methionine. However, unlike the related proteins listed above, PhzM transfers a methyl group to a nitrogen atom and our data therefore present the first efforts toward the structure of a phenazine-specific small molecule N-methyltransferase.

4.4.1.4 SAM binding site or the C-terminal domain

Like the homologous structure of PhzM the binding site for the cofactor SAM of PhzM is located in the domain III at the C-terminal ends of the first two ß-strands of the large ß sheet (Figure 3.15). SAM is bound to the protein through an extensive hydrogen bond network.
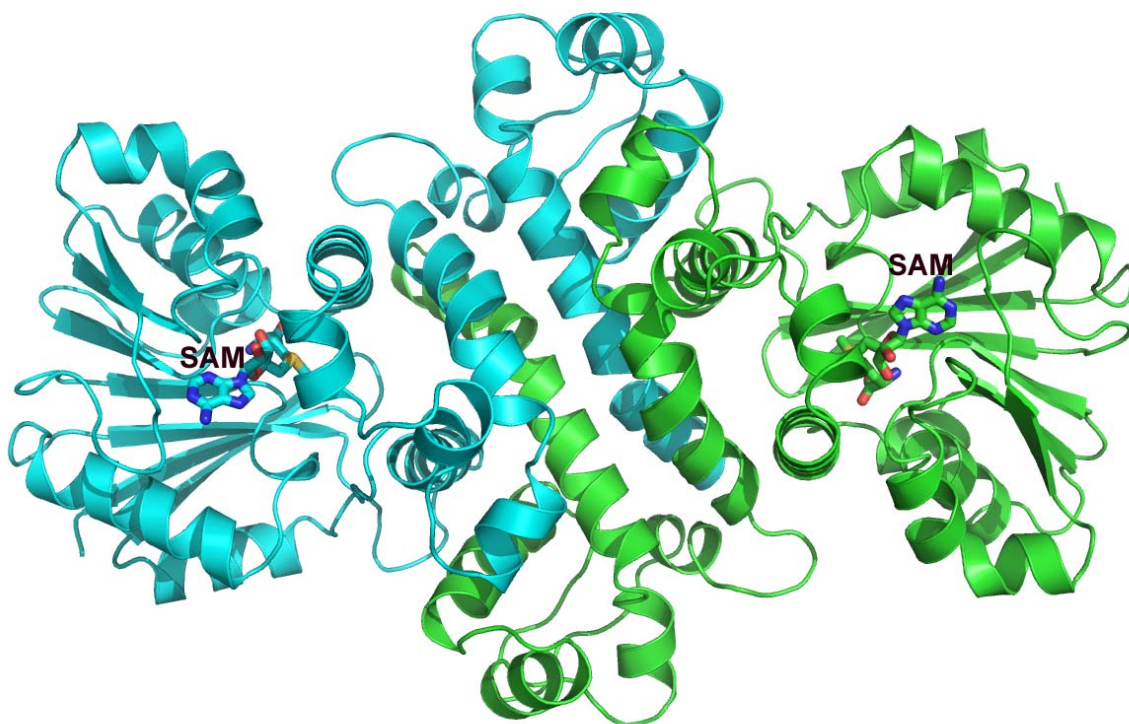
Fig 3.15 Dimer of PhzM showing the SAM binding site

The carboxyl group of the SAM molecule interacts with the hydroxyl group of side chain of Ser240 and amino group of Arg241. The amino group of SAM is anchored to the main chain carbonyl oxygen atom of Gly175. The ribose moiety forms hydrogen-bonding interactions via the two hydroxyl groups to the side chain of Asp198. The main chain carboxyl oxygen atom of Asp225 form hydrogen bonds to the amino group on the adenine ring (Figure 3.16)

84
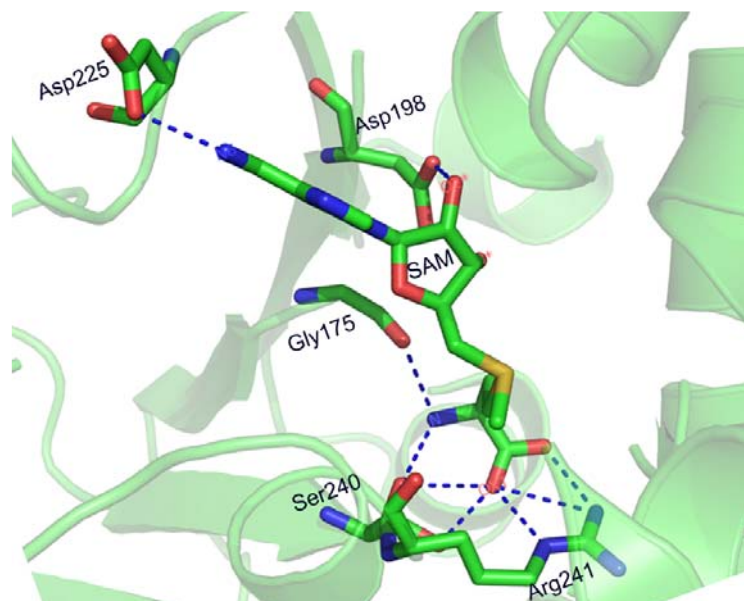
Fig 3.16 Interaction of SAM with the residues of PhzM shown by blue dotted lines

PhzM unlike the majority of methyltransferases is a dimer. The fold categorizes PhzM as a class I methyltransferase. In comparison, the two crystal forms reveal a dramatic movement of the SAM binding domain, which moves up to 8 Angstroms between the two structures (Figure 3.17).
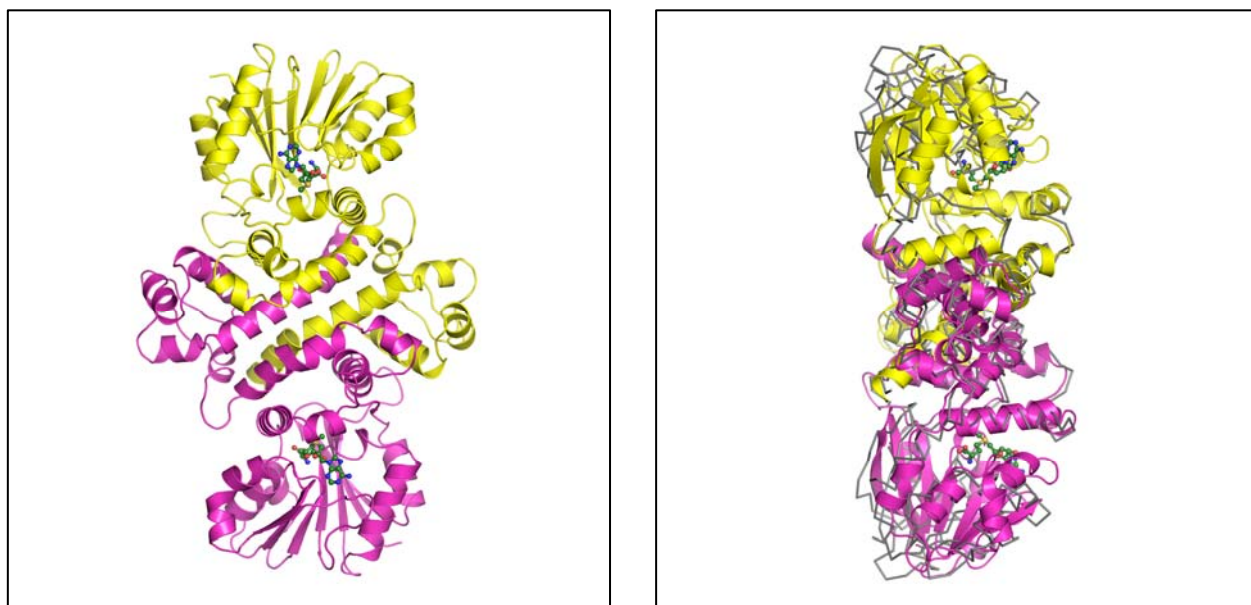
Fig 3.17 The two forms of PhzM open and closed

In the closed, SAM bound form, a substrate-binding site large enough for accepting a tricyclic phenazine molecule is generated (Figure 3.18). Modelling shows how the substrate is positioned for methyl transfer from the cofactor. In (Figure 2.18) the tricyclic phenazine molecule considered is PCA since till now studies have tried to prove PCA being the substrate. However, in this study we have found through biochemical assays that it is infact 1-oh-phenazine which is the substrate for the enzyme PhzM. Therefore, crystal structure of PhzM complexed with 1-oh-phenazine will help us to prove the same.
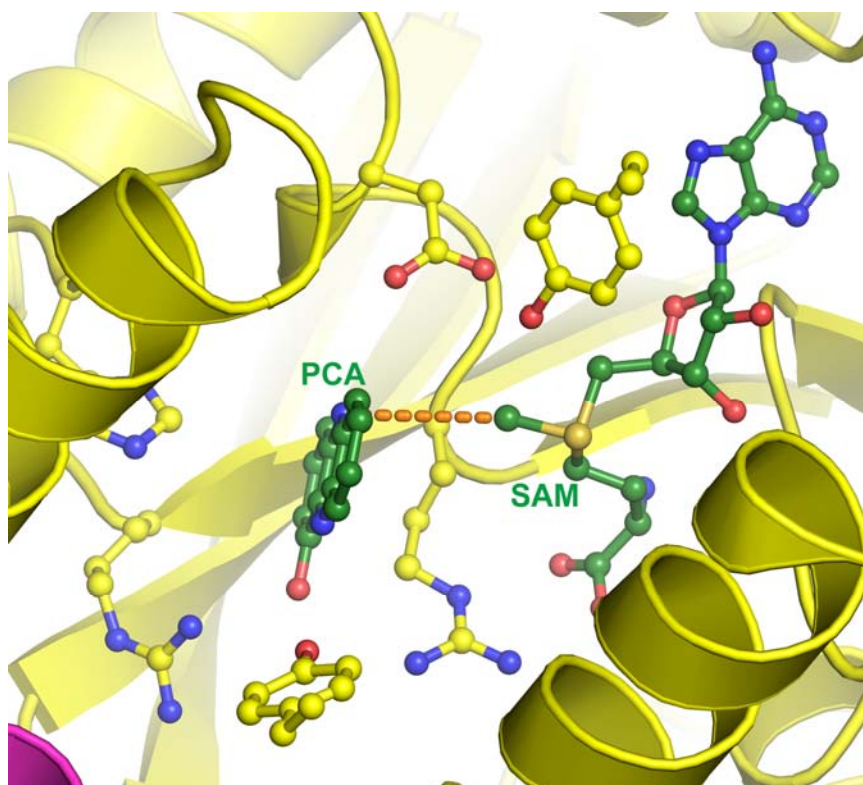
Fig 3.18 Interaction of the substrate with SAM

4.4.2 Structural Analysis of PhzS from *Pseudomonas aeruginosa*

PhzS (FAD or flavin dependent mono-oxygenase) is a dimeric protein comprising of two identical single subunits of 402 amino acids each with a monomer molecular weight of 43.6 kDa.
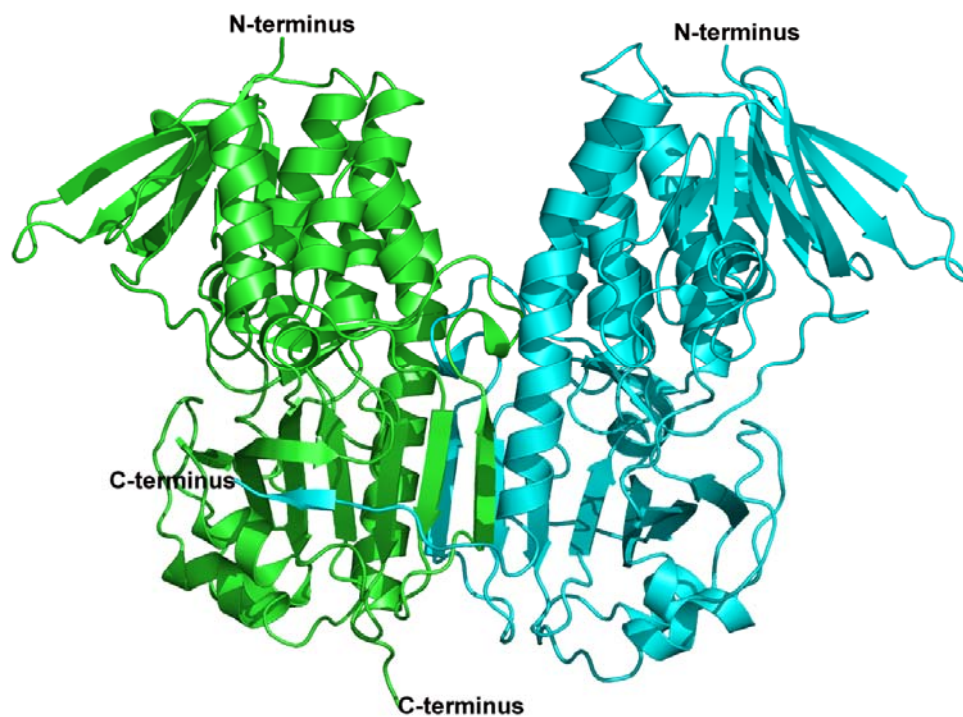
Fig 3.19 PhzS dimer with the two subunits coloured in green and blue

4.4.2.1 Monomer of PhzS

The polypeptide of PhzS is composed mainly of 3 domains (Figure 3.20).
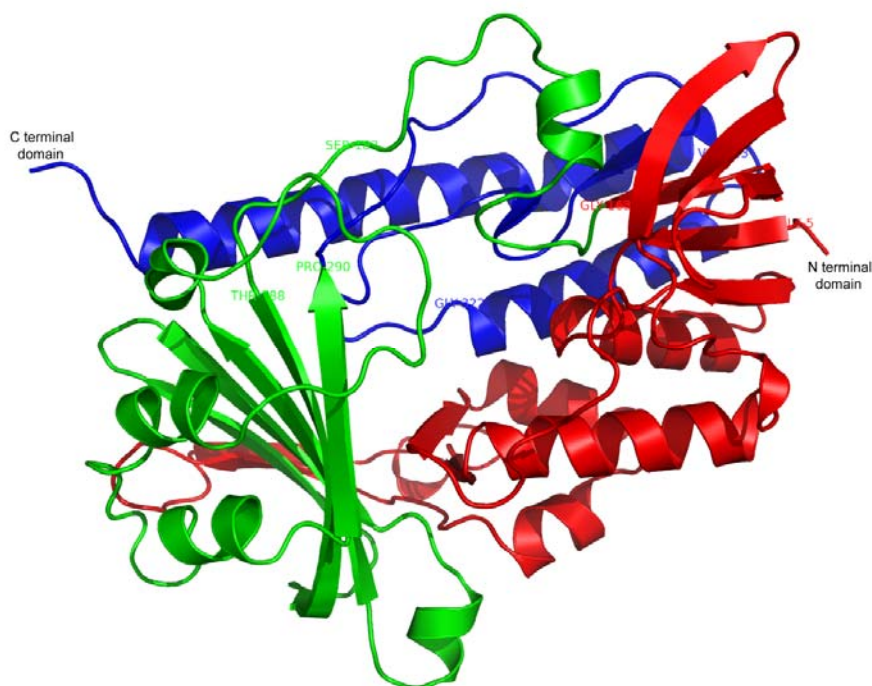
Fig 2.20 Monomer of PhzS with three domains

The N-terminal domain represents the FAD binding domain spanning residues from 4 to 163 and has a βαβ fold formed by strand A1 (6-11); helix H1 (14-28) and strand A2 (30-36).
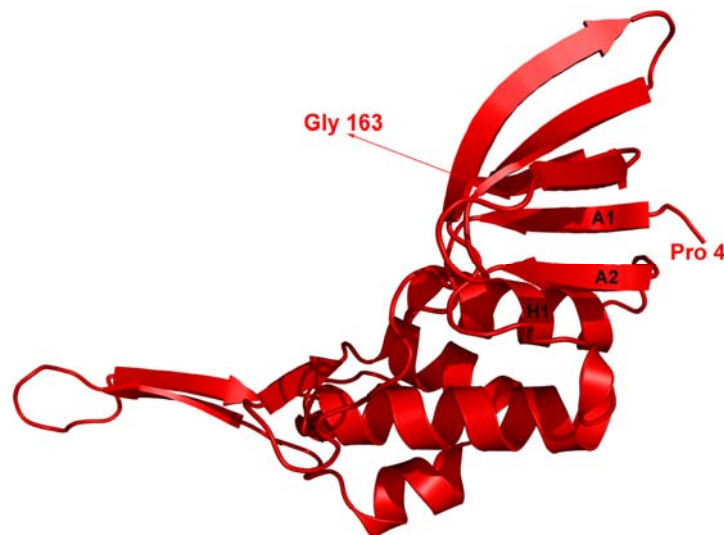
Fig 3.21 (a) showing the first domain

This fold binds the adenosine part of the FAD (Figure 2.21 (a)). The partial positive charge induced by the dipole moment of helix (H1) helps to compensate for the negative charge of the pyrophosphate moiety of the FAD. The same βαβ conformation has been observed in many NAD(P)H using enzymes(123).
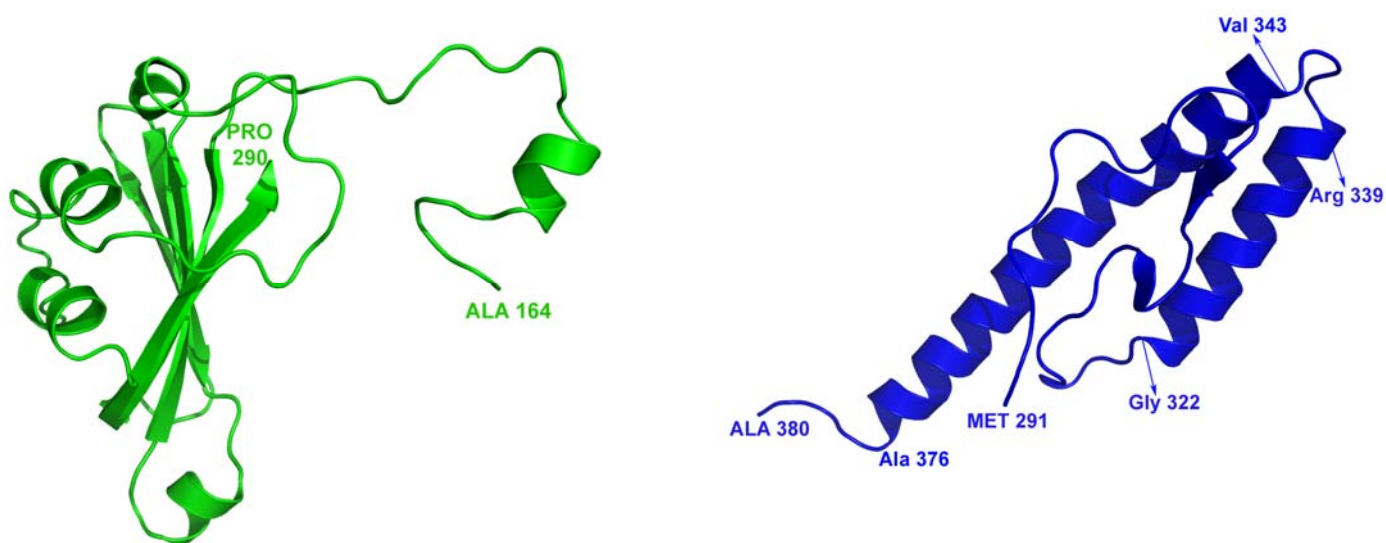
Fig 3.21 (b) and (c) showing the second and the third domain

The second domain spanning residues from 164 to 290 consists of a 'wall' of β- sheets ranging from 205 to 290 (Figure 3.21 (b)).

The third domain, the interface domain spans residues from 291 to 380. This C-terminal domain is dominated by two helices Gly322 - Arg339 and Val343 – Ala376 (Figure 3.21(c)).

4.4.2.2 The Rossmann fold

Like other dinucleotide binding proteins PhzS also exhibits conserved sequence motifs at positions crucial for binding substrates and cofactors. One of the fold is termed as the Rossamann fold (124) that consists of six parallel ß-strands interspersed by α -helices that appear on both sides of the six-stranded ß sheet. This symmetrical α/ß structure is built from two halves $ß_1 α_1 ß_2 α_2 ß_3$ and $ß_4 α_4 ß_5 α_5 ß_6$ with a crossover α helix ($α_3$) connecting $ß_3$ and $ß_4$ (Fig. 3.22).
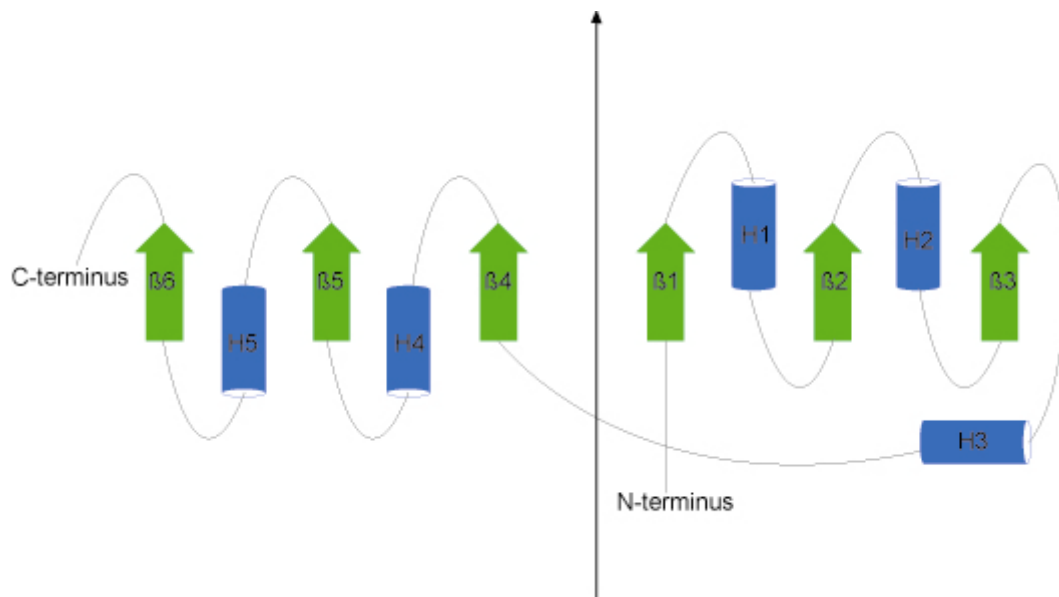
Fig 3.22 Each of the motifs is known as the classical mononucleotide-binding motif or the Rossmann fold. Cylinders represent α-helices and arrows denote ß-strands. The overall pseudo two-fold rotation symmetry between the two ßαßαß motifs is shown by an arrow.

Each of these folds is known as the classical mononucleotide binding fold or the Rossmann fold. A variation of this fold is found in the FAD binding proteins.

Amongst the entire FAD binding proteins the most thoroughly studied family is that of the glutathione reductase (GR) family. PhzS resembles the well-studied p-hydroxybenzoate hydroxylase, which belongs to the GR family and more specifically to the GR2 family. The Rossmann fold is seen in both the families, however with some exceptions.
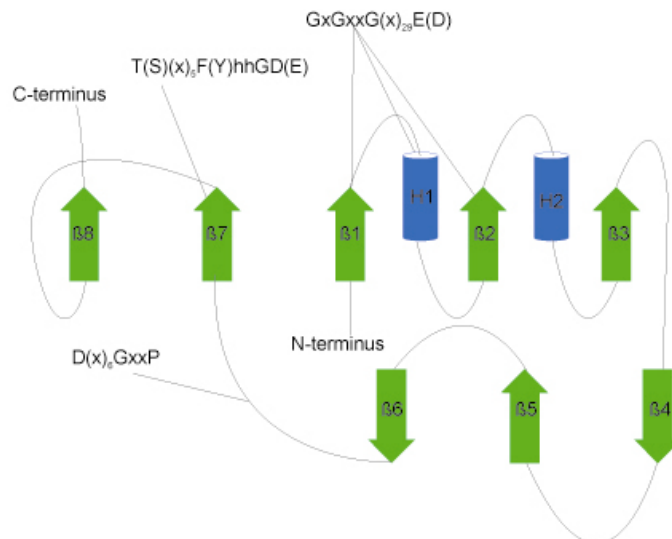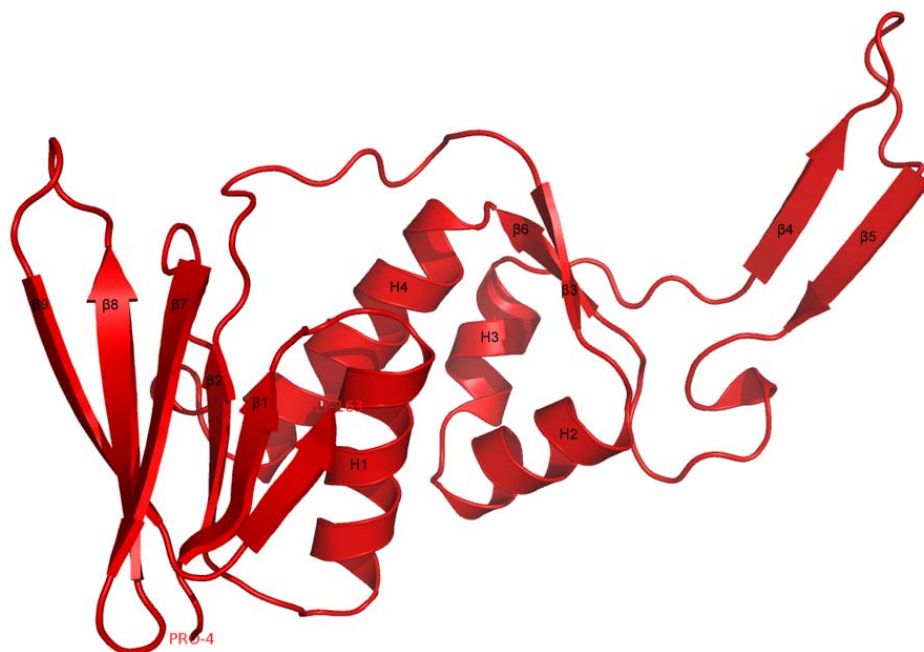

Fig 3.23 (a) FAD binding motif

Fig. 3.23 (a) shows the Rossmann fold adopted by the GR family members. PhzS also shows a more or less similar fold in the FAD binding motif. However in PhzS the β_3 and β_4 are connected through two small crossover α –helices instead of 3-strand ß-meander.
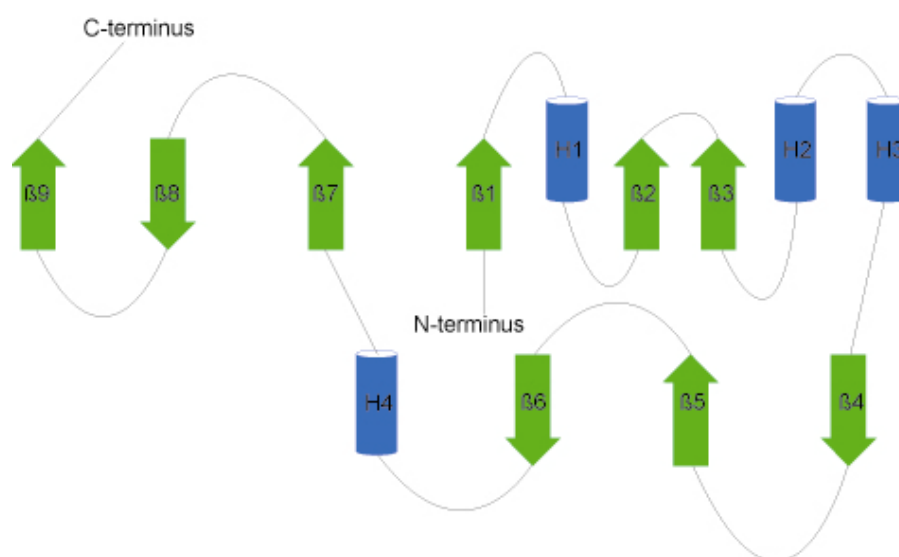
Fig 3.23 (b) FAD binding motif in PhzS

The most conserved and well-studied sequence motif is part of the Rossmann fold, xhxhGxGxxGxxxhxxh(x)8hxhE(D), where 'x' is any residue and 'h' is a hydrophobic residue (125-127) (Fig. 3.23 (b)). This motif is found at the N-terminal part of the sequence. Like the GR family PhzS also has this motif starting from residue number Ile7 to Glu35. The central part of the sequence motif of the Rossmann fold i.e., GxGxxG, is part of loop connecting the first ß-strand and α –helix in the ßαßαß fold with the N-terminal end of the α –helix pointing to the pyrophosphate moiety of FAD for charge compensation. This consensus is known as the dinucleotide binding motif (DBM) (127) or the phosphate binding sequence signature (128).

Fig 3.24 Structure of PhzS showing the Rossmann fold

In the GxGxxG motif of the FAD binding domain in PhzS, the first strictly conserved glycine residue (Gly 11) allows for the tight turn of the main chain, which is important for the positioning of the second glycine residue. This (Gly 13) residue on the other hand because of its missing side chain, permits close contact of the main chain to the pyrophosphate of FAD, specifically the oxygen atoms. The third glycine (Gly 15) allows close packing of the helix with the ß –sheet (Fig. 3.25).
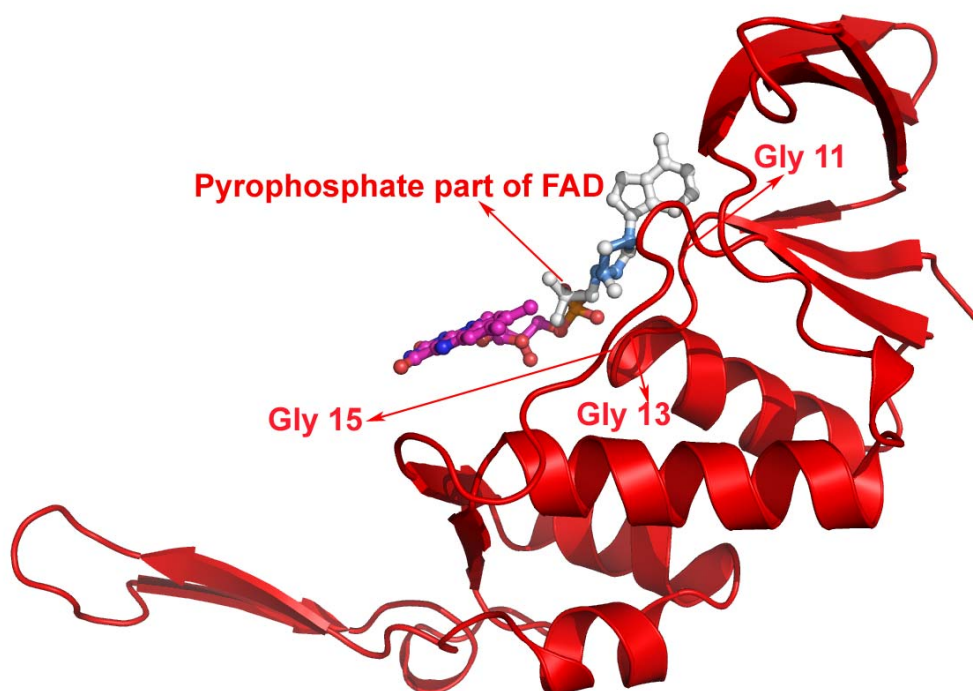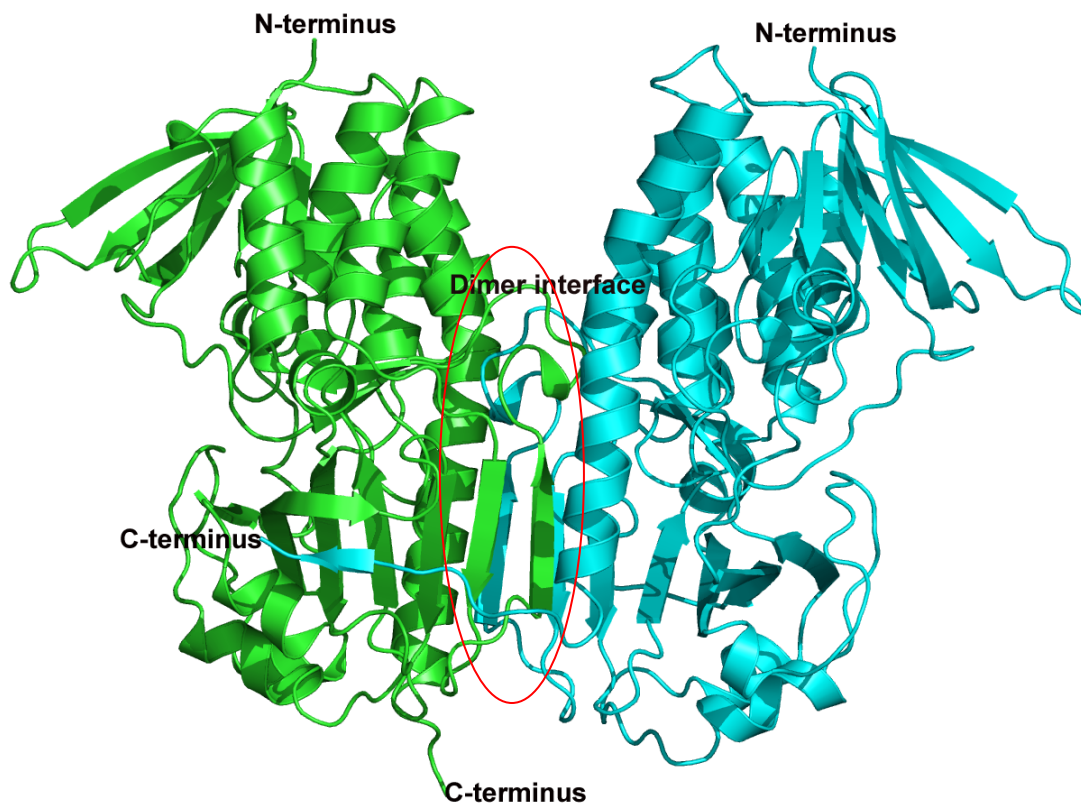
Fig 3.25 GxGxxG motif of FAD binding domain

The hydrophobic residues provide hydrophobic interactions of the alpha helix with the ß-sheet. The conserved negatively charged terminal residue (Glu35) at the end of this FAD binding motif, forms hydrogen bond with the ribose 2'-hydroxyl of the adenosine moiety.

4.4.2.3 Dimer of PhzS and dimer interface

The dimer interface is formed mainly by Domain I, the N-terminal domain comprising of five helices and one helix from the C-terminal domain. Of the residues participating in the dimer interactions, 28% are polar, 59% non-polar residues.

*Fig 3.26 The PhzS dimer showing the dimer interface*

Polar Residues	Asn48, 97; Q25, 50, 81, 101, 123, 124, 154; Thr32, 69, 73, 85, 128; Glu3, 35, 39, 55, 59, 75, 89, 94, 108, 119, 133, 137, 138; Lys30; Cys19; Tyr78, 99, 102; Asp139, 148, 159; His24, 74, 105, 150; Ser2, 8, 36-38, 82, 88, 103
Non-Polar Residues	Leu7, 17, 21, 23, 33, 34, 43, 57, 60, 62, 66, 76, 109, 121, 130, 143, 156, 161; Ala10, 12, 20, 22, 26, 52, 53, 56, 58, 65, 67, 68, 70, 84, 95, 98, 115, 116, 125, 146, 155, 158; Ile 5, 7, 9, 14, 28, 40, 47, 49, 71, 79, 104, 112, 135, 144; Val31, 45, 54, 86, 93, 117, 126, 132, 142, 160, 162; Gly11, 13, 15, 16, 27, 29, 44, 46, 61, 63, 83, 92, 96, 107, 122, 129, 131, 140, 145, 149, 151, 157, 163; Trp87; Met1, 111; Pro4, 42, 51, 64, 72, 90, 100, 153

4.4.2.4 PhzS and the homologues structure

Predictions from the fold recognition programme 3D PSSM (129) indicate that PhzS possesses significant fold similarity with FAD-dependent oxidoreductases and indicate 17% sequence similarity with p-hydroxybenzoate hydroxylase (PDB access code 1PHH;(130), a flavoprotein involved in the degradation of aromatic compounds and a model for enzymes involved in the oxygenation of a substrate (Fig. 3.27).
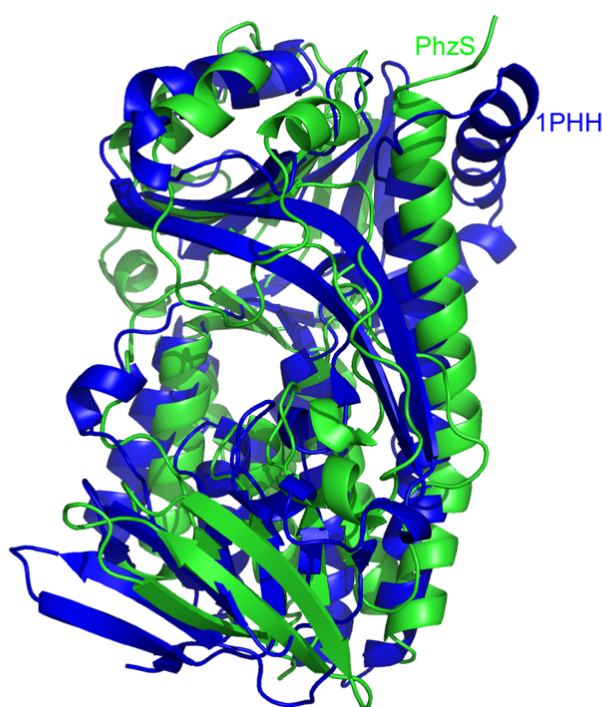

Fig 3.27 Superimposition of 1PHH and PhzS

Both PhzS and p-hydroxybenzoate hydroxylase belong to the class of FAD-dependent monooxygenases. These enzymes catalyse the insertion of one atom of dioxygen into a variety of substrates while the other oxygen atom is reduced to water. The monooxygenases use an external reducing agent to provide electrons to reduce oxygen to the level of hydrogen peroxide, which is then responsible for the insertion of oxygen into the substrate. These enzymes are reduced by NAD(P)H to give $FADH_2$, which then binds molecular oxygen to form a spectroscopically characterized highly reactive peroxide-linked flavin. This intermediate is decomposed by the nucleophilic attack of an

adjacent substrate, resulting in oxygen atom transfer(131). In PhzS, this leads to a decarboxylation of the substrate with concomitant incorporation of a hydroxyl group.

The C-terminal domain

The C-terminal region of both PhzS and 1PHH is dominated by helices. In case of 1PHH apart from the two long helices spanning residues from 298 to 358 there are two short helices as well which is not seen in PhzS. However this is because of the absence of the electron density for the last 22 residues in PhzS in one of the monomers. In 1PHH the function of helix H10 seems merely to be giving the molecule rigidity; helix H10 has an important function in catalysis. It stabilises the negative charge of the flavin ring after its reduction. Secondly plays an important role in the removal of NADP$^+$ from the active site due to electrostatic repulsion of the positively charged oxidised nicotinamide.
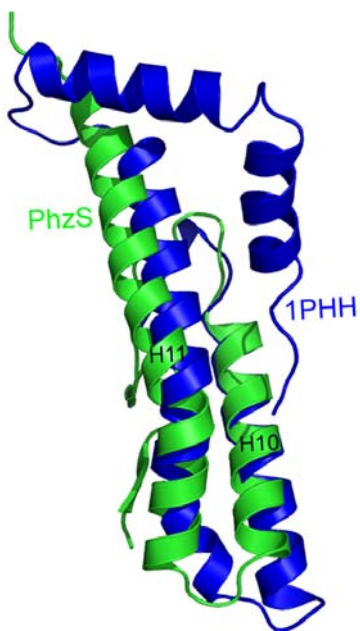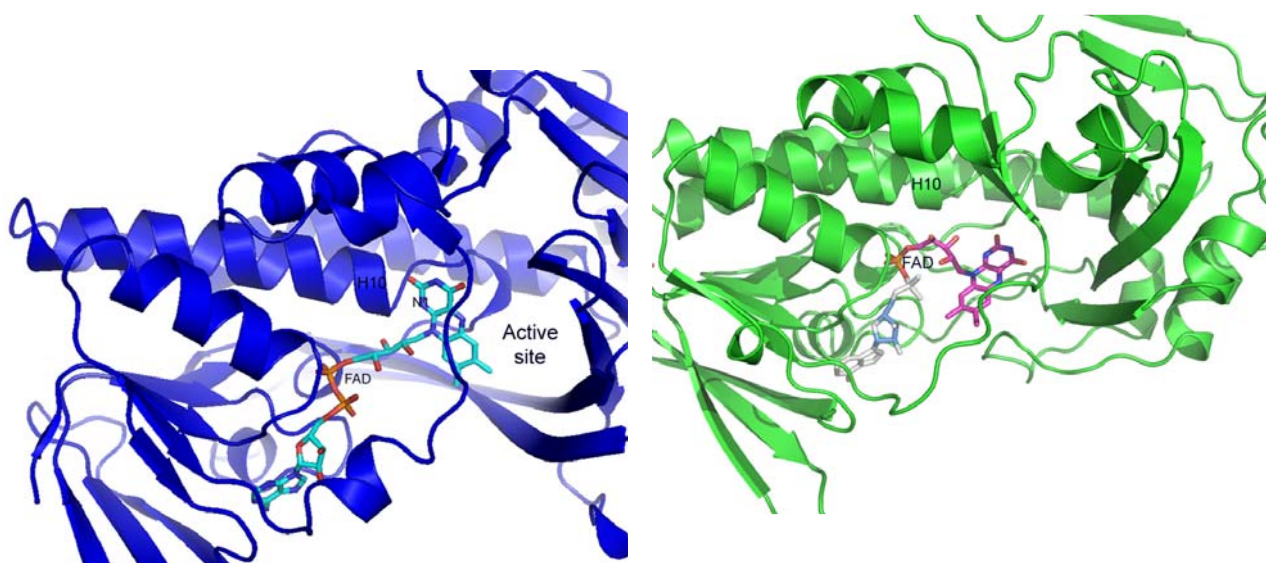
Fig 3.28 (b) The difference in the conformation of FAD in PhzS and 1PHH

However in case of PhzS although the flavin ring is in the elongated conformation but the degree of extension of the cofactor is different compared to 1PHH. This conformational flexibility allows the substrate to gain access to the active site and excludes solvent during the hydroxylation reaction.

Other than 1PHH, PhzS also shows some fold similarity with one more FAD dependent hydroxylase (1foh or phenol hydroxylase) but only to a minute extent. This is the reason why only 1PHH has been taken into consideration for better understanding of the protein being investigated.

4.4.2.4 Getting an idea about substrate binding in PhzS from the function of 1PHH

1PHH or p-Hydroxybenzoate hydroxylase catalyses the hydroxylation of p-hydroxybenzoate (pOHB) to form the catechol 3,4-dihydroxybenzoate.
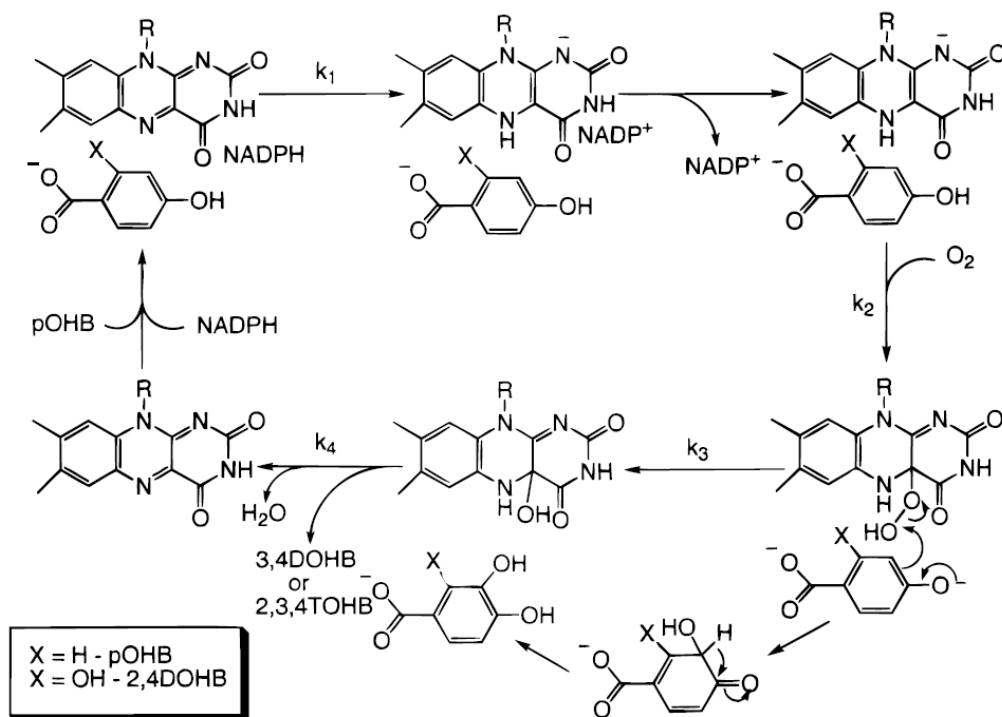
Fig 2.19 Catalytic cycle of p-hydroxybenzoate hydroxylase

1PHH, like other flavoprotein aromatic hydroxylases, activates molecular oxygen by forming a C4a-hydroperoxyflavin. The distal peroxy oxygen then incorporated into the aromatic substrate.
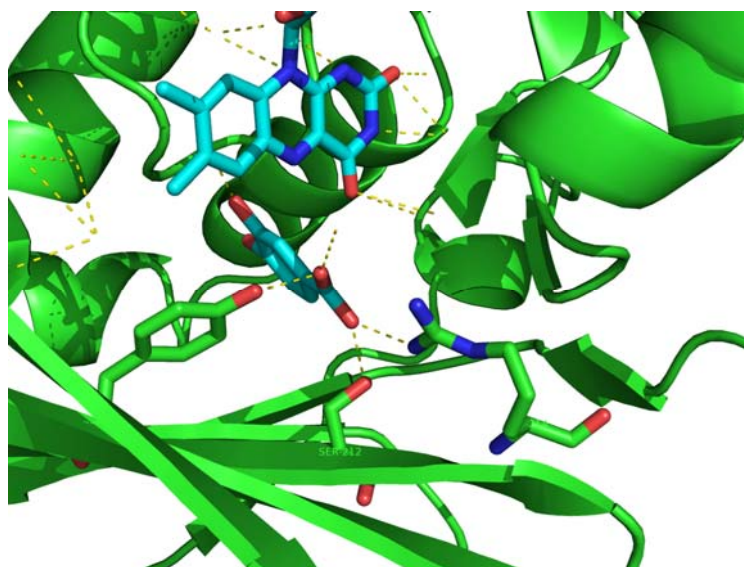

Fig 2.20 (a) 1PHH complexed with substrate

The crystal structure of 1PHH shows that the carboxyl moiety of the substrate pOHB interacts with three active site residues, Arg214, Tyr222 and Ser212 (Fig 2.20 (a)).

These residues form hydrogen bonds with the substrate carboxylate, one each from both Tyr222 and Ser212, and two from the ion paired Arg214. This helped us to construct a model of PhzS complexed with the substrate. The model reveals that in the crystal form studied in this case is in the oxidized form, expecting reduction by the cosubstrate NAD(P)H. following reduction, the isoalloxazine moiety will swing towards the substrate binding site, initiation decarboxylation-hydroxylation of the substrate phenazine-1-carboxylic acid or PCA. Thus, in normal catalysis flavin or the isoalloxazine ring moves to the out position so that the substrate can be bound, and then the flavin moves back in to exclude solvent and prevent it from interfering with the hydroxylation reaction (Fig. 2.20 (b)).
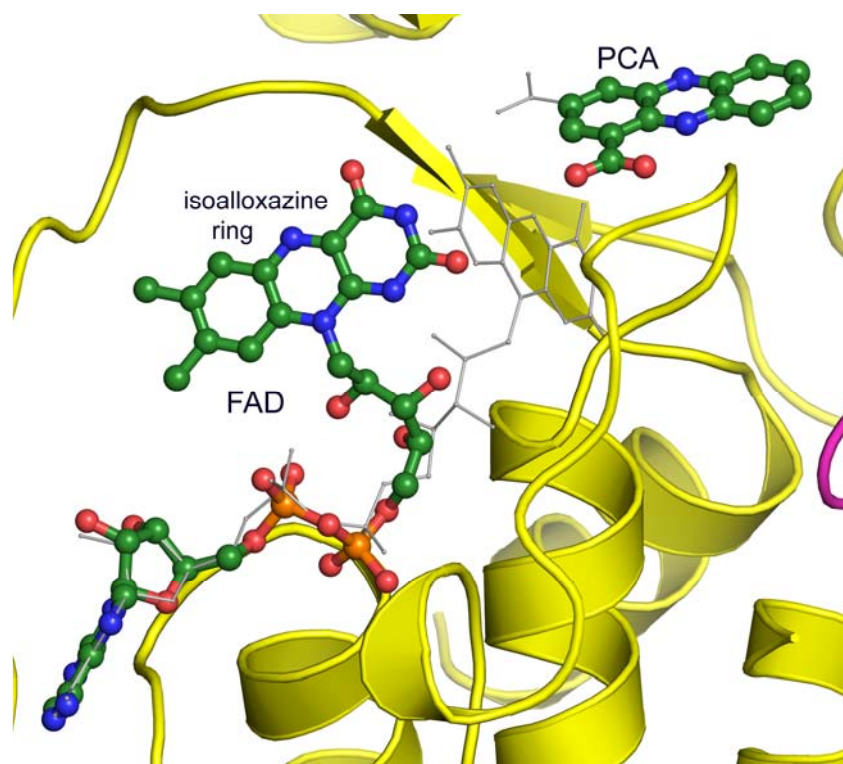
Fig 2.20 (b) The movement of the isoalloxazine ring in the PhzS structure

4.5 Biochemical analysis of proteins

4.5.1 Isothermal Titration Calorimetry

To find the interaction of SAM with PhzM we used ITC experiment. The result of the titration experiment, in which a fixed amount of PhzM was titrated against increasing concentration of SAM is shown in Figure 2.21.From the data the value of the binding constant (K_B) was found to be 1.94 x10^4 giving us the value of the dissociation constant (K_D) as 51µM using the formula

$$K_B = 1/K_D = 1/1.94 \times 10^4$$

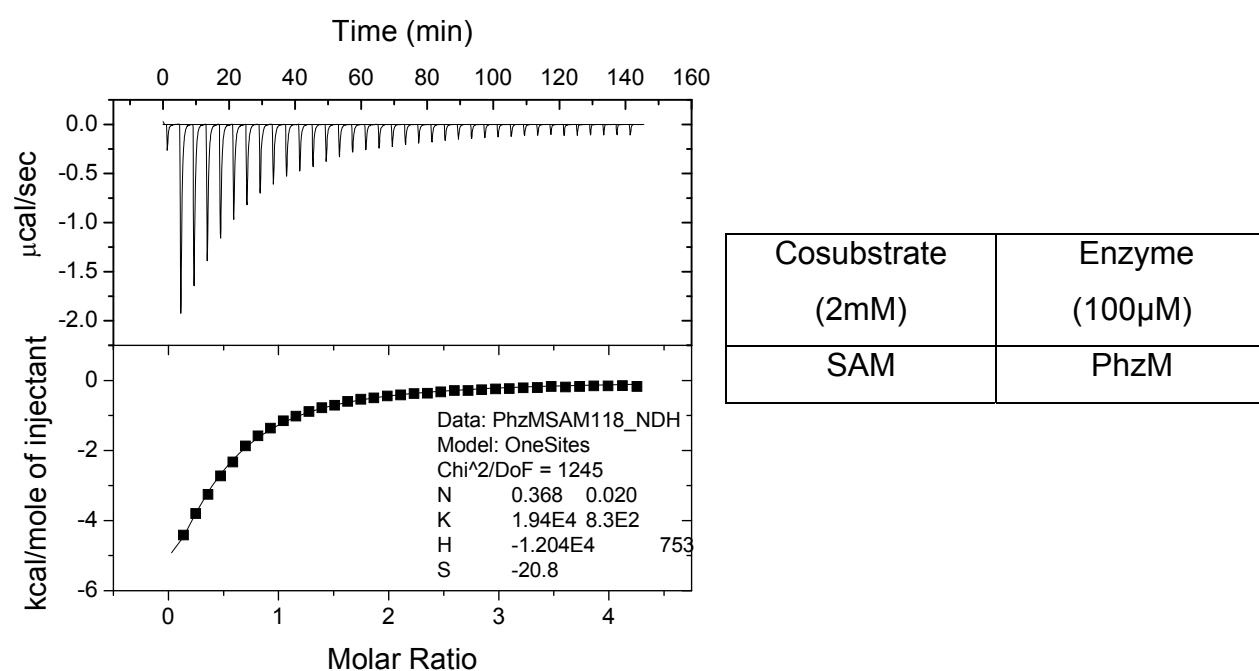| Cosubstrate (2mM)	Enzyme (100µM)
SAM	PhzM

Fig 2.21 The binding of SAM with PhzM

Although the binding of the substrate SAM with PhzM is not strong enough but it gave us an idea of cocrystallising the substrate with the enzyme to get an insight of the binding through crystallographic technique.

4.5.2 HPLC-APCI-MS

As mentioned earlier that there are two hypothetical reaction mechanisms for the biosynthesis of pyocyanin as can be seen in (Fig. 2.22). In order to get an insight to the reaction mechanism this was one of the methods employed.
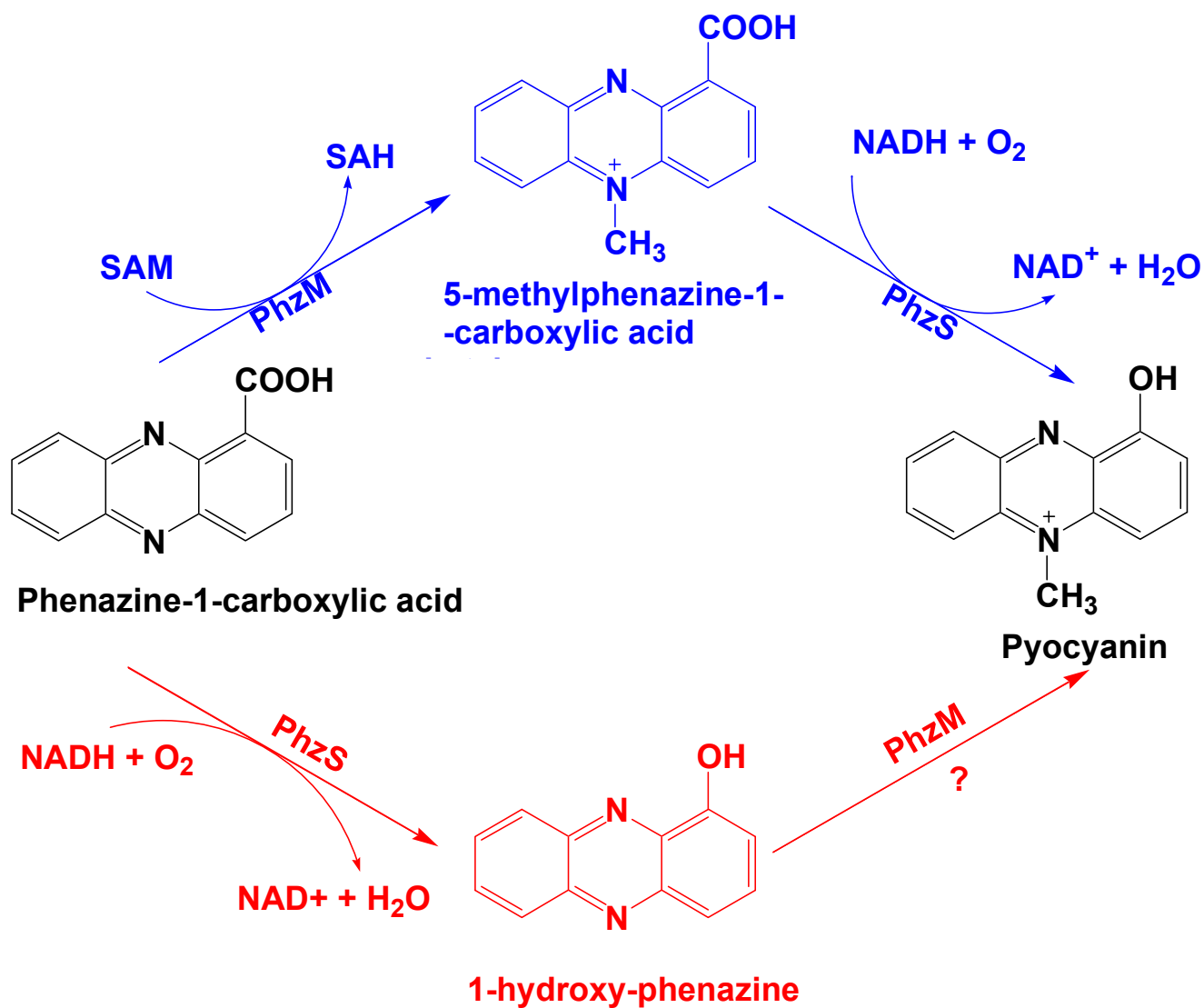

Fig 2.22 The reaction pathways
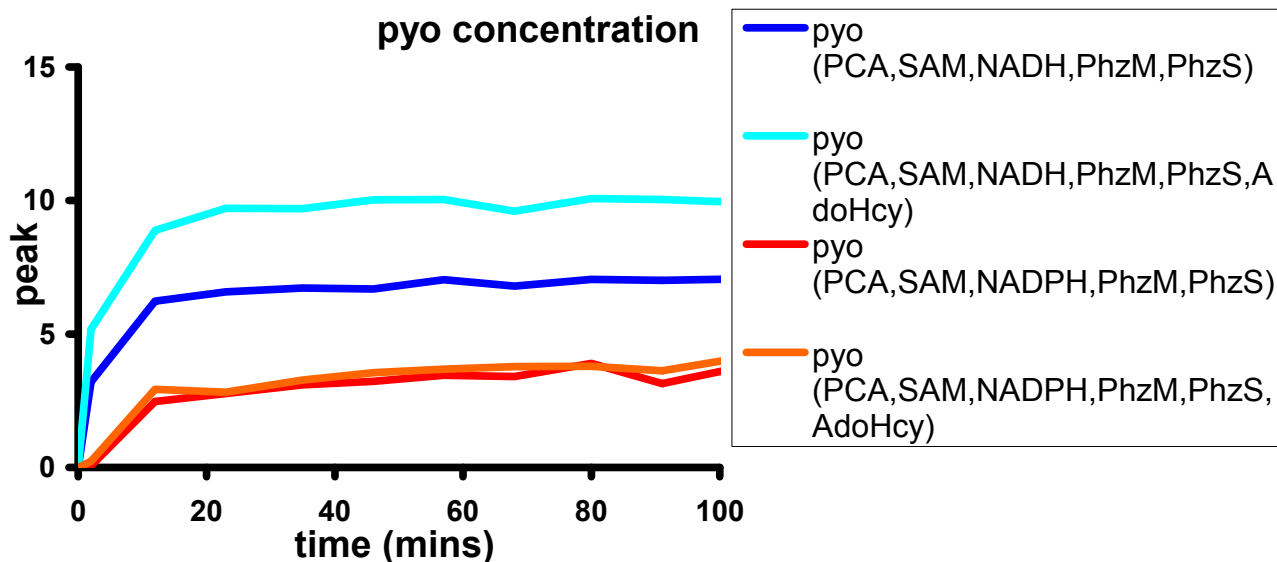
4.5.2.1 Pyocyanin biosynthesis

Fig 2.23(a) The change in the concentration of pyocyanin

Substrate (100 µM)	Cosubstrate (1mM)	Enzyme (10 µM)
PCA	SAM	PhzM
	NADH	PhzS
	NADPH	AdoHcy

First of all the overall formation of pyocyanin was monitored and was plotted as in the (Figure 2.23 a)). For the above reaction mixture as shown in the table the effect on the concentration of pyocyanin is seen when the enzymes are mixed with the specific substrates. However there is a difference in the concentration of pyocyanin formed and this variability is effected by the presence of NADPH and NADH in the reaction mixture. As we can see from the graphical representation that concentration of pyocyanin is much higher in presence of NADPH as compared to NADH. In addition to this there is one more difference that can be seen is the effect on pyocyanin in presence and absence of AdoHcy enzyme showing that this enzyme also plays certain role

in the biosynthesis of pyocyanin to some extent. As mentioned earlier in section1.8.2 AdoHcy helps in curbing the action of SAH, the negative regulator of methylation reactions.
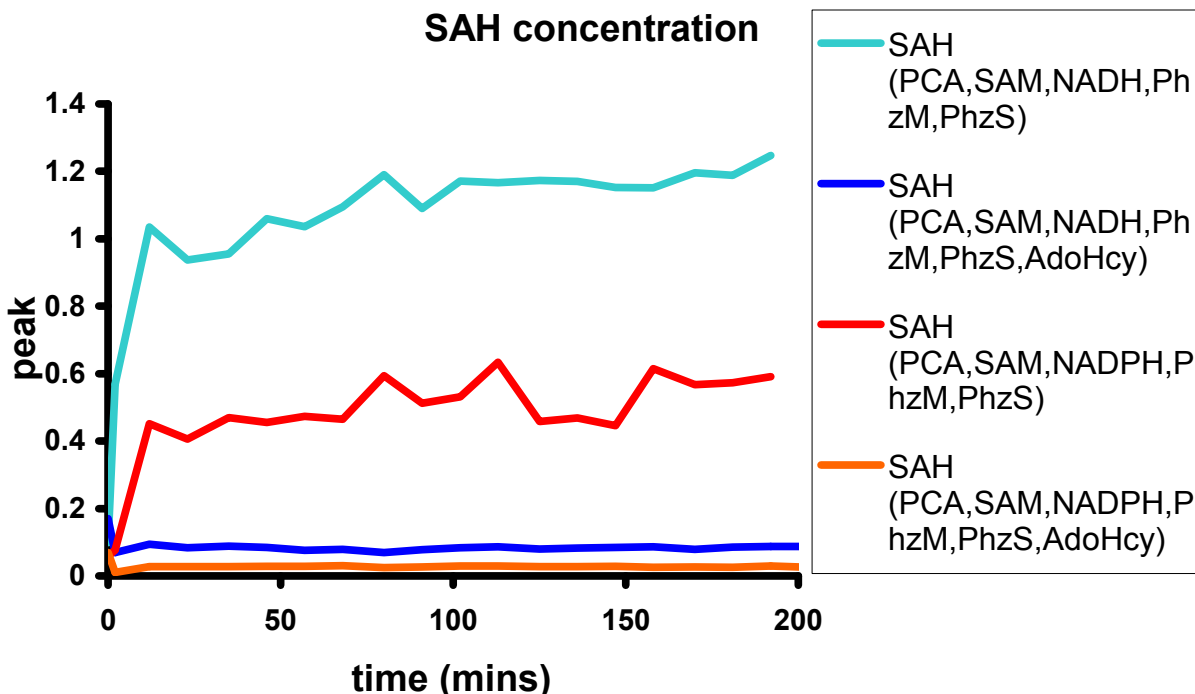

Fig 2.23(b) The effect on SAH in presence of AdoHcy

Substrate (100 µM)	Cosubstrate (1mM)	Enzyme (10 µM)
PCA	SAM, NADH, NADPH	PhzM, PhzS, AdoHcy

As we can see the concentration of SAH varies with the presence and absence of AdoHcy (Figure 2.23 (b)The amount of SAH formed in absence of AdoHcy is almost negligible compared to what is seen in presence of AdoHcy. Thus it can be concluded that for the better productivity of pyocyanin, it is much better to use AdoHcy in the reaction mixture. Thus, the hydrolysis of SAH by the nucleosidase enzyme increases the yield of pyocyanin in the reaction.

Next step was to determine the PCA concentration as the reaction proceeds leading to the formation of pyocyanin. Same reaction mixture with similar concentration was considered and the effect on the concentration of PCA was observed.

pca concentration
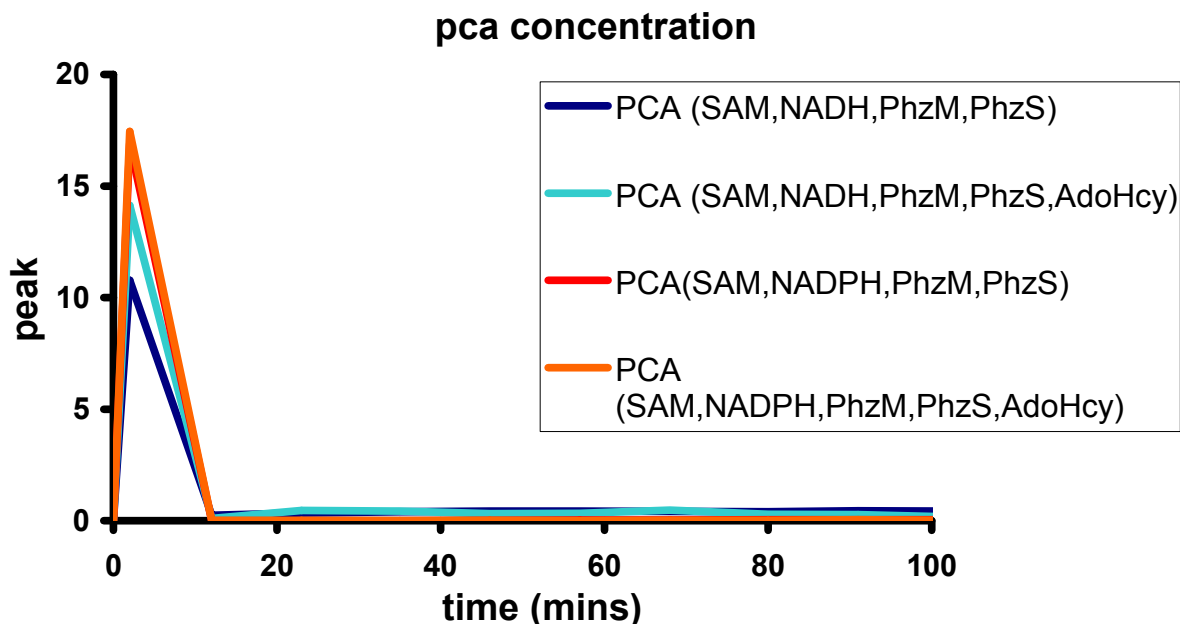
Fig 2.23(c) The consumption of PCA

Substrate (100 µM)	Cosubstrate (1mM)	Enzyme (10 µM)
PCA	SAM, NADH, NADPH	PhzM, PhzS, AdoHcy

From the Figure 2.23(c) we can see that in all the conditions leading to the formation of pyocyanin the consumption of PCA is complete. However in order to get an insight on the concentration of PCA in presence of only each of the enzyme studies were carried out in presence of either PhzM or PhzS in presence of their specific substrates. In one more study done in our group on the biosynthesis of phenazines, it was found that the end product of the 'core' phenazine biosynthesis pathway in presence of the seven enzymes PhzA-G is reduced form of PCA. So the reduced form of PCA was also used to monitor the action of either of the enzymes PhzM or PhzS. So the first test was carried

out using PhzM along with SAM and AdoHcy. In order to reduce PCA in this case two reducing agents Sodium Dithionite ($Na_2S_2O_4$) and NADPH were used.
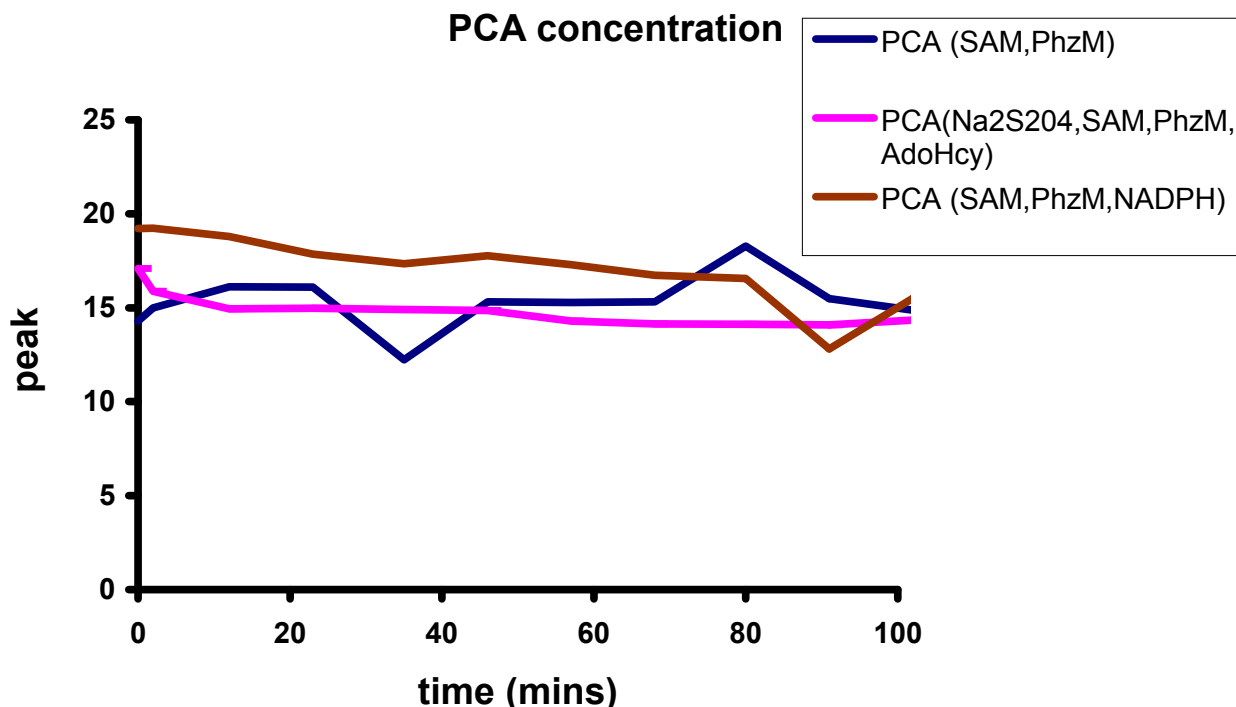
Fig 2.23(d) The consumption of reduced and oxidized PCA in presence of PhzM

Substrate (100 µM)	Cosubstrate (1mM)	Enzyme (10 µM)	Reducing agent
PCA, 1-oh-phz	SAM, NADH, NADPH	PhzM, PhzS, AdoHcy	$Na_2S_2O_4$ (5mM)

In presence of the single enzyme PhzM both, PCA as well as the reduced form PCA does not show any significant decrease in concentration (Figure 2.23(d)). This result shows that the methylation reaction didn't work efficiently implying that the PCA (oxidized and reduced form) didn't undergo methylation process and thus not a substrate of PhzM.

To check the influence of the other enzyme PhzS involved in the biosynthesis, the same technique was used. In this case also the reduced form of PCA was used as well.
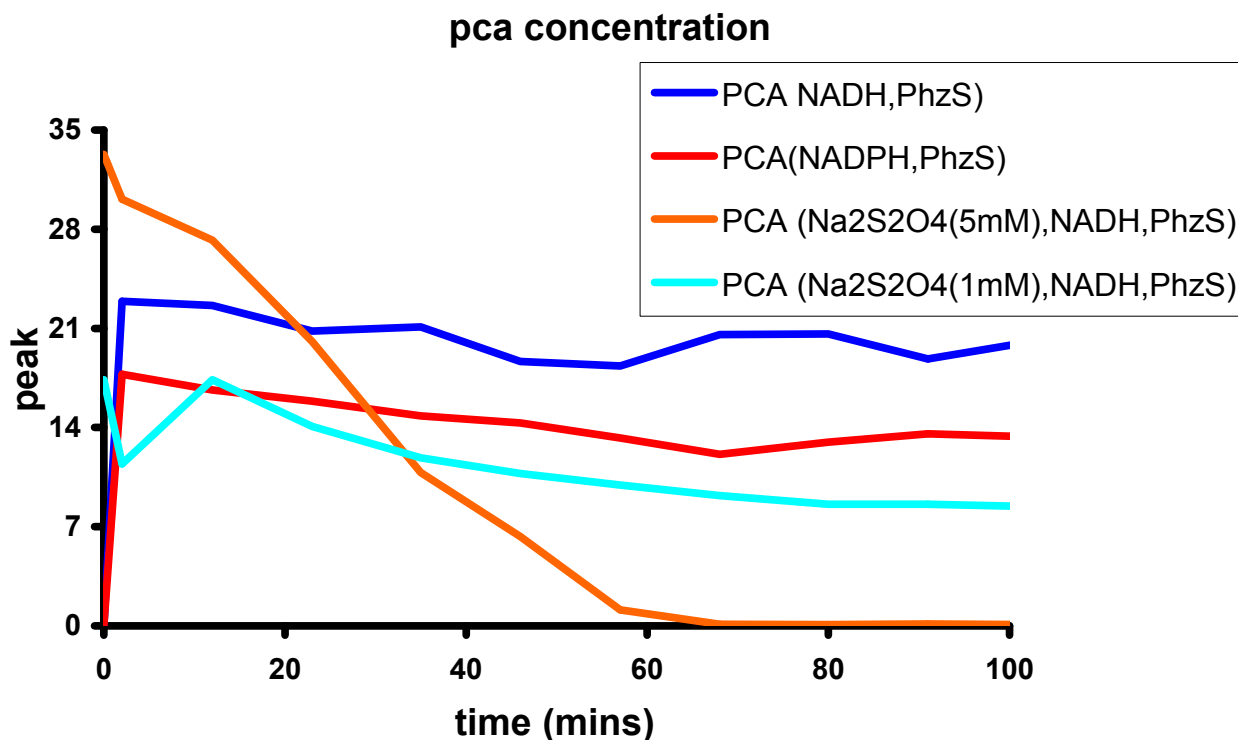
pca concentration

Fig 2.23(e) The consumption of reduced and oxidized PCA in presence of PhzS

From (Figure 2.23(e)) it can been seen that in one of the condition the reduced PCA concentration completely falls to zero compared to what it was seen in the case of PhzM. In addition to this the amount or the concentration of PCA really goes down when a higher concentration of Sodium dithionite was used. This decrease in the concentration of PCA proves that the reduced form of PCA is a good substrate for PhzS. So the next step was to check the formation of the product, which is formed by the monooxydative decarboxylation of PCA leading to the formation of 1-hydroxy-phenazine. (Figure 2.23(f)) shows the difference in the concentration of 1-hydroxy-phenazine. It can be seen that the concentration or the formation of 1-hydroxy-phenazine is highest in the presence of sodium dithionite when it was used at a high concentration.
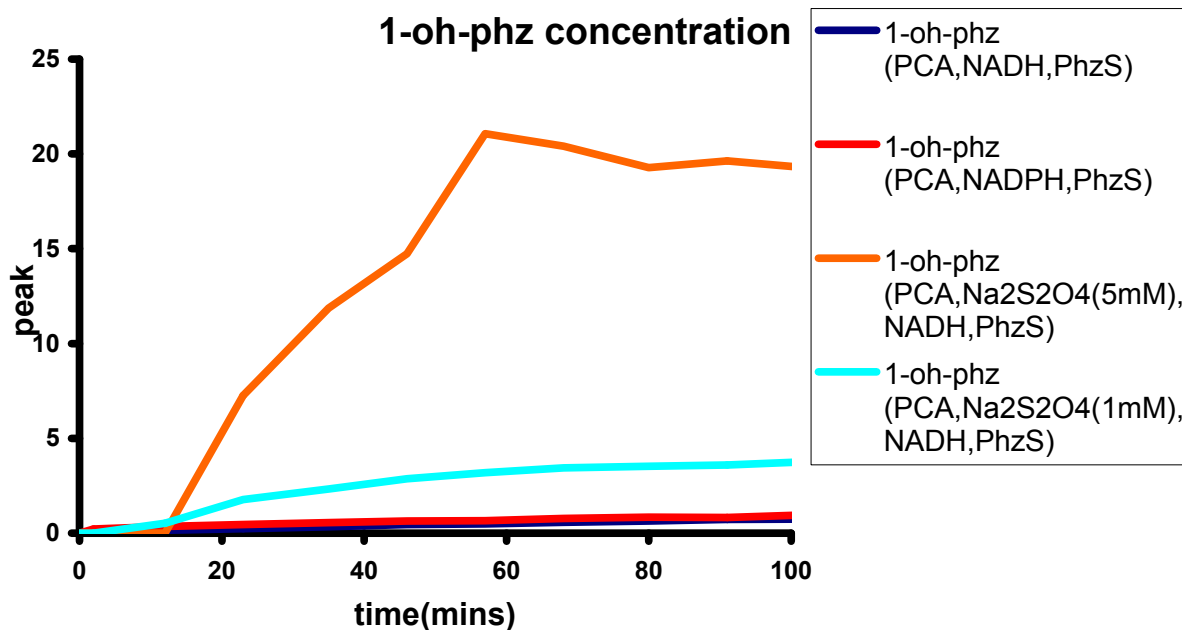
Fig 2.23(f) The formation of 1-oh-phenazine

The next in the pathway is to check the conversion of 1-hydroxy-phenazine to pyocyanin in presence of the second modifying enzyme PhzM in presence of SAM. So from (Figure 2.23(f)), the condition, which gave the highest concentration of the oxidative product from PCA, was used to check the methylation reaction. The formation of the product reaches the saturation level at a certain point and at this stage the second modifying enzyme is added along with SAM and AdoHcy enzyme (Figure 2.23(g)).

1-hydroxy-phenazine concentration
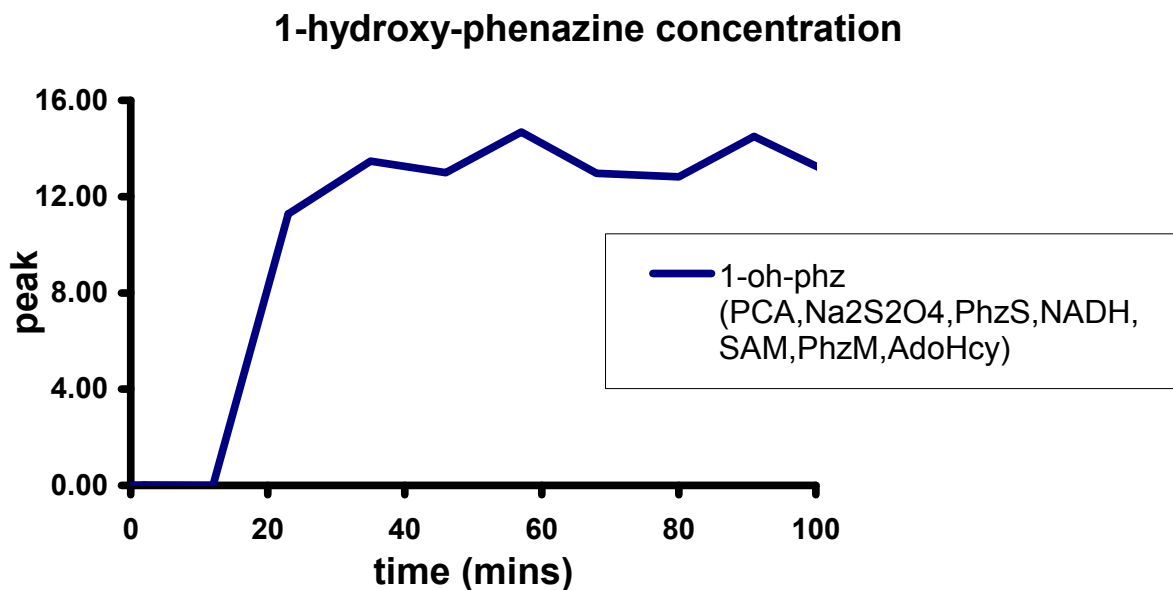
Fig 2.23(g)

However as the reaction is allowed to proceed the concentration of the substrate which is 1-hydroxy-phenazine doesn't vary showing that the methylation process is not successful and thus there is no production of pyocyanin. Theoretically it can be explained on the basis of the stability of 1-hydroxy-phenazine. When the concentration of 1-hydroxy-phenazine reaches the saturation level it is in its stable state and because of which the transfer of methyl group is not possible. But if its reduced to some extent then may be methylation will result the formation of pyocyanin.

So from the biochemical assays we can conclude that the pathway which was proposed earlier being PhzM as the first enzyme is not feasible. Moreover it is the reduced form of PCA the end product of the phenazine biosynthesis, which from our assays seems to be the starting product for pyocyanin biosynthesis. Thus the biosynthesis of pyocyanin involves the formation of 1-oh-phenazine in presence of the enzyme PhzS followed by the conversion of this reactant into the final product (Figure 2.24).
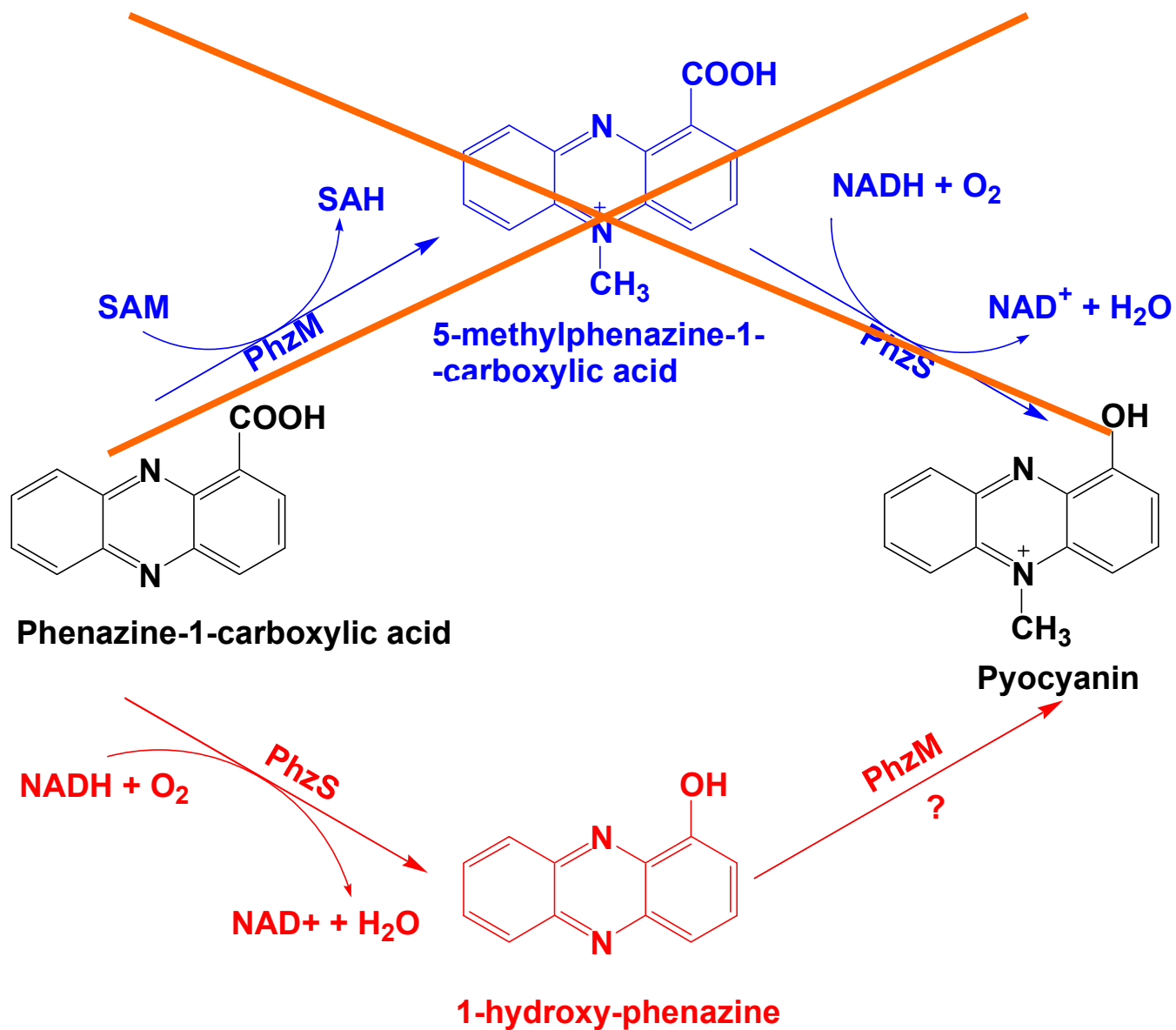
Fig 2.24 The concluded pathway

SUMMARY

5.0 Summary

Phenazines as secondary metabolites have caught the interest of the researchers since the 19th century. Amongst all the phenazine producing organisms most studies have been focussed on *Pseudomonas* species. The pathway leading to the biosynthesis of phenazines branches off from the Shikimic acid pathway. Apart from the seven gene operon leading to the biosynthesis of phenazine-1-carboxylic acid or PCA, there are some additional genes involved in the biosynthesis of other phenazine compounds. Genes *phzm* and *phzs* are couple of them, which are responsible for the conversion of PCA to pyocyanin. Pyocyanin a member of this large family of compounds called phenazines is toxic at molar concentration to a wide range of bacterial and mammalian cells. Although the research on pyocyanin dates back to early years, very little is known about the enzymes involved in its biosynthesis. This work helps us to understand the structure of the enzyme involved in its biosynthesis as well as provides an insight on the mechanism behind pyocyanin biosynthesis.

The structure of PhzM has been solved by SAD using Se-labelled protein. The final structure of native PhzM has been resolved to a resolution of 1.8Å and has R-factor of 13.9% and R_{free} of 18.4%. The structure of PhzM indicates that like other methyltransferases, it has a SAM binding site showing the Rossmann like fold and is similar to a family of previously characterised plant o-methyltransferases. The fold of the SAM binding domain of PhzM categorises this enzyme as a Class I methyltransferases. Moreover the structure of PhzM complexed with its cosubstrate SAM showed an open and close transition of PhzM and also helped to further understand and clarify its role as a methyltransferase in pyocyanin biosynthesis.

The structure of PhzS has been also solved by SAD using Se-labelled protein. The final structure of native PhzS has been resolved to a resolution of 2.4Å and has R-factor of 20.3% and R_{free} of 22.9%. Enzyme PhzS shows sequence similarity to p-hydroxybenzoate hydroxylase, of the glutathione reductase family and contains the conserved FAD binding domain. Although a complex

of PhzS bound to PCA has not been elucidated but its resemblance with other FAD-dependent monooxygenases like e.g. the well studied p-hydroxybenzoate hydroxylase or PHBH allowed us to construct a model of PhzS in complex with its substrate.

However the attempts to co-crystallise both the enzymes PhzM and PhzS with their respective substrates and products were unsuccessful so, from the crystallographic data obtained it was not possible to conclude the exact order of the reaction mechanism involved in the biosynthesis of pyocyanin. So, we carried out some biochemical assays involving APCI, to get an insight on the pathway. When both the enzymes were added with PCA in the reaction mixture with their respective substrates and cosubstrates pyocyanin was formed showing that both the enzymes were active. However, when the same experiment was carried out with single enzyme we couldn't see any conversion of PCA so it was not possible to find the exact order of the reaction. But later other results in our lab suggested that reduced PCA is infact the product of PCA biosynthesis so we decided to use chemically reduced PCA using $Na_2S_2O_4$ for studying the biosynthesis of pyocyanin. Further experiments showed that PhzS converted reduced PCA but PhzM didn't have any effect on the reduced PCA at all implying that infact in the pyocyanin biosynthetic pathway enzyme PhzS catalyses the first step followed by PhzM. Thus, in addition to better understanding of the structures of the two enzymes involved in the pyocyanin biosynthesis we also have some idea about the pathway involved in the biosynthesis.

5.0 Zusammenfassung

Phenazine sind eine Klasse von Sekundärmetaboliten, die das Interesse von Forschern seit Mitte des 19.ten Jahrhunderts auf sich gezogen haben. Unter allen phenazinproduzierenden Organismen ist *Pseudomonas* die am besten untersuchte Gattung. Die Biosynthese der Phenazine zweigt vom Shikimatweg ab. Neben dem sieben Gene enthaltenden Operon, das zur Biosynthese von Phenazine-1-carboxylat (PCA) führt, gibt es einige Gene, die an der Erzeugung von anderen Phenazinverbindungen beteiligt sind. Die Gene *phzm* und *phzs* sind hierfür ein Beispiel. Sie sind für die Umwandlung von PCA in Pyocyanin verantwortlich. Als Mitglied der großen Verbindungsklasse der Phenazine ist Pyocyanin toxisch für viele Prokaryoten und Säugetierzellen. Obwohl Pyocyanin bereits seit den frühen Jahren der Phenazinforschung untersucht wird, ist über die Enzyme, die an seiner Biosynthese beteiligt sind, nur sehr wenig bekannt. Die vorliegende Arbeit liefert einen Einblick in die Kristallstrukturen dieser Enzyme und gibt Hinweise auf die Reaktionsmechanismen der Pyocyaninbiosynthese.

Die Struktur von PhzM wurde mit der SAD-Methode unter Verwendung von Selenomethionin-markiertem Protein gelöst. Das finale Modell von nativem PhzM wurde zu einer Auflösung von 1.8Å mit R = 13.9% und R_{free} = 18.4% verfeinert. Wie andere Methyltransferasen besitzt PhzM eine SAM-Bindungsstelle mit einer Rossmann-Faltung. PhzM ist den O-Methyltransferasen aus Pflanzen am ähnlichsten, und die Topologie der SAM-Bindungsstelle kategorisiert das Enzym als Klasse-I-Methyltransferase. Es wurde außerdem die Struktur von PhzM in Gegenwart des Cosubstrats SAM bestimmt. Ein Vergleich dieses Komplexes mit der apo-Struktur zeigt große strukturelle Veränderungen zwischen der offenen, unkomplexierten und der geschlossenen, SAM-komplexierten Struktur auf, aus denen ebenfalls ein besseres Verständnis über die Rolle der Methyltransferase PhzM in der Pyocyaninbiosynthese abgeleitet werden kann.

Auch die Struktur von PhzS wurde mit der SAD-Methode aus Selenomethionin-markiertem Protein bestimmt. Das endgültige Strukturmodell

von PhzS wurde zu einer Auflösung von 2.4Å mit R = 20.3% und R$_{free}$ = 22.9% verfeinert. Das Enzym PhzS weist eine Verwandtschaft zu p-Hydroxybenzoat-Hydroxylase (PHBH) aus der Glutathion-Reduktase-Familie auf und enthält die konservierte FAD-bindende Domäne. Obwohl experimentell kein Komplex mit dem Substrat PCA hergestellt werden konnte, erlaubt die Ähnlichkeit zu PHBH die Modellierung eines solchen Komplexes.

Da weder PhzM noch PhzS in Gegenwart ihrer Substrate oder Produkte kristallisiert werden konnten, war es nicht möglich anhand der kristallografischen Daten die Abfolge der Reaktionen der Pyocyaninbiosynthese zu bestimmen. Aus diesem Grund wurden biochemische Experimente, u.a. APCI-Massenspektrometrie, durchgeführt. Wenn PCA mit beiden Enzyme und ihren Cosubstraten gleichzeitig umgesetzt wurde, kam es zu einer schnellen Bildung von Pyocyanin, was zeigt, dass beide Enzyme aktiv sind. Wenn jedoch jeweils nur ein einzelnes Enzym eingesetzt wurde, konnte kein Umsatz von PCA beobachtet werden, so dass sich aus diesen Experimenten die Reihenfolge der Reaktionen in der Pyocyaninbiosynthese zunächst ebenfalls nicht feststellen ließ. Aus einem anderen Projekt der Arbeitsgruppe gab es jedoch Hinweise darauf, dass das Endprodukt der vorgelagerten PCA-Biosynthese reduziertes PCA ist. Es wurden daher weitere Experimente mit PhzM und PhzS sowie durch Na$_2$S$_2$O$_4$ reduziertem PCA durchgeführt. In diesen Experimenten konnte PhzS reduziertes PCA umsetzen, während PhzM keinen Effekt aufwies, was anzeigt, dass PhzS die erste und PhzM die zweite Umwandlung in der Pyocyaninbiosynthese katalysiert. Die vorliegende Arbeit trägt daher nicht nur zu einem besseren Verständnis der Strukturen von Enzymen in der Pyocyaninbiosynthese bei sondern liefert auch ein Modell für die Reihenfolge der Umsetzungen in diesem Biosyntheseweg.

OUTLOOK

6.0 Outlook

While this study lays the groundwork for a detailed understanding of the conversion of PCA into pyocyanin by PhzS and PhzM, many details of the process still remain obscure. Most importantly, it is not clear why all attempts to form pyocyanin from 1-oh-phenazine were unsuccessful: neither (oxidised) commercial 1-oh-phenazine nor (reduced) 1-oh-phenazine formed from reduced PCA by PhzS were found to be substrates of PhzM. It is possible that these observations are due to special chemical properties of 1-oh-phenazine that have not been taken into account appropriately. For example, it is well known that 1-oh-phenazine polymerizes under certain conditions and that this tendency can be exploited to coat electrodes, which gives these electrodes certain electrochemical features (literature). From the results presented here, it can not be excluded that reduced 1-oh-phenazine, once formed from reduced PCA by PhzS, polymerises to a certain extend and is then not available for methylation if PhzM is added at a later stage. The 1-oh-phenazine observed in HPLC-MS would then stem from back oxidation of the product, which is no longer a substrate of PhzM. The fact that it was not possible to observe a chemically reduced form of 1-oh-phenazine by HPLC-MS may point into this direction. In the cell, this problem may not be relevant since both reactions are coupled, meaning that reduced 1-oh-phenazine produced by PhzS will be methylated to pyocyanin immediately without having time to polymerise or be back-oxidised. Further studies are required to assess these possibilities.

For more detailed insight into structure/activity relationships, crystal complexes of the two enzymes with their substrates, products or analogues are desirable. For this, more robust crystallisation conditions would have to be established, especially for PhzS, which looses crystallisability quickly after purification. This may have to do with the redox-active cofactor FAD, which probably makes PhzS sensitive to both air and light. Crystallisation under oil and with properly degassed solutions in a dark container may alleviate this situation.

Once residues that interact with ligands in the active centre have been identified, their importance should be studied by site-directed mutagenesis.

This also seems required in the light of exploiting PhzM and PhzS as targets in the development of novel pharmaceuticals, since the ability of both enzymes to escape the action of such agents by mutation and the concomitant emergence of resistance has to be assessed.

REFERENCES

REFERENCE LIST

[1] Barger,G. & Dale,H.H. (1907) Ergotoxine and some other Constituents of Ergot. *Biochem. J.*, 2, 240-299.

[2] BU'LOCK,J.D. (1961) Intermediary metabolism and antibiotic synthesis. *Adv. Appl. Microbiol.*, 3, 293-342.

[3] Price-Whelan,A., Dietrich,L.E., & Newman,D.K. (2006) Rethinking 'secondary' metabolism: physiological roles for phenazine antibiotics 2. *Nat. Chem. Biol.*, 2, 71-78.

[4] Price-Whelan,A., Dietrich,L.E., & Newman,D.K. (2006) Rethinking 'secondary' metabolism: physiological roles for phenazine antibiotics 2. *Nat. Chem. Biol.*, 2, 71-78.

[5] Villavicencio,R.T. (1998) The history of blue pus. *J. Am. Coll. Surg.*, 187, 212-216.

[6] Mavrodi,D.V., Blankenfeldt,W., & Thomashow,L.S. (2006) Phenazine compounds in fluorescent Pseudomonas spp. biosynthesis and regulation. *Annu. Rev. Phytopathol.*, 44, 417-445.

[7] Leisinger,T. & Margraff,R. (1979) Secondary Metabolites of the Fluorescent Pseudomonads 1. *Microbiological Reviews*, 43, 422-442.

[8] Costerton,J.W., Stewart,P.S., & Greenberg,E.P. (1999) Bacterial biofilms: a common cause of persistent infections. *Science*, 284, 1318-1322.

[9] Ledgham,F., Ventre,I., Soscia,C., Foglino,M., Sturgis,J.N., & Lazdunski,A. (2003) Interactions of the quorum sensing regulator QscR: interaction with itself and the other regulators of Pseudomonas aeruginosa LasR and RhlR 3. *Mol. Microbiol.*, 48, 199-210.

[10] Mavrodi,D.V., Bonsall,R.F., Delaney,S.M., Soule,M.J., Phillips,G., & Thomashow,L.S. (2001) Functional analysis of genes for biosynthesis of pyocyanin and phenazine-1-carboxamide from Pseudomonas aeruginosa PAO1. *J. Bacteriol.*, 183, 6454-6465.

[11] Costerton,J.W., Stewart,P.S., & Greenberg,E.P. (1999) Bacterial biofilms: a common cause of persistent infections. *Science*, 284, 1318-1322.

[12] Bodey,G.P., Bolivar,R., Fainstein,V., & Jadeja,L. (1983) Infections caused by Pseudomonas aeruginosa. *Rev. Infect. Dis.*, 5, 279-313.

[13] Ran,H., Hassett,D.J., & Lau,G.W. (2003) Human targets of Pseudomonas aeruginosa pyocyanin 8. *Proc. Natl. Acad. Sci. U. S. A*, 100, 14315-14320.

REFERENCES

[14] Cox,C.D. (1985) Iron transport and serum resistance in Pseudomonas aeruginosa. *Antibiot. Chemother.*, 36, 1-12.

[15] KLUYVER,A.J. (1956) Pseudomonas aureofaciens nov. spec. and its pigments 1. *J. Bacteriol.*, 72, 406-411.

[16] FRANK,L.H. & DEMOSS,R.D. (1959) On the biosynthesis of pyocyanine. *J. Bacteriol.*, 77, 776-782.

[17] Hassett,D.J., Charniga,L., Bean,K., Ohman,D.E., & Cohen,M.S. (1992) Response of Pseudomonas aeruginosa to pyocyanin: mechanisms of resistance, antioxidant defenses, and demonstration of a manganese-cofactored superoxide dismutase. *Infect. Immun.*, 60, 328-336.

[18] Stewart-Tull,D.E. & Armstrong,A.V. (1972) The effect of 1-hydroxyphenazine and pyocyanin from Pseudomonas aeruginosa on mammalian cell respiration. *J. Med. Microbiol.*, 5, 67-73.

[19] Wilson,R., Pitt,T., Taylor,G., Watson,D., MacDermot,J., Sykes,D., Roberts,D., & Cole,P. (1987) Pyocyanin and 1-hydroxyphenazine produced by Pseudomonas aeruginosa inhibit the beating of human respiratory cilia in vitro. *J. Clin. Invest*, 79, 221-229.

[20] Vukomanovic,D.V., Zoutman,D.E., Stone,J.A., Marks,G.S., Brien,J.F., & Nakatsu,K. (1997) Electrospray mass-spectrometric, spectrophotometric and electrochemical methods do not provide evidence for the binding of nitric oxide by pyocyanine at pH 7. *Biochem. J.*, 322 (Pt 1), 25-29.

[21] Hussain,A.S., Bozinovski,J., Maurice,D.H., McLaughlin,B.E., Marks,G.S., Brien,J.F., & Nakatsu,K. (1997) Inhibition of the action of nitric oxide prodrugs by pyocyanin: mechanistic studies. *Can. J. Physiol Pharmacol.*, 75, 398-406.

[22] Ras,G.J., Theron,A.J., Anderson,R., Taylor,G.W., Wilson,R., Cole,P.J., & van der Merwe,C.A. (1992) Enhanced release of elastase and oxidative inactivation of alpha-1-protease inhibitor by stimulated human neutrophils exposed to Pseudomonas aeruginosa pigment 1-hydroxyphenazine. *J. Infect. Dis.*, 166, 568-573.

[23] Lau,G.W., Ran,H., Kong,F., Hassett,D.J., & Mavrodi,D. (2004) Pseudomonas aeruginosa pyocyanin is critical for lung infection in mice 7. *Infect. Immun.*, 72, 4275-4278.

[24] Hassan,H.M. & Fridovich,I. (1980) Mechanism of the antibiotic action pyocyanine. *J. Bacteriol.*, 141, 156-163.

[25] O'Malley,Y.Q., Reszka,K.J., Rasmussen,G.T., Abdalla,M.Y., Denning,G.M., & Britigan,B.E. (2003) The Pseudomonas secretory product pyocyanin inhibits catalase activity in human lung epithelial cells. *Am. J. Physiol Lung Cell Mol. Physiol*, 285, L1077-L1086.

REFERENCES

[26] Fuhrer,T., Fischer,E., & Sauer,U. (2005) Experimental identification and quantification of glucose metabolism in seven bacterial species. *J. Bacteriol.*, 187, 1581-1590.

[27] Williams,H.D., Zlosnik,J.E., & Ryall,B. (2007) Oxygen, cyanide and energy generation in the cystic fibrosis pathogen Pseudomonas aeruginosa. *Adv. Microb. Physiol*, 52, 1-71.

[28] Price-Whelan,A., Dietrich,L.E., & Newman,D.K. (2007) Pyocyanin alters redox homeostasis and carbon flux through central metabolic pathways in Pseudomonas aeruginosa PA14. *J. Bacteriol.*, 189, 6372-6381.

[29] Lau,G.W., Hassett,D.J., Ran,H., & Kong,F. (2004) The role of pyocyanin in Pseudomonas aeruginosa infection. *Trends Mol. Med.*, 10, 599-606.

[30] Davis,G. & Thornalley,P.J. (1983) Free radical production from the aerobic oxidation of reduced pyridine nucleotides catalysed by phenazine derivatives 1. *Biochim. Biophys. Acta*, 724, 456-464.

[31] Trutko,S.M., Garagulya,A.D., Kiprianova,E.A., & Akimenko,V.K. (1988) Physiological-Role of Pyocyanine Synthesized by Pseudomonas-Aeruginosa. *Microbiology*, 57, 763-770.

[32] Dietrich,L.E., Price-Whelan,A., Petersen,A., Whiteley,M., & Newman,D.K. (2006) The phenazine pyocyanin is a terminal signalling factor in the quorum sensing network of Pseudomonas aeruginosa
1. *Mol. Microbiol.*, 61, 1308-1321.

[33] Byng,G.S., Eustice,D.C., & Jensen,R.A. (1979) Biosynthesis of phenazine pigments in mutant and wild-type cultures of Pseudomonas aeruginosa. *J. Bacteriol.*, 138, 846-852.

[34] Pierson,L.S., III, Keppenne,V.D., & Wood,D.W. (1994) Phenazine antibiotic biosynthesis in Pseudomonas aureofaciens 30-84 is regulated by PhzR in response to cell density. *J. Bacteriol.*, 176, 3966-3974.

[35] Whiteley,M., Lee,K.M., & Greenberg,E.P. (1999) Identification of genes controlled by quorum sensing in Pseudomonas aeruginosa. *Proc. Natl. Acad. Sci. U. S. A*, 96, 13904-13909.

[36] Sweet,W.J. & Peterson,J.A. (1978) Changes in cytochrome content and electron transport patterns in Pseudomonas putida as a function of growth phase. *J. Bacteriol.*, 133, 217-224.

[37] Kanthakumar,K., Taylor,G., Tsang,K.W., Cundell,D.R., Rutman,A., Smith,S., Jeffery,P.K., Cole,P.J., & Wilson,R. (1993) Mechanisms of action of Pseudomonas aeruginosa pyocyanin on human ciliary beat in vitro. *Infect. Immun.*, 61, 2848-2853.

REFERENCES

[38] Muller,P.K., Krohn,K., & Muhlradt,P.F. (1989) Effects of pyocyanine, a phenazine dye from Pseudomonas aeruginosa, on oxidative burst and bacterial killing in human neutrophils. *Infect. Immun.*, 57, 2591-2596.

[39] Price-Whelan,A., Dietrich,L.E., & Newman,D.K. (2006) Rethinking 'secondary' metabolism: physiological roles for phenazine antibiotics 2. *Nat. Chem. Biol.*, 2, 71-78.

[40] Laursen,J.B. & Nielsen,J. (2004) Phenazine natural products: biosynthesis, synthetic analogues, and biological activity. *Chem. Rev.*, 104, 1663-1686.

[41] Turner,J.M. & Messenger,A.J. (1986) Occurrence, biochemistry and physiology of phenazine pigment production. *Adv. Microb. Physiol*, 27, 211-275.

[42] Price-Whelan,A., Dietrich,L.E., & Newman,D.K. (2006) Rethinking 'secondary' metabolism: physiological roles for phenazine antibiotics2. *Nat. Chem. Biol.*, 2, 71-78.

[43] Rabaey,K., Boon,N., Hofte,M., & Verstraete,W. (2005) Microbial phenazine production enhances electron transfer in biofuel cells. *Environ. Sci. Technol.*, 39, 3401-3408.

[44] Phillips,I., Basson,S.S., Kasule,J., & Makuto,D.G. (1969) Bacteriuria of pregnancy in Kampala. A preliminary survey3. *East Afr. Med. J.*, 46, 516-519.

[45] Gamage,S.A., Rewcastle,G.W., Baguley,B.C., Charlton,P.A., & Denny,W.A. (2006) Phenazine-1-carboxamides: structure-cytotoxicity relationships for 9-substituents and changes in the H-bonding pattern of the cationic side chain11. *Bioorg. Med. Chem.*, 14, 1160-1168.

[46] Fernandez,D.U., Fuchs,R., Taraz,K., Budzikiewicz,H., Munsch,P., & Meyer,J.M. (2001) The structure of a pyoverdine produced by a Pseudomonas tolaasii-like isolate2. *Biometals*, 14, 81-84.

[47] Cerecetto,H., Gonzalez,M., Risso,M., Saenz,P., Olea-Azar,C., Bruno,A.M., Azqueta,A., De Cerain,A.L., & Monge,A. (2004) 1, 2, 4-Triazine N-oxide derivatives: studies as potential hypoxic cytotoxins. Part III. *Arch. Pharm. (Weinheim)*, 337, 271-280.

[48] Vining,L.C. (1990) Functions of secondary metabolites. *Annu. Rev. Microbiol.*, 44, 395-427.

[49] Muller,M. (1995) Scavenging of neutrophil-derived superoxide anion by 1-hydroxyphenazine, a phenazine derivative associated with chronic Pseudomonas aeruginosa infection: relevance to cystic fibrosis1. *Biochim. Biophys. Acta*, 1272, 185-189.

REFERENCES

[50] Gardner,P.R. & White,C.W. (1996) Failure of tumor necrosis factor and interleukin-1 to elicit superoxide production in the mitochondrial matrices of mammalian cells 2. *Arch. Biochem. Biophys.*, 334, 158-162.

[51] Denning,G.M., Wollenweber,L.A., Railsback,M.A., Cox,C.D., Stoll,L.L., & Britigan,B.E. (1998) Pseudomonas pyocyanin increases interleukin-8 expression by human airway epithelial cells 1. *Infect. Immun.*, 66, 5777-5784.

[52] Mahajan-Miklos,S., Tan,M.W., Rahme,L.G., & Ausubel,F.M. (1999) Molecular mechanisms of bacterial virulence elucidated using a Pseudomonas aeruginosa-Caenorhabditis elegans pathogenesis model 1. *Cell*, 96, 47-56.

[53] Hassett,D.J., Charniga,L., Bean,K., Ohman,D.E., & Cohen,M.S. (1992) Response of Pseudomonas aeruginosa to pyocyanin: mechanisms of resistance, antioxidant defenses, and demonstration of a manganese-cofactored superoxide dismutase 2. *Infect. Immun.*, 60, 328-336.

[54] O'Malley,Y.Q., Abdalla,M.Y., McCormick,M.L., Reszka,K.J., Denning,G.M., & Britigan,B.E. (2003) Subcellular localization of Pseudomonas pyocyanin cytotoxicity in human lung epithelial cells. *Am. J. Physiol Lung Cell Mol. Physiol*, 284, L420-L430.

[55] Lau,G.W., Hassett,D.J., Ran,H., & Kong,F. (2004) The role of pyocyanin in Pseudomonas aeruginosa infection. *Trends Mol. Med.*, 10, 599-606.

[56] Lau,G.W., Ran,H., Kong,F., Hassett,D.J., & Mavrodi,D. (2004) Pseudomonas aeruginosa pyocyanin is critical for lung infection in mice 7. *Infect. Immun.*, 72, 4275-4278.

[57] Hassett,D.J., Schweizer,H.P., & Ohman,D.E. (1995) Pseudomonas aeruginosa sodA and sodB mutants defective in manganese- and iron-cofactored superoxide dismutase activity demonstrate the importance of the iron-cofactored form in aerobic metabolism 1. *J. Bacteriol.*, 177, 6330-6337.

[58] Price-Whelan,A., Dietrich,L.E., & Newman,D.K. (2006) Rethinking 'secondary' metabolism: physiological roles for phenazine antibiotics 2. *Nat. Chem. Biol.*, 2, 71-78.

[59] Hernandez,M.E. & Newman,D.K. (2001) Extracellular electron transfer 1. *Cell Mol. Life Sci.*, 58, 1562-1571.

[60] Look,D.C., Stoll,L.L., Romig,S.A., Humlicek,A., Britigan,B.E., & Denning,G.M. (2005) Pyocyanin and its precursor phenazine-1-carboxylic acid increase IL-8 and intercellular adhesion molecule-1 expression in human airway epithelial cells by oxidant-dependent mechanisms 1. *J. Immunol.*, 175, 4017-4023.

REFERENCES

[61] Brown,K.A., Carpenter,E.P., Watson,K.A., Coggins,J.R., Hawkins,A.R., Koch,M.H.J., & Svergun,D.I. (2003) Twists and turns: a tale of two shikimate-pathway enzymes 1. *Biochemical Society Transactions*, 31, 543-547.

[62] McDonald,M., Mavrodi,D.V., Thomashow,L.S., & Floss,H.G. (2001) Phenazine biosynthesis in Pseudomonas fluorescens: branchpoint from the primary shikimate biosynthetic pathway and role of phenazine-1,6-dicarboxylic acid 1. *J. Am. Chem. Soc.*, 123, 9459-9460.

[63] Floss,H.G. (1997) Natural products derived from unusual variants of the shikimate pathway 4. *Nat. Prod. Rep.*, 14, 433-452.

[64] Hollstein,U. & McCamey,D.A. (1973) Biosynthesis of phenazines. II. Incorporation of (6-14C)-D-shikimic acid into phenazine-1-carboxylic acid and iodinin 1. *J. Org. Chem.*, 38, 3415-3417.

[65] Byng,G.S. & Turner,J.M. (1977) Incorporation of [14C]shikimate into plenazines and their further metabolism by Pseudomonas phenazinium 3. *Biochem. J.*, 164, 139-145.

[66] MILLICAN,R.C. (1963) A THIOBARBITURIC ACID ASSAY FOR SHIKIMIC ACID. *Anal. Biochem.*, 6, 181-192.

[67] LEVITCH,M.E. & STADTMAN,E.R. (1964) STUDY OF THE BIOSYNTHESIS OF PHENAZINE-1-CARBOXYLIC ACID 1. *Arch. Biochem. Biophys.*, 106, 194-199.

[68] Chang,P.C. & Blackwood,A.C. (1968) Simultaneous biosynthesis of pyocyanine, phenazine-1-carboxylic acid, and oxychloroaphine from labelled substrates by Pseudomonas aeruginosa Mac 436 1. *Can. J. Biochem.*, 46, 925-929.

[69] Podojil,M. & Gerber,N.N. (1970) Biosynthesis of 1,6-phenazinediol 5,10-dioxide (iodinin). Incorporation of shikimic acid. *Biochemistry*, 9, 4616-4618.

[70] MILLICAN,R.C. (1963) A THIOBARBITURIC ACID ASSAY FOR SHIKIMIC ACID 2. *Anal. Biochem.*, 6, 181-192.

[71] CARTER,C.H. (1961) 4,7-Phenanthroline-5,6-quinone, a new agent for amebiasis 1. *Antibiot. Chemother.*, 11, 637-639.

[72] Pierson,L.S., III, Gaffney,T., Lam,S., & Gong,F. (1995) Molecular analysis of genes encoding phenazine biosynthesis in the biological control bacterium. Pseudomonas aureofaciens 30-84 1. *FEMS Microbiol. Lett.*, 134, 299-307.

REFERENCES

[73] Mavrodi,D.V., Ksenzenko,V.N., Bonsall,R.F., Cook,R.J., Boronin,A.M., & Thomashow,L.S. (1998) A seven-gene locus for synthesis of phenazine-1-carboxylic acid by Pseudomonas fluorescens 2-79 1. *J. Bacteriol.*, 180, 2541-2548.

[74] Mavrodi,D.V., Bonsall,R.F., Delaney,S.M., Soule,M.J., Phillips,G., & Thomashow,L.S. (2001) Functional analysis of genes for biosynthesis of pyocyanin and phenazine-1-carboxamide from Pseudomonas aeruginosa PAO1. *J. Bacteriol.*, 183, 6454-6465.

[75] Mavrodi,D.V., Ksenzenko,V.N., Bonsall,R.F., Cook,R.J., Boronin,A.M., & Thomashow,L.S. (1998) A seven-gene locus for synthesis of phenazine-1-carboxylic acid by Pseudomonas fluorescens 2-79. *J. Bacteriol.*, 180, 2541-2548.

[76] Blankenfeldt,W., Kuzin,A.P., Skarina,T., Korniyenko,Y., Tong,L., Bayer,P., Janning,P., Thomashow,L.S., & Mavrodi,D.V. (2004) Structure and function of the phenazine biosynthetic protein PhzF from Pseudomonas fluorescens 4. *Proc. Natl. Acad. Sci. U. S. A*, 101, 16431-16436.

[77] Chin,A.W.T., Thomas-Oates,J.E., Lugtenberg,B.J., & Bloemberg,G.V. (2001) Introduction of the phzH gene of Pseudomonas chlororaphis PCL1391 extends the range of biocontrol ability of phenazine-1-carboxylic acid-producing Pseudomonas spp. strains 2. *Mol. Plant Microbe Interact.*, 14, 1006-1015.

[78] Stover,C.K., Pham,X.Q., Erwin,A.L., Mizoguchi,S.D., Warrener,P., Hickey,M.J., Brinkman,F.S., Hufnagle,W.O., Kowalik,D.J., Lagrou,M., Garber,R.L., Goltry,L., Tolentino,E., Westbrock-Wadman,S., Yuan,Y., Brody,L.L., Coulter,S.N., Folger,K.R., Kas,A., Larbig,K., Lim,R., Smith,K., Spencer,D., Wong,G.K., Wu,Z., Paulsen,I.T., Reizer,J., Saier,M.H., Hancock,R.E., Lory,S., & Olson,M.V. (2000) Complete genome sequence of Pseudomonas aeruginosa PA01, an opportunistic pathogen 1. *Nature*, 406, 959-964.

[79] Bosch,R., Moore,E.R., Garcia-Valdes,E., & Pieper,D.H. (1999) NahW, a novel, inducible salicylate hydroxylase involved in mineralization of naphthalene by Pseudomonas stutzeri AN10 1. *J. Bacteriol.*, 181, 2315-2322.

[80] Walker,R.D. & Duerre,J.A. (1975) S-adenosylhomocysteine metabolism in various species. *Can. J. Biochem.*, 53, 312-319.

[81] Hoffman,D.R., Cornatzer,W.E., & Duerre,J.A. (1979) Relationship between tissue levels of S-adenosylmethionine, S-adenylhomocysteine, and transmethylation reactions. *Can. J. Biochem.*, 57, 56-65.

[82] Caudill,M.A., Wang,J.C., Melnyk,S., Pogribny,I.P., Jernigan,S., Collins,M.D., Santos-Guzman,J., Swendseid,M.E., Cogger,E.A., & James,S.J. (2001) Intracellular S-adenosylhomocysteine concentrations

predict global DNA hypomethylation in tissues of methyl-deficient cystathionine beta-synthase heterozygous mice 2. *J. Nutr.*, 131, 2811-2818.

[83] Hendricks,C.L., Ross,J.R., Pichersky,E., Noel,J.P., & Zhou,Z.S. (2004) An enzyme-coupled colorimetric assay for S-adenosylmethionine-dependent methyltransferases. *Anal. Biochem.*, 326, 100-105.

[84] Caudill,M.A., Wang,J.C., Melnyk,S., Pogribny,I.P., Jernigan,S., Collins,M.D., Santos-Guzman,J., Swendseid,M.E., Cogger,E.A., & James,S.J. (2001) Intracellular S-adenosylhomocysteine concentrations predict global DNA hypomethylation in tissues of methyl-deficient cystathionine beta-synthase heterozygous mice2. *J. Nutr.*, 131, 2811-2818.

[85] Hendricks,C.L., Ross,J.R., Pichersky,E., Noel,J.P., & Zhou,Z.S. (2004) An enzyme-coupled colorimetric assay for S-adenosylmethionine-dependent methyltransferases. *Anal. Biochem.*, 326, 100-105.

[86] Wang,C., Leffler,S., Thompson,D.H., & Hrycyna,C.A. (2005) A general fluorescence-based coupled assay for S-adenosylmethionine-dependent methyltransferases 1. *Biochem. Biophys. Res. Commun.*, 331, 351-356.

[87] Chugani,S.A., Whiteley,M., Lee,K.M., D'Argenio,D., Manoil,C., & Greenberg,E.P. (2001) QscR, a modulator of quorum-sensing signal synthesis and virulence in Pseudomonas aeruginosa 6. *Proc. Natl. Acad. Sci. U. S. A*, 98, 2752-2757.

[88] Costerton,J.W., Stewart,P.S., & Greenberg,E.P. (1999) Bacterial biofilms: a common cause of persistent infections 2. *Science*, 284, 1318-1322.

[89] Bodey,G.P., Bolivar,R., Fainstein,V., & Jadeja,L. (1983) Infections caused by Pseudomonas aeruginosa1. *Rev. Infect. Dis.*, 5, 279-313.

[90] Lee,J.H., Lequette,Y., & Greenberg,E.P. (2006) Activity of purified QscR, a Pseudomonas aeruginosa orphan quorum-sensing transcription factor 5. *Mol. Microbiol.*, 59, 602-609.

[91] Lequette,Y., Lee,J.H., Ledgham,F., Lazdunski,A., & Greenberg,E.P. (2006) A distinct QscR regulon in the Pseudomonas aeruginosa quorum-sensing circuit 3. *J. Bacteriol.*, 188, 3365-3370.

[92] Dietrich,L.E., Price-Whelan,A., Petersen,A., Whiteley,M., & Newman,D.K. (2006) The phenazine pyocyanin is a terminal signalling factor in the quorum sensing network of Pseudomonas aeruginosa. *Mol. Microbiol.*, 61, 1308-1321.

[93] Dietrich,L.E., Price-Whelan,A., Petersen,A., Whiteley,M., & Newman,D.K. (2006) The phenazine pyocyanin is a terminal signalling

factor in the quorum sensing network of Pseudomonas aeruginosa. *Mol. Microbiol.*, 61, 1308-1321.

[94] Van Duyne,G.D., Standaert,R.F., Karplus,P.A., Schreiber,S.L., & Clardy,J. (1993) Atomic structures of the human immunophilin FKBP-12 complexes with FK506 and rapamycin. *J. Mol. Biol.*, 229, 105-124.

[95] Laemmli,U.K. (1970) Cleavage of structural proteins during the assembly of the head of bacteriophage T4 1. *Nature*, 227, 680-685.

[96] Ossipow,V., Laemmli,U.K., & Schibler,U. (1993) A simple method to renature DNA-binding proteins separated by SDS-polyacrylamide gel electrophoresis. *Nucleic Acids Res.*, 21, 6040-6041.

[97] Doublie,S. (1997) Preparation of selenomethionyl proteins for phase determination. *Methods Enzymol.*, 276, 523-530.

[98] Fairall,L., Schwabe,J.W., Chapman,L., Finch,J.T., & Rhodes,D. (1993) The crystal structure of a two zinc-finger peptide reveals an extension to the rules for zinc-finger/DNA recognition 1. *Nature*, 366, 483-487.

[99] Romero,A.J. & Rhodes,C.T. (1993) Stereochemical aspects of the molecular pharmaceutics of ibuprofen 2. *J. Pharm. Pharmacol.*, 45, 258-262.

[100] Cudney,R., Patel,S., Weisgraber,K., Newhouse,Y., & McPherson,A. (1994) Screening and optimization strategies for macromolecular crystal growth 2. *Acta Crystallogr. D. Biol. Crystallogr.*, 50, 414-423.

[101] Jancarik,J., Scott,W.G., Milligan,D.L., Koshland,D.E., Jr., & Kim,S.H. (1991) Crystallization and preliminary X-ray diffraction study of the ligand-binding domain of the bacterial chemotaxis-mediating aspartate receptor of Salmonella typhimurium 2. *J. Mol. Biol.*, 221, 31-34.

[102] Milburn,M.V., Prive,G.G., Milligan,D.L., Scott,W.G., Yeh,J., Jancarik,J., Koshland,D.E., Jr., & Kim,S.H. (1991) Three-dimensional structures of the ligand-binding domain of the bacterial aspartate receptor with and without a ligand 1. *Science*, 254, 1342-1347.

[103] Rossmann,M.G. & van Beek,C.G. (1999) Data processing. *Acta Crystallogr. D. Biol. Crystallogr.*, 55, 1631-1640.

[104] Kabsch,W. (1993) Automatic Processing of Rotation Diffraction Data from Crystals of Initially Unknown Symmetry and Cell Constants 1. *Journal of Applied Crystallography*, 26, 795-800.

[105] Schneider,T.R. & Sheldrick,G.M. (2002) Substructure solution with SHELXD 1. *Acta Crystallogr. D. Biol. Crystallogr.*, 58, 1772-1779.

REFERENCES

[106]   Murshudov,G.N., Vagin,A.A., & Dodson,E.J. (1997) Refinement of macromolecular structures by the maximum-likelihood method 2. *Acta Crystallogr. D. Biol. Crystallogr.*, 53, 240-255.

[107]   Emsley,P. & Cowtan,K. (2004) Coot: model-building tools for molecular graphics 1. *Acta Crystallogr. D. Biol. Crystallogr.*, 60, 2126-2132.

[108]   Brunger,A.T., Adams,P.D., Clore,G.M., DeLano,W.L., Gros,P., Grosse-Kunstleve,R.W., Jiang,J.S., Kuszewski,J., Nilges,M., Pannu,N.S., Read,R.J., Rice,L.M., Simonson,T., & Warren,G.L. (1998) Crystallography & NMR system: A new software suite for macromolecular structure determination. *Acta Crystallogr. D. Biol. Crystallogr.*, 54, 905-921.

[109]   Jancarik,J. & Kim,S.H. (1991) Sparse-Matrix Sampling - A Screening Method for Crystallization of Proteins. *Journal of Applied Crystallography*, 24, 409-411.

[110]   Cudney,B., Patel,S., Weisgraber,K., & Newhouse,Y. (1994) Screening and Optimization Strategies for Macromolecular Crystal-Growth. *Acta Crystallographica Section D-Biological Crystallography*, 50, 414-4123.

[111]   Schiltz,M., Shepard,W., Fourme,R., Prange,T., de la,F.E., & Bricogne,G. (1997) High-pressure krypton gas and statistical heavy-atom refinement: a successful combination of tools for macromolecular structure determination 1. *Acta Crystallogr. D. Biol. Crystallogr.*, 53, 78-92.

[112]   Jones,T.A., Zou,J.Y., Cowan,S.W., & Kjeldgaard,M. (1991) Improved methods for building protein models in electron density maps and the location of errors in these models. *Acta Crystallogr. A*, 47 (Pt 2), 110-119.

[113]   Cowtan,K. & Main,P. (1998) Miscellaneous algorithms for density modification. *Acta Crystallogr. D. Biol. Crystallogr.*, 54, 487-493.

[114]   Cowtan,K. (2008) Fitting molecular fragments into electron density 1. *Acta Crystallogr. D. Biol. Crystallogr.*, 64, 83-89.

[115]   Cowtan,K.D. & Main,P. (1996) Phase combination and cross validation in iterated density-modification calculations. *Acta Crystallogr. D. Biol. Crystallogr.*, 52, 43-48.

[116]   Laskowski,R.A., Moss,D.S., & Thornton,J.M. (1993) Main-chain bond lengths and bond angles in protein structures. *J. Mol. Biol.*, 231, 1049-1067.

[117]   Cowtan,K. (1998) Modified phased translation functions and their application to molecular-fragment location. *Acta Crystallogr. D. Biol. Crystallogr.*, 54, 750-756.

REFERENCES

[118] Cowtan,K. (1999) Error estimation and bias correction in phase-improvement calculations. *Acta Crystallogr. D. Biol. Crystallogr.*, 55, 1555-1567.

[119] Cowtan,K.D. & Main,P. (1993) Improvement of macromolecular electron-density maps by the simultaneous application of real and reciprocal space constraints. *Acta Crystallogr. D. Biol. Crystallogr.*, 49, 148-157.

[120] Cowtan,K.D. & Zhang,K.Y. (1999) Density modification for macromolecular phase improvement. *Prog. Biophys. Mol. Biol.*, 72, 245-270.

[121] Zubieta,C., Kota,P., Ferrer,J.L., Dixon,R.A., & Noel,J.P. (2002) Structural basis for the modulation of lignin monomer methylation by caffeic acid/5-hydroxyferulic acid 3/5-O-methyltransferase. *Plant Cell*, 14, 1265-1277.

[122] Martin,J.L. & McMillan,F.M. (2002) SAM (dependent) I AM: the S-adenosylmethionine-dependent methyltransferase fold 1. *Curr. Opin. Struct. Biol.*, 12, 783-793.

[123] Rossmann,M.G. & Argos,P. (1978) The taxonomy of binding sites in proteins. *Mol. Cell Biochem.*, 21, 161-182.

[124] Rao,S.T. & Rossmann,M.G. (1973) Comparison of Super-Secondary Structures in Proteins 1. *Journal of Molecular Biology*, 76, 241-&.

[125] Schulz,G.E. & Schirmer,R.H. (1974) Topological comparison of adenyl kinase with other proteins 1. *Nature*, 250, 142-144.

[126] Schulz,G.E., Schirmer,R.H., & Pai,E.F. (1982) FAD-binding site of glutathione reductase 1. *J. Mol. Biol.*, 160, 287-308.

[127] Wierenga,R.K., Drenth,J., & Schulz,G.E. (1983) Comparison of the three-dimensional protein and nucleotide structure of the FAD-binding domain of p-hydroxybenzoate hydroxylase with the FAD- as well as NADPH-binding domains of glutathione reductase 3. *J. Mol. Biol.*, 167, 725-739.

[128] Moller,W. & Amons,R. (1985) Phosphate-binding sequences in nucleotide-binding proteins 1. *FEBS Lett.*, 186, 1-7.

[129] Kelley,L.A., MacCallum,R.M., & Sternberg,M.J. (2000) Enhanced genome annotation using structural profiles in the program 3D-PSSM. *J. Mol. Biol.*, 299, 499-520.

[130] Schreuder,H.A., van der Laan,J.M., Hol,W.G., & Drenth,J. (1988) Crystal structure of p-hydroxybenzoate hydroxylase complexed with its reaction product 3,4-dihydroxybenzoate. *J. Mol. Biol.*, 199, 637-648.

REFERENCES

[131] Dong,C., Flecks,S., Unversucht,S., Haupt,C., van Pee,K.H., & Naismith,J.H. (2005) Tryptophan 7-halogenase (PrnA) structure suggests a mechanism for regioselective chlorination. *Science*, 309, 2216-2219.

ACKNOWLEDGEMENTS

ACKNOWLEDGEMENTS

This whole work presented here wouldn't have been possible without the help of many people including my friends and colleagues in and outside the institute. Here I would like to thank the following people with all my heart whom.I owe, for their constant help and support.

First and foremost my sincere gratitude to Dr.Roger Goody who allowed and gave me an opportunity to work in this wonderful department and also for his constant support throughout these years.

My sincere thanks to my supervisor Dr. Wulf Blankenfeldt. whose ever encouraging nature helped me to step forward in both my work field and personal life. I sincerely thank him for his generosity, time, patience and lot of useful discussions.and am grateful for his constant support, constructive guidance and active encouragement throughout my work which helped me a lot in understanding the subject and undertaking several problems with fruitful solutions.

I would like to thank Dr. Henning Mootz, my third supervisor for taking time to offer words of encouragement and for his helpful comments on my thesis.

I thank Dr. Petra Janning, for her invaluable help with all the mass spectroscopic work and introducing and helping me with the instrument.

Dr. Linda Thomashow and Dr. Dmitri Mavrodi, our collaborators in US who helped me with some useful informations and ideas

Petra Herde, without whose help I wouldn't have been confident enough in working with all the equipments with ease. I am grateful to her for being so